

AMPHIPHILIC DIBLOCK COPOLYMERS:
STUDY OF INTERPOLYELECTROLYTE COMPLEXATION IN
ORGANIC MEDIA AND
NANOENCAPSULATION OF MELATONIN

DISSERTATION

zur Erlangung des akademischen Grades eines
Doktors der Naturwissenschaften (Dr. rer. nat.)
im Fach Chemie der Fakultät für Biologie, Chemie und Geowissenschaften der
Universität Bayreuth

vorgelegt von

Evis Karina Penott Chang

Geboren in Valencia/Venezuela

Bayreuth, 2011

Die vorliegende Arbeit wurde in der Zeit von Septembert 2003 bis Mai 2011 in Bayreuth am Lehrstuhl Makromolekulare Chemie II unter Betreuung von Herrn Prof. Dr. Axel H. E. Müller angefertigt.

Vollständiger Abdruck der von Fakultät für Biologie, Chemie und Geowissenschaften der Universität Bayreuth genehmigten Dissertation zur Erlangung des akademischen Grades eines Doktors der Naturwissenschaften (Dr. rer. nat.).

Dissertation eingereicht am:	08.05.2011
Zulassung durch die Promotionskommission:	18.05.2011
Wissenschaftliches Kolloquium:	22.07.2011

Amtierender Dekan: Prof. Dr. Stephan Clemens

Prüfungsausschuß:

Prof. Dr. A. H. E. Müller (Erstgutachter)
Prof. Dr. S. Föster (Zweitgutachter)
Prof. Dr. P. Strohrigl (Vorsitzender)
Prof. Dr. B. Weber

To all who supported me in this journey!

A ti Jorge, por siempre

SUMMARY

Two oppositely charged homopolyelectrolytes poly(2-(methacryloyloxy)ethyl-dimethyl-ethylammonium bromide) (PDMAEMAQ) and poly(acrylic acid) (PAA), and amphiphilic diblock copolymers based on polystyrene and the ionizable block poly(acrylic acid) were synthesized via Atom Transfer Radical Polymerization (ATRP). All polymers were characterized using ^1H NMR and gel permeation chromatography to confirm their structure, molecular weight distribution and to follow the conversion. Poly(2-(dimethylamino)ethyl methacrylate), PDMAEMA, was quaternized with ethyl bromide to produce PDMAEMAQ with a quaternization degree of 98%. Furthermore, poly(acrylic acid) segments were obtained after hydrolysis of the poly(*t*-butyl acrylate) block.

After characterization of all polymers, interpolyelectrolyte complexation in chloroform was carried out. A novel method was developed to transfer the insoluble polyelectrolytes into the organic solvent and subsequently form polymer/polymer interpolyelectrolyte (IPECs) in organic media. Therein, the polyelectrolyte were first reacted with oppositely charged low molecular weight surfactants (sodium dodecyl sulfate, SDS, and cetyltrimethylammonium bromide, CTAB) to form polyelectrolyte-surfactant complexes (PESCs). In organic solvents, analogously to the formation of IPECs in aqueous media, interpolyelectrolyte complexation takes place upon the direct mixing of organic solutions of two complementary PESCs. This process is accompanied by an entropically favorable release of the surfactant counterions (in the form of ion pairs or their aggregates in low polarity organic solvents), which were previously associated with the ionic groups of the polyelectrolytes in solution. These reactions are fast and lead to frozen and non-equilibrium macromolecular co-assemblies.

The size and the morphologies of the IPECs in chloroform were extensively investigated using transmission electronic microscopy (TEM), scanning force microscopy (SFM), dynamic/static light scattering techniques, ^1HMR and turbidimetric titrations, for two different systems: (i) homopolyelectrolyte/homopolyelectrolyte and (ii) homopolycation/negatively charged amphiphilic diblock copolymer. For the first system, the possible particle structures consist either of particles with a core formed by IPECs stabilized by fragments of the excess polymeric component or of vesicles (polymersomes). In system (ii), particles of micellar type with a core assembled from electrostatically coupled segments of the polymeric components can be found, surrounded by a corona built

up either from a mixture of polystyrene blocks and excess segments of PDMAEMAQ⁺DS⁻ chains or from a mixture of polystyrene blocks and excess parts of PA⁻CTA⁺ blocks, depending on which polymeric component was present in surplus during the interpolyelectrolyte complexation.

Finally, nanocapsules loaded with melatonin were fabricated using a simple nanoprecipitation route employing a mixture of a diblock copolymer based on poly(methyl methacrylate) and PDMAEMA (PMMA-*b*-PDMAEMA) in combination with poly(ϵ -caprolactone), PCL. The diblock copolymers were synthesized via ATRP using PMMA-macroinitiators for the DMAEMA polymerization. Shape and size of the nanocarriers were visualized by TEM, cryogenic TEM and scanning electron microscopy (SEM). Standard TEM for nanocapsules showed an oily core surrounded by a thin layer composed of PCL/PMMA-*b*-PDMAEMA. Cryo-TEM also indicated the presence of spherical nanoobjects with a diffuse polymer corona. Encapsulation efficiencies were determined assaying the nanoparticles by HPLC and values of ca. 30-35% are shown by the nanocapsules. DLS measurements further confirmed well-defined unimodal particle size distributions for all formulations. It was also possible to successfully incorporate platinum nanoparticles into the nanocarrier, as evidenced by TEM, which opens up possibilities for promising applications like monitoring the circulation of the drug carrier within the body.

ZUSAMMENFASSUNG

Zwei entgegengesetzt geladene Homopolyelectrolyte, Poly(2-(Methacryloyloxy)ethyl dimethylammonium bromid) (PDMAEMAQ) und Polyacrylsäure (PAA), sowie amphiphile Diblockcopolymeren auf Basis von Polystyrol und einem ionisierbaren Polyacrylsäure-block wurden mittels Atom Transfer Radical Polymerisation (ATRP) synthetisiert. Alle Polymere wurden über $^1\text{H-NMR}$ - und Gelpermeationschromatographie auf die Struktur und die Molekulargewichtsverteilung hin untersucht. Poly(2(dimethylamino)ethyl methacrylat), PDMAEMA, wurde mit Ethylbromid zu PDMAEMAQ bis zu einem Quaternisierungsgrad von 98% reagiert. Die Poly(acrylsäure)segmente wurden hingegen durch eine Hydrolyse der Poly(*t*-butylacrylat)blöcke erhalten.

Nach der Charakterisierung aller Polymere erfolgte eine Interpolyelektrolyt-Komplexbildung dieser verschiedenen Polymere in Chloroform. Eine neue Methode wurde hierbei entwickelt um die Polyelektrolyte in das organische Lösungsmittel zu übertragen und eine anschließende Polymer/Polymer Komplexbildung durchzuführen. Hierzu war es zuerst nötig die Polyelektrolyte mit entgegengesetzt geladenen niedermolekularen Tensiden (Natriumdodecylsulfat, SDS, und Cetyltrimethylammoniumbromid, CTAB) zu Polyelektrolyt/Tensid-Komplexen (PESCs) umzusetzen. Analog der Bildung von Interpolyelektrolyt-Komplexen (IPECs) in wässrigen Medien ist die anschließende Komplexierung der Polymere durch die direkte Mischung zweier organischer Lösungen mit zwei komplementären PESCs zu erreichen. Dieser Prozess wird durch eine entropisch günstige Freigabe der Tensid-Gegenionen (in Form von Ionenpaaren oder deren Aggregaten in organischen Lösemitteln geringer Polarität), die zuvor an die ionischen Gruppen der Polyelektrolytblöcke in Lösung angebunden waren, ermöglicht. Diese sehr schnellen Austauschreaktionen führen zu gefroren Nichtgleichgewichtsstrukturen der beiden aggregierenden Polymere. Die Größe und die Morphologie der IPECs in Chloroform wurde daher umfassend mit Hilfe der Transmissionselektronenmikroskopie (TEM), Rasterkraftmikroskopie (SFM), dynamischer/statischer Lichtstreuung, $^1\text{H-NMR}$ und turbidimetrischer Titration für zwei verschiedene Systeme untersucht: (i) Homopolyelectrolyt / Homopolyelectrolyt und (ii) Homopolykation / negativ geladenes Diblockcopolymer.

Für das erste System bestehen die möglichen Aggregatstrukturen zum einen aus Partikeln mit einem IPEC-Kern der durch Teile des überschüssigen Polymers stabilisiert wird, oder es bilden sich Vesikel (Polymersome) aus. Im System (ii) sind die Aggregate aus einem Mizellaren IPEC Kern und einer Korona zusammengesetzt, die entsprechend der Stochiometrie aus einer Mischung an PS und überschüssigen PDMAEMAQ⁺DS⁻ Ketten oder aus einem Gemisch von PS und überzähligen PAA⁻CTA⁺ Blocksegmenten besteht.

Darüber hinaus wurden mit Melatonin geladene Nanokapseln mittels einer Nanoausfällung eines Diblockcopolymeres auf Basis von Poly(methyl methacrylat) und PDMAEMA (PMMA-b-PDMAEMA) in Kombination mit Poly(ϵ -Caprolacton), PCL, hergestellt. Die Diblockcopolymeren wurden per ATRP unter der Verwendung eines PMMA-Makroinitiators für die DMAEMA Polymerisation synthetisiert. Form und Größe der Nanoträger ergaben sich aus TEM, cryo-TEM- und Rasterelektronenmikroskopie (REM) Untersuchungen. Standard TEM der Nanokapseln zeigte einen öligen Kern, der von einer dünnen Schicht an PCL/PMMA-b-PDMAEMA umgeben ist. Cryo-TEM offenbarte ebenfalls die Anwesenheit von sphärischen Nanoobjekten mit einer diffusen und gequollenen Polymerkorona. Die Verkapselungseffizienzen der Nanopartikel, welche mittels HPLC bestimmt wurden, betragen angemessene Werte von ca. 30-35%. DLS-Messungen bestätigten überdies unimodale Teilchengrößenverteilung für alle Formulierungen. Es konnten ebenfalls Platin-Nanopartikel erfolgreich in die Nanokapseln integriert werden, was Möglichkeiten für viel versprechende Anwendungen, wie der Überwachung der Zirkulation der Wirkstoffträger im Körper, eröffnet.

TABLE OF CONTENT

SUMMARY.....	4
ZUSAMMENFASSUNG.....	6
1. INTRODUCTION	11
1.1 ATRP basics	11
1.1.1 <i>Conventional Radical Polymerization.....</i>	<i>11</i>
1.1.2 <i>Basic Principles of LRP.....</i>	<i>12</i>
1.1.3 <i>Atom Transfer Radical Polymerization</i>	<i>12</i>
1.2 Interpolyelectrolyte Complexation	18
1.2.1 <i>Interpolyelectrolyte Complexation in Water</i>	<i>18</i>
1.2.2 <i>Interpolyelectrolyte Complexation in Organic Media</i>	<i>20</i>
1.3 Drug Encapsulation. Nanocontainers	23
1.3.1 <i>Synthetic Polymers for Drug Delivery System (DDS).....</i>	<i>24</i>
1.3.2 <i>Polymeric Nanoparticles for Drug Delivery</i>	<i>25</i>
1.3.3 <i>Clearance and Opsonization</i>	<i>28</i>
1.3.4 <i>Other drug nanocarrier formulations.</i>	<i>30</i>
1.3.5 <i>How is the drug released?.....</i>	<i>31</i>
Objective of this Thesis	32
References	33
2. OVERVIEW OF THIS THESIS.....	46
Individual Contributions to Joint Publications	54
3. INTERPOLYELECTROLYTE COMPLEXATION IN CHLOROFORM	56
Abstract	57
3.1 Introduction	58
3.2 Experimental Section	60
3.2.1 <i>Materials.....</i>	<i>60</i>
3.2.2 <i>Polymer Synthesis.....</i>	<i>60</i>
3.2.2.1 <i>Synthesis and quaternization of poly(2-dimethylaminoethyl methacrylate) (PDMAEMA).</i>	<i>61</i>
.....	61
3.2.2.2 <i>Synthesis of poly(acrylic acid) (PAA).</i>	<i>61</i>

3.2.3 Preparation of Polyelectrolyte-Surfactant Complexes (PESCs).....	62
3.2.4 Characterization.....	62
3.3 Results and Discussion	63
3.3.1 Interpolyelectrolyte Complexation in Chloroform	63
3.3.2 Characterization of IPECs	67
3.4 Conclusions	71
Acknowledgements	72
References.....	72
4. INTERPOLYELECTROLYTE COMPLEXES OF DIBLOCK COPOLYMERS VIA INTERACTION OF COMPLEMENTARY POLYELECTROLYTE-SURFACTANT COMPLEXES IN CHLOROFORM	74
Abstract	75
4.1 Introduction	76
4.2 Experimental Part	78
4.2.1 Materials.....	78
4.2.2 Synthesis of Polymers	78
4.2.2.1 Synthesis of Polystyrene Macroinitiator.....	79
4.2.2.2 Synthesis of Polystyrene-block-Poly(acrylic acid) (PS- <i>b</i> -PAA _x) Diblock Copolymers.....	79
4.2.3 Preparation of Polyelectrolyte-Surfactant Complexes (PESCs).....	81
4.2.4. Characterization.....	82
Gel Permeation Chromatography (GPC).	82
Turbidimetric Titrations	82
Dynamic Light Scattering (DLS).	83
Static Light Scattering (SLS).	83
Transmission Electron Microscopy (TEM).	83
4.3 Results and Discussions.....	84
4.3.1. Interpolyelectrolyte Complexation in Chloroform	84
4.3.2 Characterization of IPECs	86
4.4 Conclusions	92
Acknowledgements.....	93
References.....	93
5. AMPHIPHILIC DIBLOCK COPOLYMER AND POLYCAPROLACTONE BLENDS TO PRODUCE NEW VESICULAR NANOCARRIERS	95

Abstract	96
5.1. Introduction	97
5.2. Experimental Section	100
5.2.1 <i>Materials</i>	100
5.2.2 <i>Synthesis of Poly(methyl methacrylate) macroinitiator</i>	100
5.2.3 <i>Synthesis of Poly(methyl methacrylate)-b-poly(2-dimethylaminoethyl methacrylate)</i>	100
5.2.4 <i>Preparation and Loading of Nanocapsules</i>	101
5.2.5 <i>Platinum-melatonin loaded nanoparticles</i>	101
5.2.6 <i>Notation</i>	101
5.3. Results and Discussions	104
5.3.1 <i>Physico-Chemical Characterization</i>	104
5.3.2 <i>Morphological Study</i>	107
5.3.3 <i>Encapsulation Efficiency (EE)</i>	110
5.4. Conclusions	111
Acknowledgments	112
References	112
ACKNOWLEDGMENTS	118
LIST OF PUBLICATIONS	120
ERKLÄRUNG	121

1. INTRODUCTION

This section is divided in three parts; each one intends to give a brief overview of some theoretical aspects related with the topic of the present work. Since the polymers used here were synthesized by atom transfer radical polymerization, the first part of this introduction deals with the most relevant basic principles of this polymerization method. The second part is about interpolyelectrolyte complexation, which has been reported in most of the cases in aqueous media and to lesser extent in low-polar organic solvents. Here, details about interpolyelectrolyte complexation in organic solvent are given as a proposal to obtain new macromolecular structures which can lead to new promising applications. And finally, the third part includes some fundamentals of drug delivery systems, drug encapsulation and some aspects that should be taken into account for the preparation of a pharmaceutical formulation.

1.1 ATRP basics

1.1.1 Conventional Radical Polymerization

Conventional Radical Polymerization (CRP) has played a dominant role in the industrial process of polymeric materials because a large variety of monomers can be polymerized and copolymerized under mild experimental conditions. However, CRP is difficult to control and very often yield polymers with ill-controlled molecular weight and broad polydispersity, as a consequence of irreversible biradical termination processes (coupling and disproportionation reactions).^{1, 2} Recently, synthesis of well-defined polymers via so-called controlled/"living" radical polymerization (LRP) is possible since bimolecular terminations are minimized and the life-time of living polymers is prolonged through the introduction of dormant states for the propagating species. With LRP, the final molecular weight can be predicted and adjusted by varying the initial ratio monomer-to-initiator, maintaining a narrow molecular weight distribution ($1.04 < M_w/M_n < 1.5$).³

Traditionally, well-defined polymer architectures such as block copolymer were prepared via living ionic polymerization techniques. Recent advances in controlled LRP have made possible the synthesis of well controlled architectures which were only accessible by living ionic polymerization. Chain polymerizations without chain-breaking reactions are highly

desirable because they allow the synthesis of block copolymers by sequential addition of different monomers (Eq.1). When the polymerization of the monomer M1 is completed, the “living” reactive centers are intact because of the absence of chain-breaking reaction. Sequential addition of a second monomer (third and so) leads to the formation of a block copolymer containing M1.⁴



1.1.2 Basic Principles of LRP

Nowadays, the three most effective methods of controlling radical polymerizations, with future commercial promise include: Nitroxide Mediated Polymerization (NMP), Atom Transfer Radical Polymerization (ATRP) and Reversible Addition-Fragmentation chain Transfer Polymerization (RAFT). All these methods have their advantages and limitations.⁵⁻⁹ But independently of the method, a LRP requires all chains to begin growing (reversibly via exchange process) practically at the same time and to retain their functionalities until the very end of the reaction. This is contrast with what occurs in conventional radical polymerization, where all chains terminate and initiation is never completed, even when all monomer is consumed. Therefore, the three basic prerequisites for LRP are:¹⁰

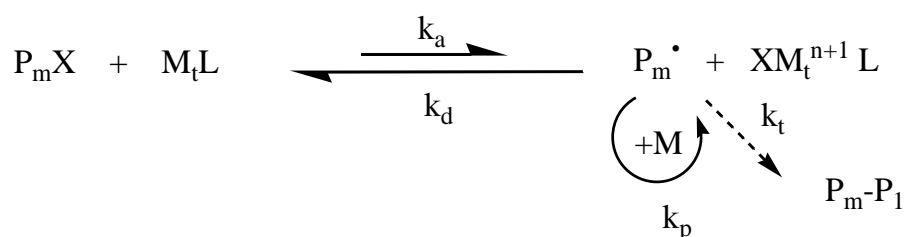
1. Initiation should be completed at low monomer conversions.
2. Relatively low MW ($DP < 1000$) should be targeted to avoid chain transfer. This requires high concentration of growing and dormant chains (e.g., $> 10^{-2}$ M for bulk polymerization)
3. Concentration of propagating radicals ($[P^\circ] < 10^{-7}$ M) should be sufficiently low to enable growth of chains to sufficiently high MW, before they terminate.

1.1.3 Atom Transfer Radical Polymerization

A general mechanism for ATRP is shown in Scheme 1. This method utilizes a reversible halogen abstraction step in which a lower oxidation state metal (M_t complexed

by ligand L) reacts with an alkyl halide (P_m-X) to generate a radical (P_m^\bullet) and a higher oxidation state metal complex ($XM_t^{n+1}L$, at a rate constant of activation, k_a). This radical adds monomer to generate the polymer chain (with a rate constant of propagation, k_p). The higher oxidation state metal can then deactivate the growing radical to generate a dormant chain and the lower oxidation state metal (with a rate constant of deactivation, k_d). The molecular weight is controlled because both initiation and deactivation are fast, allowing for all chains to begin growing at approximately the same time while maintaining a low concentration of active species.

Scheme 1. Equilibrium/Propagation Expression for ATRP



There are, thus, some parameters which play an important role for a successful ATRP: the catalyst, it includes a transition metal compound and ligands, a suitable initiator and appropriate polymerization conditions to lead to a living process, i.e., linear increase of the molecular weight with conversion and low polydispersities.

Kinetics.

ATRP kinetics is discussed in term of copper-based catalyst. According to Scheme 1, using the assumption that contribution of termination becomes insignificant due to the persistent radical effect (PRE)¹¹⁻¹³ and using a fast equilibrium approximation, which is necessary for observed low polydispersities, the rate law can be derived as follows:

$$R_p = k_p \frac{k_a}{k_d} [M][I]_0 \times \frac{[Cu^I]}{[X - Cu^{II}]} \quad (\text{eq. 2})$$

$$\frac{M_w}{M_n} = 1 + \left(\frac{k_p [I]_0}{k_d [X - Cu^{II}]} \right) \left(\frac{2}{Xp} - 1 \right) \quad (\text{eq. 3})$$

Equations 2 and 3 give more precise descriptions about how the catalyst controls the polymerization through the atom transfer equilibrium. In these equations, $[I]_0$ refers to the initial concentration of the initiator. In eq. 2, the rate of polymerization, R_p , is first order with respect to the monomer, $[M]$, and the Cu(I) concentration, $[Cu^I]$, in solution. A high concentration of Cu(II), $[X-Cu^{II}]$, slows down the rate of polymerization. Not only does the rate constant of propagation, k_p , which is specific for each monomer, affect R_p , but also equilibrium constant of activation, k_a and deactivation, k_d . A high value for the equilibrium constant gives a higher rate of polymerization as well. Equation 3 illustrates how the polydispersity index in ATRP in the absence of significant chain termination and transfer, relates to the concentrations of initiator $[I]_0$ and deactivator $[X-Cu^{II}]$, the rate constants of propagation (k_p) and deactivation (k_d), and the monomer conversion (Xp). This equation holds for conditions when initiator is completely consumed and degrees of polymerization are sufficiently high; otherwise the Poisson term should be added.¹⁴ The molecular weight distribution, M_w/M_n , decreases with conversion, Xp . A narrower molecular weight distribution is obtained at higher conversion, higher k_d relative to k_p , higher concentration of deactivator, and higher molecular weights, i.e., $1/[I]_0$.

Monomer

Several monomers have been successfully polymerized by ATRP: styrenes,^{15, 16} (meth)acrylates,^{17, 18} (meth)acrylamides^{19, 20} and acrylonitrile,^{15, 21, 22} which contain substituent that can stabilize the propagating radicals.^{23, 24} However, controlled polymerization of (meth)acrylic acid by ATRP presents a problem because the acid can poison the catalysts by coordinating to the transition metal. By this method, polymerization requires of protected acid monomers, further hydrolysis leads to the respective polyacid.^{25, 26} In addition, nitrogen-containing ligands, can be protonated which interferes with the metal complexation ability monomers. Each monomer has its own unique atom transfer equilibrium constant for its active and dormant species. In the absence of any side reactions other than radical termination by coupling or disproportionation, a high

equilibrium constant will lead to a large amount of termination because of high radical concentration. Each monomer possesses also its own intrinsic radical propagation rate. For a specific monomer, the concentration of propagating radicals and the rate of the radical deactivation needs to be adjusted to maintain polymerization control.

Initiators

The initiators have the main role of determining the number of growing polymer chains (Eq.4).²⁷ If the initiation is fast and the transfer and termination negligible, then the number of growing chains is constant and equal to the initial initiator concentration.

$$M_{n,theo} = M_{w,monomer} \times \frac{[M]_0}{[I]_0} \times Xp \quad (\text{eq. 4})$$

A variety of initiators, typically alkyl halides R-X, have been used successfully in ATRP. To obtain well-defined polymers with narrow molecular weight distributions, the halide group, X, must rapidly and selectively migrate between the growing chain and the transition-metal complex. When X is either bromine or chlorine, the molecular weight control is the best. Iodine works well for acrylate polymerizations in copper-mediated ATRP.²⁸ Fluorine is not used because the C-F bond is too strong to undergo homolytic cleavage. In general, any alkyl halide with activating substituents on the α -carbon, such as aryl, carbonyl, or allyl groups, can potentially be used as ATRP initiators. Polyhalogenated compounds (e.g., CCl₄ and CHCl₃) and compounds with a weak R-X bond, such as N-X, S-X, and O-X, can be also be used. When the initiating moiety is attached to macromolecular species, macroinitiators are formed and can be used to synthesize block/graft copolymers.

The basic requirement for a good ATRP initiator is that it should have a reactivity at least comparable to that of the subsequently formed growing chains. This also indicates that not all initiators are good for all monomers. For successful initiation, the structure of the alkyl group (R) in the initiator should be similar to that of the dormant polymer species. Tertiary alkyl halides are better initiators than secondary ones, which are better than primary alkyl halides. These have been partially confirmed by measurements of activation rate constants.²⁹⁻³¹ Benzyl-substituted halides are useful initiators for the polymerization of

styrene and its derivatives due to their structural resemblance.³² However, they fail in the polymerization of more reactive monomers in ATRP such as MMA. On the other hands, 2-bromopropionates are good initiators for the ATRP of acrylates.

Catalyst: transition metals and ligands

The ideal catalyst for ATRP should be highly selective for atom transfer and should not participate in other reactions. The catalyst is the key to ATRP since it determines the position of the atom transfer equilibrium and the dynamics of exchange between the dormant and active species. There are several prerequisites for an efficient transition metal catalyst. First, the metal center must have at least two readily accessible oxidation states separated by one electron. Second, the metal center should have reasonable affinity toward a halogen. Third, the coordination sphere around the metal should be expandable upon oxidation to selectively accommodate a (pseudo)halogen. Fourth, the ligand should complex the metal relatively strongly. A number of different transition metal complexes based on Fe,³³ Ru,³⁴ Ni,³⁵ Pd³⁶ have been used in ATRP. However, Cu-catalyst is the most successful and common one, and superior in terms of versatility and cost.

The main role of the ligand in ATRP is to solubilize the transition-metal salt in the organic media and to adjust the redox potential of the metal center for appropriate reactivity and dynamics for the atom transfer.

Nitrogen-based polydentate ligands have been shown to be very efficient ligands for copper catalysts in terms of controlling the polymerization reaction. A wide range of monomers like (meth)acrylates, styrenes, acrylonitrile, acrylamides, and vinylpyridines have been polymerized and copolymerized successfully with Cu-based catalysts using ligands with amine, pyridine, or imine substructures.^{5, 31, 37-39} These investigations revealed that the ligand played a crucial role in tuning the activity of the related catalyst in the activation and deactivation steps of the ATRP mechanism (Scheme 1). This equilibrium is affected by the electronic and steric effects of the ligand in the following ways. First, bulky ligands reduce the rate of activation, as the Cu center is harder to access for the bromine atom. The second, and more predominant factor, is based mainly on the electronic interactions of the ligand with the Cu center in the complex. For example, good π -acceptor

ligands efficiently stabilize the lower oxidation state of the metal center. This shifts the atom transfer equilibrium toward the dormant species PnX .³¹

Solvent, Temperature and Reaction Time

ATRP can be carried out either in bulk, in solution, or in a heterogeneous system (e.g., emulsion, suspension). A solvent is sometimes necessary, especially when the obtained polymer is insoluble in its monomer (e.g., polyacrylonitrile). Several factors affect the solvent choice. Chain transfer to solvent should be minimal. In addition, interactions between solvent and the catalytic system should be considered to avoid catalyst poisoning by the solvent (e.g., carboxylic acids or phosphine in copper based ATRP)³⁸ and solvent-assisted side reactions, such as elimination of HX from polystyryl halides, which is more pronounced in a polar solvent,³ should be minimized.

The rate of polymerization in ATRP increases with increasing temperature due to the increase of both the radical propagation rate constant and the activation equilibrium constant. As a result of the higher activation energy for the radical propagation than for the radical termination, higher k_p/k_t ratios and better control (“livingness”) may be observed at higher temperatures. However, chain transfer and other side reactions become more pronounced at elevated temperatures.³ In general, the solubility of the catalyst increases at higher temperatures; however, catalyst decomposition may also occur with the temperature increase.^{40, 41} The optimal temperature depends mostly on the monomer, the catalyst, and the targeted molecular weight.

At high monomer conversions, the rate of propagation slows down considerably; however, the rate of any side reaction does not change significantly, as most of them are monomer concentration independent. Prolonged reaction times leading to nearly complete monomer conversion may not increase the polydispersity of the final polymer but will induce loss of end groups. Thus, to obtain polymers with high end-group functionality or to subsequently synthesize block copolymers, conversion must not exceed 95% to avoid end-group loss.

1.2 Interpolyelectrolyte Complexation

During the last decades, growing attention has been paid to the design of novel “intelligent” (or “smart”) polymeric architectures, which can demonstrate high response and sensitivity to slight variations of conditions of the surrounding medium. One of the possible approaches to the design of such architectures is to utilize assembly processes proceeding in multi-component polymer systems. In particular, one can exploit electrostatic interactions between oppositely charged amphiphilic block copolymers which is expected to result in formation of novel, yet unexplored, interpolyelectrolyte complexes (IPECs), and are expected to exist in the micellar form in appropriate organic solvents (or their mixtures).

1.2.1 Interpolyelectrolyte Complexation in Water

It is well known that polyelectrolytes (PE) can form stable complexes with oppositely charged species because of the strong cooperative Coulombic attraction forces and the release of small counterions.

The simplest route to prepare such IPECs is a direct interaction of anionic and cationic amphiphilic block copolymers either in aqueous or organic solutions (Figure 1). In these cases, however, macromolecular micelles (common in aqueous media or reverse in organic media) rather than individual macromolecules (unimers) are expected to interact each other because critical micellization concentrations of amphiphilic block copolymers are usually very low. In connection with this, the formation of the IPECs can be sufficiently off-equilibrium and, therefore, hardly controlled process which may lead to so called “frozen” non-equilibrium structures.

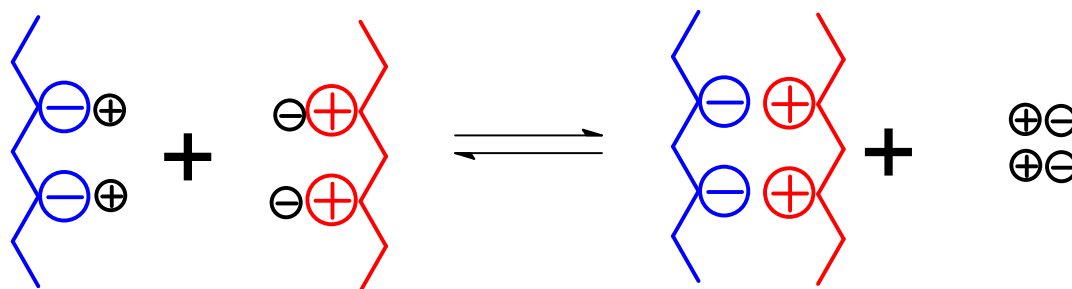


Figure 1. Interpolyelectrolyte complexation

IPECs have been extensively studied for their potential and promising application in different fields such as medicine, biotechnology, ecology and industry. They might be used as membranes and ion-exchange resins⁴²⁻⁴⁴ flocculants⁴⁵⁻⁴⁷, layer by layer (LBL) assembly,⁴⁸⁻⁵⁰ for separation and purification of biopolymers,^{51, 52} for micro- and nanoencapsulation,⁵³⁻⁵⁶ drug delivery^{57, 58} and gene delivery therapy.⁵⁹⁻⁶³

The formation and structure of the interpolyelectrolyte complexes depends on several factors such as the chemical structures of both polymers, their chain lengths, and their environments such as the solvent, pH, salinity, mixing ratio and temperature.⁶⁴⁻⁷¹ Complexations may lead to colloiddally stable nanoparticles or to macroscopically phase separation in the form of flocculates or coacervates.^{72, 73} The driving force for this type of phase separation is the gain in entropy related to the liberation of small counterions originally constrained, via electrostatic attraction, in close proximity to the macroions.

Consequently, phase separation can be suppressed by high salt concentrations, or by careful selection of the molecular characteristics of the polyelectrolyte pair. Macroscopic phase separation of IPECs can be controlled much more effectively by means of a double-hydrophilic block copolymer (DHBC), defined as a macromolecule consisting of a nonionic water-soluble chain linked to one end of a polyelectrolyte⁷⁴ as shown in the Figure 2. Complexation between such a diblock copolymer and an oppositely charged homopolyelectrolyte leads to the formation of micelles known as polyion complex (PIC) micelles or block ionomer complexes (BICs)⁷⁵⁻⁷⁷ or vesicles.⁷⁸

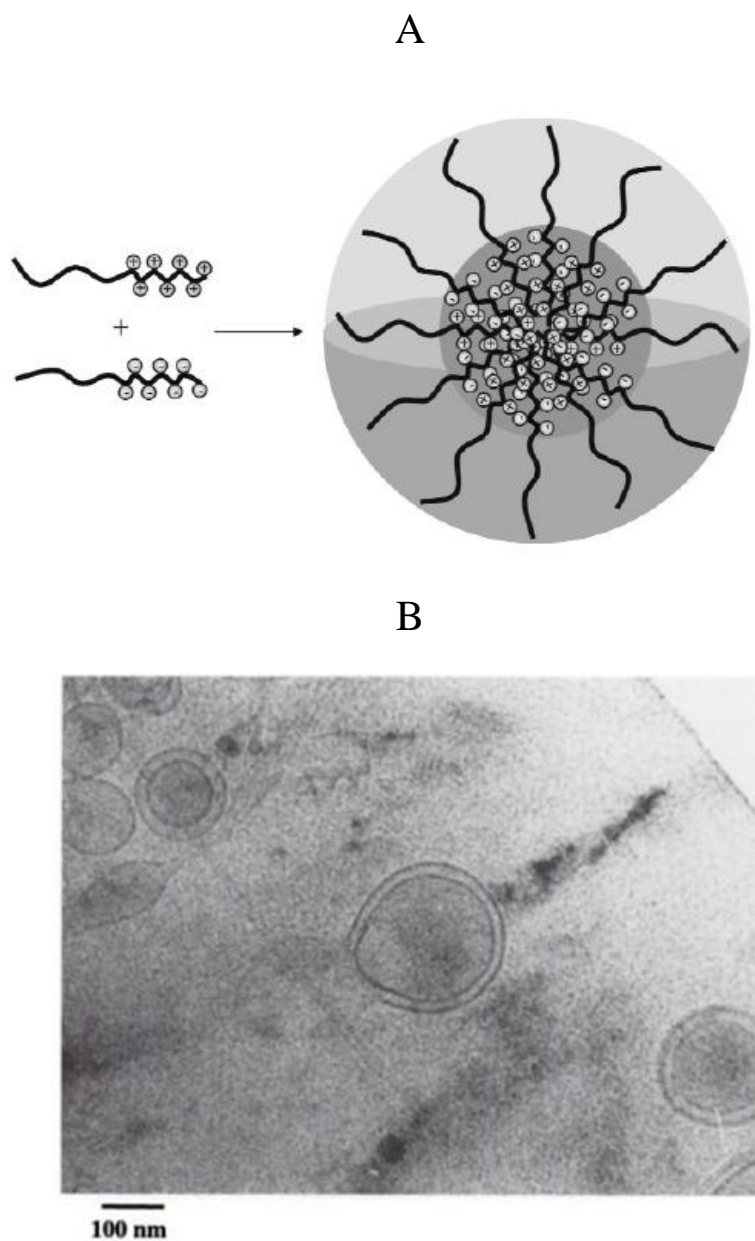


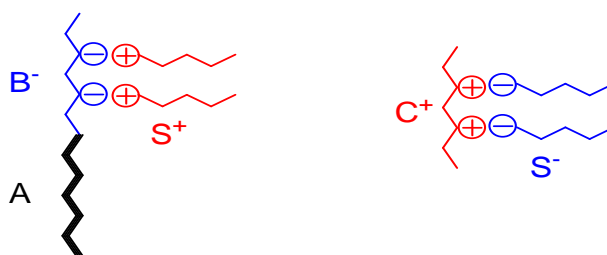
Figure 2. Formation of a micellar-type interpolyelectrolyte complex (A) Taken from [79]. Vesicles of PMAA49-PDMAEMA11 in water at pH = 9 (B). Taken from [78]

1.2.2 Interpolyelectrolyte Complexation in Organic Media

Interpolyelectrolyte complexation in water is well documented, though in organic solvents the situation is rather different because, in most of the cases, direct complexation is impossible due to poor solubility of the polymeric components of a system.

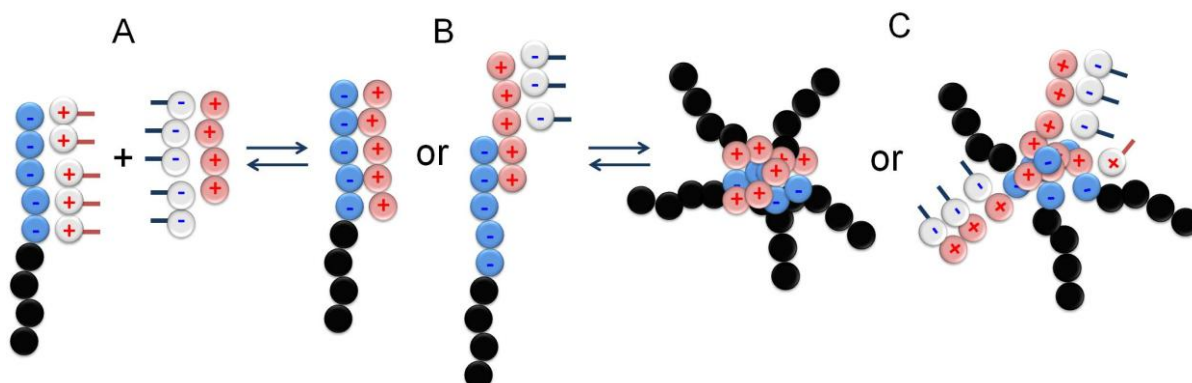
In this project a *two-step approach* is used to the design of novel polymeric architectures based on IPECs of homopolyelectrolytes and ionic amphiphilic diblock copolymers. The *first step* is a modification of the ionic (co)polymers via their interaction with oppositely charged surfactants in aqueous media. This enables to dissolve the products of the modification, i.e., complexes of ionic (co)polymers with oppositely charged surfactants, for example, $\text{AB}^- \cdot \text{S}^+$ or $\text{C}^+ \cdot \text{S}^-$, being S^- and S^+ surfactant counterions (Scheme 1), in low polarity organic solvents, e.g., chloroform, toluene, etc. In the appropriate organic solvents (or their mixtures), such complexes are expected to be *molecularly dispersed*, that is, to exist in the state of individual polyions (unimers) complexed with surfactant counterions, as was observed for a number of polyelectrolyte-surfactant complexes.

Scheme 1. Ionic block copolymer-surfactant complexes $\text{AB}^- \cdot \text{S}^+$ and $\text{C}^+ \cdot \text{S}^-$.



The *second step* is a complexation reaction between the molecularly dispersed complexes of the ionic (co)polymer with oppositely charged surfactants, $\text{AB}^- \cdot \text{S}^+$ and $\text{C}^+ \cdot \text{S}^-$, in low polarity organic solvents (or their mixtures) (Scheme 2A). This reaction is expected to result in the formation of the complex copolymers $\text{A}(\text{B}^- \cdot \text{C}^+)$ or $\text{A}(\text{B}^- \cdot (\text{C}^+)_n)\text{C}^+ \text{S}^-$ (Scheme 2B) stabilized by the electrostatic interaction of their oppositely charged fragments. The surfactant counterions previously associated with charged groups of the original ionic amphiphilic diblock copolymers are thought to be released into the bulk solution since it is entropically favorable.

Due to insolubility of common IPECs in low polarity organic solvents, such complex copolymers are thought to undergo self-assembly to generate novel complex polymeric architectures (Scheme 2C). In general, the formed macromolecular architectures can be of various morphological types, e.g., lamellae, vesicles, spherical or cylindrical micelles.

Scheme 2. Expected formation of micellar IPECs in low polarity organic media.

Bakeev, *et al.*,^{79, 80} reported a first attempt to prepare IPECs by using previous complexation of the polyelectrolyte with oppositely charged surfactant. Stoichiometric polyelectrolyte-surfactant complexes (PESCs), which are insoluble in water, could be redissolved in low-polar organic solvents, retaining their integrity due to the strong electrostatic attraction between the polyion units and surfactant ionic heads in low permittivity media, while solubility is provided by the affinity of the hydrocarbon tails to and organic solvent.⁷⁹⁻⁸¹ Thus far, polycations and polyanions could be transferred into low-polar organic solvents and an exchange reaction is expected to take place. The aim of Bakeev's work was to introduce conducting doped polyaniline (PANI) into an IPEC with polystyrenesulfonate (PSS) anion. Later, Lokshin *et al.*,⁸² reported the formation of IPECs between PANI complexed with surfactant and DNA as well as PSS. More recently, Pergushov *et al.*, reported the first reaction between polymethacrylate anions and poly(N-ethyl-4-vinylpyridinium) cations containing surfactant ions as counterions (dimethyldistearylammonium cations and dodecylsulfate anions, respectively) in chloroform yielding IPECs.⁸³ Also, an investigation of complexation between DNA and a cationic surfactant was carried out by Sergeyev *et al.*, demonstrating that DNA-surfactant complexes were soluble in chloroform and heptanes existing as individual components with a 1:1 stoichiometry.⁸⁴

Being insoluble in various non-polar solvents, IPECs demonstrate high swelling in aqueous media. The micellar cores of the formed complex polymeric architectures are therefore expected to change their properties from a glassy state to a viscous liquid one in dependence on the content of water, which can be solubilized by such micellar species from low polarity organic solvents. This provides a unique possibility for controlled

reorganization of the formed polymeric architectures, especially, upon adding to their organic solutions some aqueous solutions of low molecular weight electrolytes, which are known to destroy interpolymer ionic bonds.

Micellar coronas can include the desired number of different non-ionic blocks, whose content in the formed complex polymeric architectures are determined by the chemical structures of the original diblock copolymers and their amounts, as well as degrees of polymerization of the blocks. Under appropriate conditions (if the complex cores are not “frozen”), the non-polar blocks differing in chemical nature are expected to demonstrate *segregation* into the different domains on the level of a single micelle, leading to a *microphase separation* in its micellar corona. In the simplest case, this process is thought to result in the formation of mixed, “patchy” or Janus micelles (Figure 3).

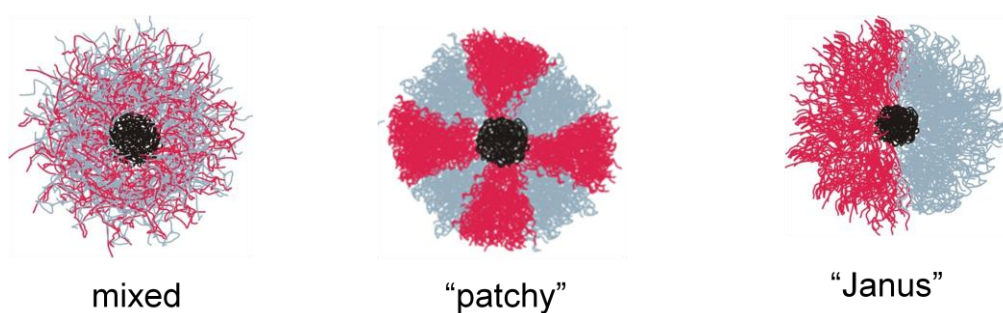


Figure 3. Structures of micelles expected via interpolyelectrolyte complexation.

1.3 Drug Encapsulation. Nanocontainers

Over the past few decades, there has been an increasing interest in developing novel drug delivery systems (DDS). This marked interest has several reasons: One is the fact that colloidal drug carriers have shown potential applications and advantages, enhancing the *in vivo* efficiency of many drugs. Secondly, and not less important, is that, pharmaceutical market trend indicates nowadays that DDS are playing an important role on their sales and developments. The imperative necessity for searching new drug delivery methods will result not only in more effective and efficacious treatments against many diseases that can improve pharmaceutical sales and profit but also will generate new niche to provide greater intellectual property protection to the already existing formulations. Another reason,

related with the latter one, is that patent expirations are forcing to the pharmaceutical companies to consider product reformulations and here again, new delivery methods are needed to develop new formulations of “off-patent” and “soon-to-be off patent” drugs. The reformulation of those products has to deal with the reduction of side/toxic effects, increase the patient compliance and reduce health care cost.⁸⁵

1.3.1 Synthetic Polymers for Drug Delivery System (DDS)

Nanotechnology has impacted significantly the field of drug delivery systems (DDS). It provides new materials in the nanometer range which can have potential applications in clinical medicine and research. Even more, it offers the advantages of a more targeted drug delivery and a more controllable release of the therapeutic compound.⁸⁶

A DDS has several functions: to protect the therapeutically active molecules against *in vivo* degradation, to prevent harmful side/toxic effects, to increase the bioavailability and the fraction of the drug accumulated in the targeted zone, to improve the pharmacokinetics and pharmacodynamics of the delivered drug.⁸⁶⁻⁸⁸

There are some requirements a polymeric material has to fulfill before being applied with therapeutically purposes. Two main mechanisms can be distinguished for addressing the desired sites for the drug release: (i) passive and (ii) active targeting. When it is not a drug itself it should provide a passive function as a drug carrier and active function when the nanocarriers surface is functionalized with ligands that are selectively recognized by a receptor on the surface of the cell.⁸⁷ Some of the following properties are expected for a nanocarrier: (a) prolonged circulation in the blood; (b) ability to accumulate – specifically or non-specifically; (c) responsiveness to local stimuli, such as pH and/or temperature changes; (d) allow for an effective intracellular drug delivery and further to individual cell organelles, and (e) bear a contrast/reporter moiety allowing for the real-time observation of its accumulation inside the target. Some other properties can be added to the list, such as magnetic sensitivity.^{89, 90} Depending on the reticular requirements a multifunctional pharmaceutical nanocarrier can be constructed, having specific properties and function. In the Figure 4 there is a schematic representation of multifunctional nanocarriers given by Torchilin,⁸⁹ explanations are given in the text of the figure.

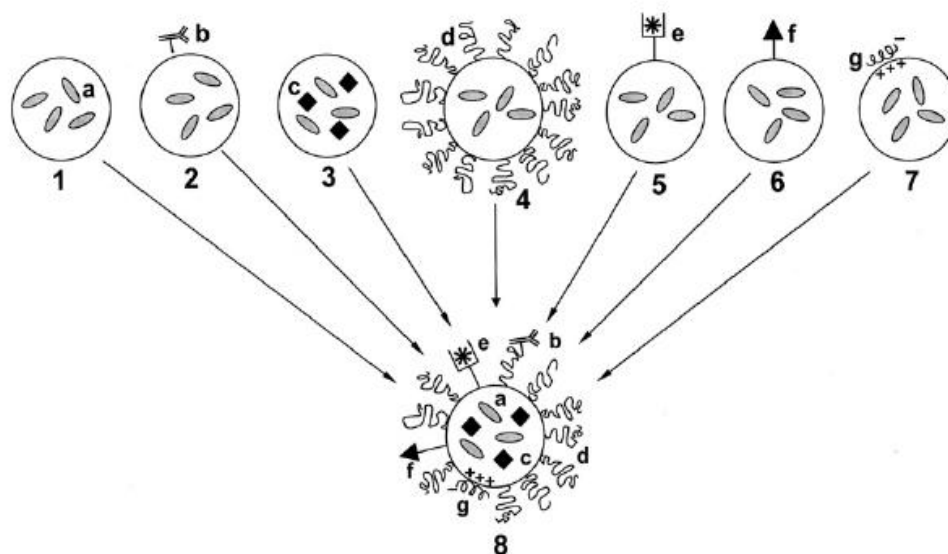


Figure 4. Schematic representation of the assembly on the multifunctional pharmaceutical nanocarrier. **1** – Traditional “plain” nanocarrier (a: drug loaded into the carrier); **2** – targeted nanocarrier or immunocarrier (b: specific targeting ligand, usually a monoclonal antibody, attached to the carrier surface); **3** – magnetic nanocarrier (c: magnetic particles loaded into the carrier together with the drug and allowing for the carrier sensitivity towards the external magnetic field and its use as contrast agent for magnetic resonance imaging); **4** – long-circulating nanocarrier (d: surface-attached protecting polymer (usually PEG) allowing for prolonged circulation of the nanocarrier in the blood); **5** – contrast nanocarrier for imaging purposes (e: heavy metal atom – ^{111}In , $^{99\text{m}}\text{Tc}$, Gd, Mn – loaded onto the nanocarrier via the carrier-incorporated chelating moiety for gamma- or MR imaging application); **6** – cell-penetrating nanocarrier (f: cell-penetrating peptide, CPP, attached to the carrier surface and allowing for the carrier enhanced uptake by the cells); **7** – DNA-carrying nanocarrier such as lipoplex or polyplex (g: DNA complexed by the carrier via the carrier surface positive charged); **8** – hypothetical multifunctional nanocarrier combining the properties of the carriers No. 1-7. Figure taken from [90].

1.3.2 Polymeric Nanoparticles for Drug Delivery

Synthetic polymers have been investigated as drug carriers, as a polymeric drug itself or in combination with small molecule drugs or biomacromolecules such as protein and poly(nucleic acids). It is expected that the polymer be water-soluble, non-toxic, non-immunogenic and it needs to be safe at all stages of the drug delivery process, i.e., before and after drug releases, including a safe excretion. If the polymer is non-degradable (e.g. poly(meth)acrylates the size need to be below the renal threshold ensuring that it is not accumulated in the body. On the other hands, if the polymer is degradable (e.g. polyesters), the toxicity and/or the immune response of the degradation products have to be considered as well.⁹⁰ When the polymer is a drug itself, it is a new chemical entity and has to be assessed as such.

Various types of systems have been developed to achieve controlled parental and peroral drug delivery or targeting to specific tissues. Colloidal drug carriers are in the

range between 10-600 nm, and include: liposomes, emulsions, micelles, vesicle, liquid crystal, micro and nanoparticles.

Polymeric nanoparticles refer to those nanocarriers prepared using polymers, i.e., nanocapsules and nanospheres. Nanoparticles have the advantage of being able to cross the membrane barriers, particularly in the absorptive epithelium of the small intestine.⁸⁵ These drug carriers are interesting since small diameter particles have a large relative surface area. Particles 200 nm or greater in diameter can be cleared from the circulatory system faster.⁸⁵

Figure 5 shows a schematic representation for the most used polymeric nanoparticles in drug delivery. A nanocapsule (NC) has a vesicular structure, composed of a central oily core surrounded by a thin polymer wall, whereas a nanosphere (NS) only consists of a polymer matrix. A nanoemulsion (NE), also used as nanocarrier, is prepared without polymer. NC, NS, and NE are stabilized by surfactants at the interface particle/water, preventing particle agglomeration and/or drug leakage. Theoretically nanocapsules are superior to nanoemulsions because the polymer shell protects the encapsulated drug against the outer environment, thus, degradation is minimized. Comparing NC versus NS, the former one have the advantages over the NS of their low polymer content and a high loading capacity for lipophilic drugs.⁹¹

These colloidal systems mentioned above can be prepared either by (i) polymerization of the dispersed monomers, so called interfacial polymerization, or (ii) using pre-formed polymers, with so called nanoprecipitation, also called interfacial deposition,^{92, 93} solvent evaporation,⁹⁴ or emulsion-diffusion techniques.⁹⁵ Since, each method offers advantages and disadvantages, a detailed explanation of each one is not within the scope of this introduction; for this reason only the two more important and most common used method are explained.

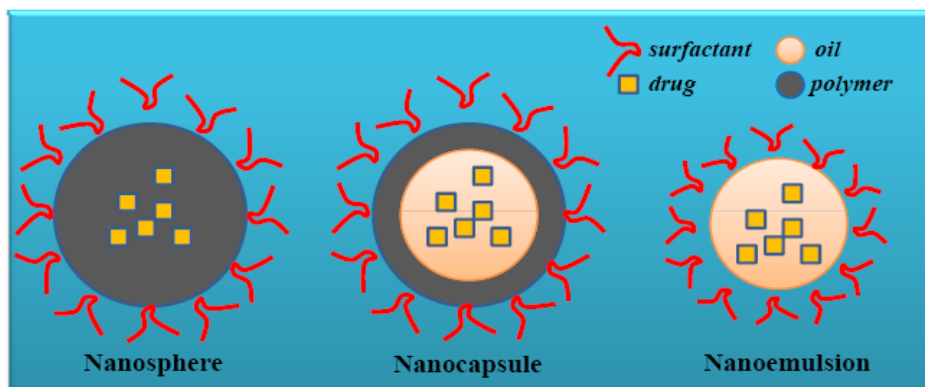


Figure 5. Schematic representation of polymeric nanoparticles used for drug delivery systems.

Biodegradable nanocapsules obtained by interfacial polymerization of alkyl α -cyanoacrylate monomers have been commonly used. This preparation method was developed by Al Khouri.⁹⁶⁻⁹⁹ Briefly, the cyanoacrylate monomer is polymerized together with the lipophilic drug. Both, monomer and drug are previously dissolved in a mixture of oil and lipophilic solvent (such as ethanol). The mixture contains the drug either in dissolved or dispersed form. It is then slowly added to a non-ionic surfactant aqueous solution. Due to the large excess of the lipophilic solvent, the oil phase is finely dispersed in the aqueous phase, and the monomer is polymerized at the oil/water interphase, and nanocapsules with oily core are formed. But, the presence of residual monomers or oligomers or reagent from the polymerization as well as cross-reaction between the content of the nanocapsules, especially the drug molecules and the acrylic monomer¹⁰⁰ might limit the potential use of the nanocapsules. This problem was overcome by Fessi by means of interfacial deposition of preformed polymers.⁹³

Among the other methods to obtain nanocapsules using preformed polymer, interfacial deposition is nowadays one of the employed methods, because it is one of the simplest and most advantageous one, which allows using several biodegradable polymers, resulting in nanoparticles with well-defined shape and particle size. Figure 6 shows a schematic representation of nanoparticles preparation. By this method, nanocapsules are formed instantaneously by the fast diffusion of a water-miscible solvent (such as acetone) containing the polymer, the lipophilic drug, oil (with or without a lipophilic surfactant) into an aqueous phase containing a hydrophilic surfactant under moderate magnetic stirring.

The formation of the nanocapsule is explained by the interfacial turbulence generated during the fast diffusion of the water-soluble solvent in water which also provides the energy for oil droplet formation. Once the solvent diffusion is complete, the polymer aggregates around the oil droplets. The aqueous phase becomes milky with bluish opalescence yielding in one step nanocapsules with a spherical vesicular shape consisting of an oily core (where the drug is solubilized) surrounded by a thin wall of polymer deposited at the interphase.^{101, 102}

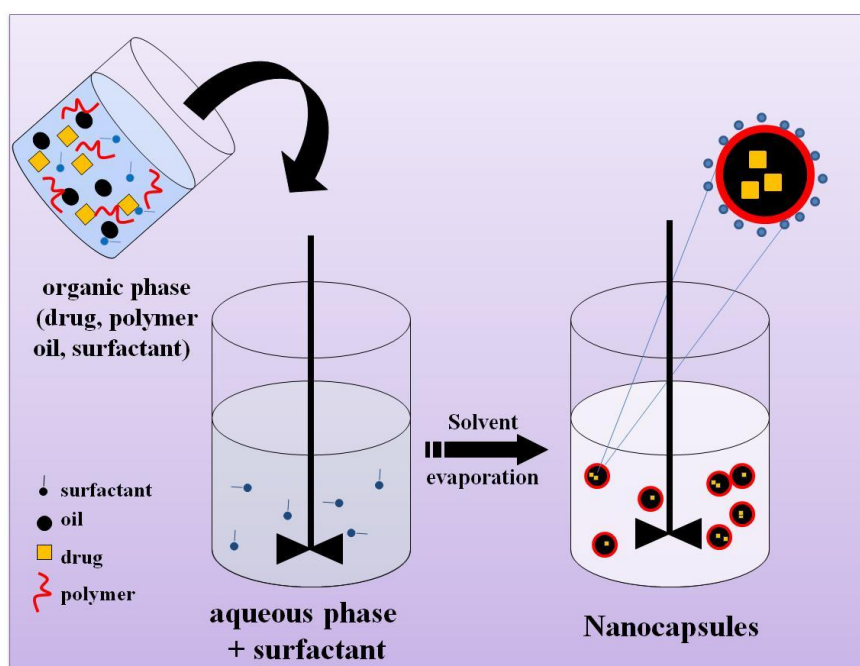


Figure 6. Schematic representation of nanocapsule preparation via interfacial nanoprecipitation.

1.3.3 Clearance and Opsonization

The body defense system reacts once that a foreign particle is introduced. Since, a pharmaceutical nanocarrier is a foreign body an opsonization and clearance process begins in order to remove it prior to completion of its function. Thus, “basic” function of any nanocarrier is its longevity in the body.⁸⁹ The body distributes nutrients, clears waste, and distributes systematically administered drugs via the vascular and lymphatic system. Intravenously injected particles are scavenged and cleared from the circulation by so-called Kupffer cells and macrophages in a process that is facilitated by surface deposition of

blood opsonic factor and complement proteins on the injected drug particle.⁸⁵ The opsonization is the process by which bacteria (or other foreign cells) are altered by so-called opsonins (antibodies in blood serum) to make them more susceptible to the action of phagocytes.

The clearance pharmacokinetics and behavior and tissue distribution of a drug carrier orally or intravenously administered are greatly influenced by its size and surface characteristic.^{85, 103, 104} On exposure to the blood, particles of different surface characteristic, size and morphology attract different arrays of opsonins as well as another plasma proteins, which may be taken into account for the different pattern in the rate and site of the particle clearance from the vasculature.¹⁰³ Understanding how the human body clears particles is vital to develop a nanocarrier that target not only a relevant macrophage population but also to engineer a long-circulating or macrophage-evading particles.^{85, 103}

To overcome the recognition by the mononuclear phagocyte system formulations “invisible” to macrophages have been developed. Coating the nanoparticles with a hydrophilic shell such as poly(ethyleneglycol) (PEG) suppress macrophage recognition by reducing protein adsorption and surface opsonization.^{105, 106} This evasion prolongs the circulation of the nanoparticles allowing a controlled release of the therapeutics in the blood.⁸⁵ There are a vast amount of research work focused to the better understanding of the PEG coating to extent the particle blood circulation. Also copolymers based PEG and polylactide-glycol (PEG-PLAGA) have been prepared for long-circulating particles, and experiments in BALB/c mice have demonstrated that protective effect of PEG depends on the content of this block.^{89, 107} Clearance and liver accumulation patterns reveal that the higher content of PEG blocks, the lower the clearance and the better the protection from the liver uptake.⁸⁹ Even when hydrophilicity has been considered as the main requirement, it is not sufficient. It has been proposed^{108, 109} that chain flexibility is also necessary to provide long-circulating particles. The different conformations that PEG block can adopt due to its transient, flexibility and rapidly changing structure, the immune system would have difficult in modeling an antibody around it.¹¹⁰

1.3.4 Other drug nanocarrier formulations.

The administration route is a very important parameter as the drug itself for the therapeutic success. New formulations have to enhance the circulation time in the body, to avoid opsonization and macrophages recognition, to cross a particular physical barrier or even to find an alternative for the drug delivery of the new generation protein-based different that the peroral one, where drug degradation can occur during its transit along the gastrointestinal tract. In this sense, nanotechnology is opening new therapeutic opportunities for agents that cannot be used effectively as conventional drug formulations due to poor bioavailability or drug instability. The choice of the administration route is driven mainly by patient acceptability, drug properties, access to the disease location or effectiveness in dealing with the specific disease. The most frequently used one is the peroral route (oral administration), but certain numbers of drugs (as protein- and peptide-based) do not easily cross the mucosal surfaces and biological membranes.¹¹¹ However, it is still the most intensively investigated because it offers the advantages of convenience and cheapness of administration and potential manufacturing cost savings. On the other hands, parenteral routes, i.e., intravenous, intramuscular and subcutaneous, are very important but more invasive than peroral (and transdermal) drug administration. Nanoscale drug carriers have a great potential for improving the delivery of drugs through nasal and sublingual routes, both of which avoid first-pass metabolism; and for difficult-access ocular, brain and intra-articular cavities.

The type of the release is also important for the therapeutic success of the drug delivery. It can be sustained (or continues) or pulsed. Sustained release¹¹² of the drug involves polymeric nanocarriers which release the drug at controlled rate, by diffusion out of the polymer or by degradation of the polymer over the time. Pulsed, highly preferred, mimics closely the way as the body naturally produces hormones like insulin. The drug is released rapidly within a short period of time, as a result of a biological or external trigger, after a specific lag time.¹¹³ It can be achieved using polymers which respond to specific stimuli, e.g., exposure to the light, changes in the pH or temperature.¹¹⁴

1.3.5 How is the drug released?

A central physical characteristic of the drug carrier systems is the drug release profile, which in its most fundamental form is the fraction of drug released from the disperse system as a function of the time after the system has been administered. This release can be driven by a number of processes, the most important one being:¹¹⁴

1. The drug may diffuse out of the carrier by diffusion in the solid matrix. This process is negligibly slow for macroscopic delivery systems, but can be fast for submicron carriers. Diffusion in solid is characterized by diffusion coefficients of 10^{-18} to 10^{-20} m²/s or less, resulting in release time of the order of hours or minutes for a particle with a diameter in the hundred nanometer range. The carrier retains its structural integrity in this situation. This process can be seen as a perturbation of partition equilibrium, before dilution the carrier is dispersed in a small volume of continuous phase and the drug is partitioned between the carrier phase, $[D]_{\text{part}}$, and the continuous phase, $[D]_{\text{cont}}$, being $[D]$ = drug concentration. On dilution the drug will diffuse out of the carrier until the partition equilibrium is re-established, as shown in the Figure 7. The rates of the forward (k_f) and reverse (k_r) processes may be functions of concentration and time, and need not to be first order. If the degree of dilution is large, $[D]_{\text{cont}}$ will be small, and the drug will partition largely into the aqueous phase. At infinite dilution $[D]_{\text{cont}}$ be zero and so the reverse rate will be zero. If the degree of dilution is large the drug will leave the carrier completely and accumulate in the continuous phase (although at zero concentration). The rate at which this occurs will be $k_f[D]_{\text{cont}}$. The theoretical situation of infinite dilute is known as a perfect sink (although perfect sink conditions are never attainable in practice). The kinetics of the release is determined only by the drug-carrier interaction, and is not influenced by the drug in the sink medium.
2. The solvent may penetrate the microparticle and dissolve the drug, which then diffuses out in solution. The solvent may gain entry by percolation through pores, or hydration of the particle.
3. The carrier may be degraded or dissolved by its surroundings, the drug being sufficiently immobile to diffuse from the carrier over the same timescale. In this case the accumulation of drug in the continuous phase follows the degradation of the carrier.

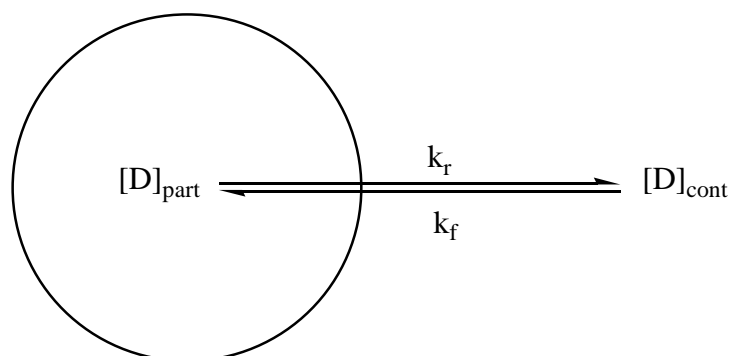


Figure 7. Diffusion equilibrium of drug between particle and continuous phase. Figure taken from [115].

Objective of this Thesis

The main objective of this thesis is to evaluate the behavior of amphiphilic diblock copolymers, commonly used in aqueous applications, to develop (i) novel interpolyelectrolyte complexes in a low polarity organic solvent, traditionally performed in aqueous media, and (ii) to formulate novel vesicular nanocarriers for drug encapsulation.

Due to the well known interest on polyelectrolyte complexation, the method here employed allowed to synthesize in organic media materials substantially water-free with novel nanoarchitectures that can be practically fully dried from a volatile organic solvent to form highly porous powders, which may be interesting, for instance, for design of novel separation membranes.

Moreover, the investigations of amphiphilic diblock copolymers in the field of pharmaceutical applications are mostly focused in the properties of these polymers to self-assemble to form micelles that can be loaded with a therapeutic agent. Here, we are interested in using these copolymers to design a novel nanocontainer to load melatonin. To attempt this objective, interfacial deposition in water is employed to successfully obtain well nanostructured particles.

References

1. Wang, J.-L.; Grimaud, T.; Matyjaszewski, K., Kinetic Study of the Homogeneous Atom Transfer Radical Polymerization of Methyl Methacrylate. *Macromolecules* **1997**, 30, (21), 6507-6512.
2. Chen, X.-P.; Qiu, K.-Y., Synthesis of Well-Defined Polystyrene by Radical Polymerization Using 1,1,2,2-Tetraphenyl-1,2-ethanediol/FeCl₃/PPh₃ Initiation System. *Journal of Applied Polymer Science* **2000**, 77, 1607-1613.
3. Matyjaszewski, K.; Davis, K.; Patten, T. E.; Wei, M., Observation and Analysis of a Slow Termination Process in the Atom Transfer Radical Polymerization of Styrene. *Tetrahedron* **1997**, 53, (45), 15321-15329.
4. Odian, G., *Principles of Polymerization*. Fourth ed.; Wiley-Interscience: New York, **2004**.
5. Wang, J.-S.; Matyjaszewski, K., Controlled/"Living" Radical Polymerization. Atom Transfer Radical Polymerization in the Presence of Transition-Metal Complexes. *Journal of the American Chemical Society* **1995**, 117, (20), 5614-5615.
6. Matyjaszewski, K.; Xia, J., Atom Transfer Radical Polymerization. *Chemical Reviews* **2001**, 101, (9), 2921-2990.
7. Mayadunne, R. T. A.; Rizzardo, E.; Chiefari, J.; Chong, Y. K.; Moad, G.; Thang, S. H., Living Radical Polymerization with Reversible Addition-Fragmentation Chain Transfer (RAFT Polymerization) Using Dithiocarbamates as Chain Transfer Agents. *Macromolecules* **1999**, 32, (21), 6977-6980.
8. Chiefari, J.; Chong, Y. K.; Ercole, F.; Krstina, J.; Jeffery, J.; Le, T. P. T.; Mayadunne, R. T. A.; Meijs, G. F.; Moad, C. L.; Moad, G.; Rizzardo, E.; Thang, S. H., Living Free-Radical Polymerization by Reversible Addition-Fragmentation Chain Transfer: The RAFT Process. *Macromolecules* **1998**, 31, (16), 5559-5562.
9. Hawker, C. J.; Bosman, A. W.; Harth, E., New Polymer Synthesis by Nitroxide Mediated Living Radical Polymerizations. *Chemical Reviews* **2001**, 101, (12), 3661-3688.

10. Matyjaszewski, K.; Davis, T. P.; Ed., Handbook of Radical Polymerization. *Handbook of Radical Polymerization*. Wiley-Interscience: New York. **2002**.
11. Fischer, H., The Persistent Radical Effect in "Living" Radical Polymerization. *Macromolecules* **1997**, 30, (19), 5666-5672.
12. Fischer, H., The Persistent Radical Effect in Controlled Radical Polymerizations. *Journal of Polymer Science: Part A: Polymer Chemistry* **1999**, 37, (13), 1885-1901.
13. Shipp, D. A.; Matyjaszewski, K., Kinetic Analysis of Controlled/"Living" Radical Polymerizations by Simulations. 1. The Importance of Diffusion-Controlled Reactions. *Macromolecules* **1999**, 32, (9), 2948-2955.
14. Matyjaszewski, K., The Importance of Exchange Reactions in Controlled/Living Radical Polymerization in the Presence of Alkoxyamines and Transition Metals. *Macromolecular Symposia* **1996**, 111, (1), 47-61.
15. Al-Harhi, M.; Sardashti, A.; Soares, J. B. P.; Simon, L. C., Atom Transfer Radical Polymerization (ATRP) of Styrene and Acrylonitrile with Monofunctional and Bifunctional Initiators. *Polymer* **2007**, 48, (7), 1954-1961.
16. Percec, V.; Barboiu, B., "Living" Radical Polymerization of Styrene Initiated by Arenesulfonyl Chlorides and CuI(bpy)_nCl. *Macromolecules* **1995**, 28, (23), 7970-7972.
17. Magenau, A. J. D.; Kwak, Y.; Matyjaszewski, K., ATRP of Methacrylates Utilizing CuIIX₂/L and Copper Wire. *Macromolecules* **2010**, 43, (23), 9682-9689.
18. Grimaud, T.; Matyjaszewski, K., Controlled/"Living" Radical Polymerization of Methyl Methacrylate by Atom Transfer Radical Polymerization. *Macromolecules* **1997**, 30, (7), 2216-2218.
19. Teodorescu, M.; Matyjaszewski, K., Atom Transfer Radical Polymerization of (Meth)Acrylamides. *Macromolecules* **1999**, 32, (15), 4826-4831.
20. Xia, Y.; Yin, X.; Burke, N. A. D.; Stöver, H. D. H., Thermal Response of Narrow-Disperse Poly(N-isopropylacrylamide) Prepared by Atom Transfer Radical Polymerization. *Macromolecules* **2005**, 38 (14), 5937-5943.

21. Matyjaszewski, K.; Jo, S. M.; Paik, H.-j.; Shipp, D. A., An Investigation into the CuX/2,2'-Bipyridine (X = Br or Cl) Mediated Atom Transfer Radical Polymerization of Acrylonitrile. *Macromolecules* **1999**, 32, (20), 6431-6438.
22. Matyjaszewski, K.; Jo, S. M.; Paik, H.-j.; Gaynor, S. G., Synthesis of Well-Defined Polyacrylonitrile by Atom Transfer Radical Polymerization. *Macromolecules* **1997**, 30, (20), 6398-6400.
23. Patten, T. E.; Matyjaszewski, K., Atom-Transfer Radical Polymerization and the Synthesis of Polymeric Materials. *Advanced Materials* **1998**, 10, (12), 901-915.
24. Matyjaszewski, K., Transition Metal Catalysis in Controlled Radical Polymerization: Atom Transfer Radical Polymerization. *Chemistry - A European Journal* **1999**, 5, (11), 3095-3102.
25. Mori, H.; Chan Seng, D.; Lechner, H.; Zhang, M.; Müller, A. H. E., Synthesis and Characterization of Branched Polyelectrolytes 1. Preparation of Hyperbranched Poly(acrylic acid) via Self-Condensing Atom Transfer Radical Copolymerization. *Macromolecules* **2002**, 35, (25), 9270-9281.
26. Davis, K. A.; Charleux, B.; Matyjaszewski, K., Preparation of Block Copolymers of Polystyrene and Poly(t-butyl acrylate) of Various Molecular Weights and Architectures by Atom Transfer Radical Polymerization. *Journal of Polymer Science Part A: Polymer Chemistry* **2000**, 38, (12), 2274-2283.
27. Davis, K. A.; Matyjaszewski, K., Atom Transfer Radical Polymerization of tert-Butyl Acrylate and Preparation of Block Copolymers. *Macromolecules* **2000**, 33, (11), 4039-4047.
28. Davis, K.; O'Malley, J.; Paik, H.-J.; Matyjaszewski, K., Effect of the Counteranion in Atom Transfer Radical Polymerization Using Alkyl (Pseudo)Halide Initiators. *Polymer Preprints (American Chemical Society, Division of Polymer Chemistry)* **1997**, 38, (1), 687-688.
29. Matyjaszewski, K.; Paik, H.-j.; Zhou, P.; Diamanti, S. J., Determination of Activation and Deactivation Rate Constants of Model Compounds in Atom Transfer Radical Polymerization. *Macromolecules* **2001**, 34, 5125-5131.

30. Goto, A.; Fukuda, T., Determination of the Activation Rate Constants of Alkyl Halide Initiators for Atom Transfer Radical Polymerization. *Macromolecular Rapid Communications* **1999**, 20, (12), 633-636.
31. Matyjaszewski, K.; Göbelt, B.; Paik, H.-j.; Horwitz, C. P., Tridentate Nitrogen-Based Ligands in Cu-Based ATRP: A Structure-Activity Study. *Macromolecules* **2001**, 34, 430-440.
32. Matyjaszewski, K.; Davis, K.; Patten, T. E.; Wei, M., Observation and Analysis of a Slow Termination Process in the Atom Transfer Radical Polymerization of Styrene. *Tetrahedron* **1997**, 53, (45), 15321-15329.
33. Matyjaszewski, K.; Wei, M.; Xia, J.; McDermott, N. E., Controlled/"Living" Radical Polymerization of Styrene and Methyl Methacrylate Catalyzed by Iron Complexes. *Macromolecules* **1997**, 30, (26), 8161-8164.
34. Takahashi, H.; Ando, T.; Kamigaito, M.; Sawamoto, M., Half-Metallocene-Type Ruthenium Complexes as Active Catalysts for Living Radical Polymerization of Methyl Methacrylate and Styrene. *Macromolecules* **1999**, 32, (11), 3820-3823.
35. Uegaki, H.; Kotani, Y.; Kamigaito, M.; Sawamoto, M., NiBr₂(Pn-Bu₃)₂-Mediated Living Radical Polymerization of Methacrylates and Acrylates and Their Block or Random Copolymerizations. *Macromolecules* **1998**, 31, (20), 6756-6761.
36. Lecomte, P.; Drapier, I.; Dubois, P.; Teyssie, P.; Jerome, R., Controlled Radical Polymerization of Methyl Methacrylate in the Presence of Palladium Acetate, Triphenylphosphine, and Carbon Tetrachloride. *Macromolecules* **1997**, 30, (24), 7631-7633.
37. Wang, J.-S.; Matyjaszewski, K., Controlled/"Living" Radical Polymerization. Halogen Atom Transfer Radical Polymerization Promoted by a Cu(I)/Cu(II) Redox Process. *Macromolecules* **1995**, 28, (23), 7901-7910.
38. Matyjaszewski, K.; Patten, T. E.; Xia, J., Controlled/"Living" Radical Polymerization. Kinetics of the Homogeneous Atom Transfer Radical Polymerization of Styrene. *Journal of the American Chemical Society* **1997**, 119, (4), 674-680.

39. Qiu, J.; Matyjaszewski, K., Polymerization of Substituted Styrenes by Atom Transfer Radical Polymerization. *Macromolecules* **1997**, 30, (19), 5643-5648.
40. Percec, V.; Barboiu, B.; Neumann, A.; Ronda, J. C.; Zhao, M., Metal-Catalyzed "Living" Radical Polymerization of Styrene Initiated with Arenesulfonyl Chlorides. From Heterogeneous to Homogeneous Catalysis. *Macromolecules* **1996**, 29, (10), 3665-3668.
41. Uegaki, H.; Kotani, Y.; Kamigaito, M.; Sawamoto, M., Nickel-Mediated Living Radical Polymerization of Methyl Methacrylate. *Macromolecules* **1997**, 30, (8), 2249-2253.
42. Schwarz, H. H.; Richau, K.; Paul, D., Membranes from Polyelectrolyte Complexes. *Polymer Bulletin* **1991**, 25, (1), 95-100.
43. Michaels, A. S.; Mir, L.; Schneider, N. S., A Conductometric Study of Polycation--Polyanion Reactions in Dilute Aqueous Solution. *The Journal of Physical Chemistry* **1965**, 69, (5), 1447-1455.
44. Michael, A. S.; Miekka, R. G., Polycation-Polyanion complexes: Preparation and Properties of Poly(vinylbenzyltrimethylammonium) Poly(styrenesulfonate). *The Journal of Physical Chemistry* **1961**, 65, (10), 1765-1773.
45. Yu, X.; Somasundaran, P., Enhanced Flocculation With Double Flocculants. *Colloids and Surfaces, A: Physicochemical and Engineering Aspects* **1993**, 81, (1-3), 17-23.
46. Petzold, G.; Nebel, A.; Buchhammer, H. M.; Lunkwitz, K., Preparation and Characterization of Different Polyelectrolyte Complexes and their Application as Flocculants. *Colloid and Polymer Science* **1998**, 276, (2), 125-130.
47. Dragan, S.; Dragan, D.; Cristea, M.; Airinei, A.; Ghimici, L., Polyelectrolyte Complexes. II. Specific Aspects of the Formation of Polycation/dye/Polyanion Complexes. *Journal of Polymer Science, Part A: Polymer Chemistry* **1999**, 37, (4), 409-418.
48. Decher, G., Fuzzy Nanoassemblies: Toward Layered Polymeric Multicomposites. *Science* **1997**, 277, (5330), 1232-1237.

49. Yoshida, K.; Sato, K.; Anzai, J., Layer-by-Layer Polyelectrolyte Films Containing Insulin for pH-Triggered Release. *Journal of Materials Chemistry* **2010**, 20, (8), 1546-1552.
50. Weiyong, Y.; Zhisong, L.; Chang, M. L., Controllably Layer-by-Layer Self-Assembled Polyelectrolytes/Nanoparticle Blend Hollow Capsules and their Unique Properties. *Journal of Materials Chemistry* **2011**, 21, (13), 5148-5155.
51. Trinh, C. K.; Schnabel, W., Polyelectrolyte Complexes of Binary and Ternary Systems Containing Poly(sodium styrene sulfonate), Poly(sodium phosphate), and Poly(N-ethyl-4-vinylpyridinium bromide). *Angewandte Makromolekulare Chemie* **1994**, 221, (1), 127-35.
52. Yu, J.; Liu, H.; Chen, J., Flocculation and Characterization of Protein by Anionic Copolymer Containing Reactive Functional Groups. *Colloids and Surfaces, A: Physicochemical and Engineering Aspects* **2000**, 163, (2), 225-232.
53. Pommersheim, R.; Schrezenmeir, J.; Vogt, W., Immobilization of Enzymes by Multilayer Microcapsules. *Macromolecular Chemistry and Physics* **1994**, 195, (5), 1557-1567.
54. General, S.; Rudloff, J.; Thünemann, A. F., Hollow Nanoparticles Via Stepwise Complexation and Selective Decomplexation of Poly(ethylene imine). *Chemical Communications* **2002**, (5), 534-535.
55. Gittins, D. I.; Caruso, F., Multilayered Polymer Nanocapsules Derived from Gold Nanoparticle Templates. *Advanced Materials* **2000**, 12, (24), 1947-1949.
56. Antipov, A. A.; Sukhorukov, G. B., Polyelectrolyte Multilayer Capsules as Vehicles with Tunable Permeability. *Advances in Colloid and Interface Science* **2004**, 111, (1-2), 49-61.
57. Moustafine, R. I.; Salachova, A. R.; Frolova, E. S.; Kemenova, V. A.; Van den Mooter, G., Interpolyelectrolyte Complexes of Eudragit® E PO with Sodium Alginate as Potential Carriers for Colonic Drug Delivery: Monitoring of Structural Transformation and Composition Changes During Swellability and Release Evaluating. *Drug Development and Industrial Pharmacy* **2009**, 35, (12), 1439-1451.

58. Said, A. E.-H. A., Radiation Synthesis of Interpolymer Polyelectrolyte Complex and Its Application as a Carrier for Colon-Specific Drug Delivery System. *Biomaterials* **2005**, 26, (15), 2733-2739.
59. Kabanov, A. V.; Kabanov, V. A., Interpolyelectrolyte and Block Ionomer Complexes for Gene Delivery: Physico-Chemical Aspects. *Advanced Drug Delivery Reviews* **1998**, 30, (1-3), 49-60.
60. Munier, S.; Messai, I.; Delair, T.; Verrier, B.; Ataman-Oenal, Y., Cationic PLA nanoparticles for DNA delivery: Comparison of three surface polycations for DNA binding, protection and transfection properties. *Colloids and Surfaces, B: Biointerfaces* **2005**, 43, (3-4), 163-173.
61. Wakebayashi, D.; Nishiyama, N.; Yamasaki, Y.; Itaka, K.; Kanayama, N.; Harada, A.; Nagasaki, Y.; Kataoka, K., Lactose-Conjugated Polyion Complex Micelles Incorporating Plasmid DNA as a Targetable Gene Vector System: Their Preparation and Gene Transfecting Efficiency Against Cultured HepG2 cells *Journal of Controlled Release* **2004**, 95, (3), 653-664.
62. Van de Wetering, P.; Cherng, J.-Y.; Talsma, H.; Crommelin, D. J. A.; Hennink, W. E., 2-(dimethylamino)ethyl methacrylate Based (Co)Polymers as Gene Transfer Agents. *Journal of Controlled Release* **1998**, 53, (1-3), 145-153.
63. Leong, K. W.; Mao, H.-Q.; Truong-Le, V. L.; Roy, K.; Walsh, S. M.; August, J. T., DNA-Polycation Nanospheres as Non-Viral Gene Delivery Vehicles. *Journal of Controlled Release* **1998**, 53, (1-3), 183-193.
64. Synatschke, C. V.; Schacher, F. H.; Förtsch, M.; Drechsler, M.; Müller, A. H. E., Double-Layered Micellar Interpolyelectrolyte Complexes - How Many Shells to a Core? *Soft Matter* **2011**, 7, (5), 1714-1725.
65. Iliopoulos, I.; Audebert, R., Complexation of Acrylic Acid Copolymers with Polybases: Importance of Cooperative Effects. *Macromolecules* **1991**, 24, (9), 2566 - 2575.
66. Kiriy, A.; Yu, J.; Stamm, M., Interpolyelectrolyte Complexes: A Single-Molecule Insight. *Langmuir* **2006**, 22, (4), 1800-1803.

67. Yancheva, E.; Paneva, D.; Maximova, V.; Mespouille, L.; Dubois, P.; Manolova, N.; Rashkov, I., Polyelectrolyte Complexes between (Cross-linked) N-Carboxyethylchitosan and (Quaternized) Poly[2-(dimethylamino)ethyl methacrylate]: Preparation, Characterization, and Antibacterial Properties. *Biomacromolecules* **2007**, *8*, (3), 976-984.
68. Pergushov, D. V.; Remizova, E. V.; Feldthusen, J.; Zezin, A. B.; Müller, A. H. E.; Kabanov, V. A., Novel Water-Soluble Micellar Interpolyelectrolyte Complexes. *Journal of Physical Chemistry B* **2003**, (107), 8093-8096.
69. Pergushov, D. V.; Remizova, E. V.; Gradzielski, M.; Lindner, P.; Feldthusen, J.; Zezin, A. B.; Müller, A. H. E.; Kabanov, V. A., Micelles of Polyisobutylene-block-Poly(methacrylic acid) Diblock Copolymers and their Water-Soluble Inter-Polyelectrolyte Complexes Formed with Quaternized Poly(4-vinylpyridine). *Polymer* **2004**, *45*, (2), 367-378.
70. Voets, I. K.; de Keizer, A.; Stuart, M. A. C.; Justynska, J.; Schlaad, H., Irreversible Structural Transitions in Mixed Micelles of Oppositely Charged Diblock Copolymers in Aqueous Solution. *Macromolecules (Washington, DC, United States)* **2007**, *40*, (6), 2158-2164.
71. Voets, I. K.; de Keizer, A.; de Waard, P.; Frederik, P. M.; Bomans, P. H. H.; Schmalz, H.; Walther, A.; King, S. M.; Leermakers, F. A. M.; Cohen Stuart, M. A., Double-Faced Micelles From Water-Soluble Polymers. *Angewandte Chemie, International Edition* **2006**, *45*, (40), 6673-6676.
72. Philipp, B.; Dautzenberg, H.; Linow, K.-J.; Kötz, J.; Dawydoff, W., Polyelectrolyte Complexes — Recent Developments and Open Problems *Progress in Polymer Science* **1989**, *14*, (1), 91-172.
73. Holappa, S.; Kantonen, L.; Andersson, T.; Winnik, F.; Tenhu, H., Overcharging of Polyelectrolyte Complexes by the Guest Polyelectrolyte Studied by Fluorescence Spectroscopy. *Langmuir* **2005**, *21*, (24), 11431-11438.

74. Colfen, H., Double-Hydrophilic Block Copolymers: Synthesis and Application as Novel Surfactants and Crystal Growth Modifiers. *Macromolecular Rapid Communications* **2001**, 22, (4), 219-252.
75. Kabanov, A. V.; Bronich, T. K.; Kabanov, V. A.; Yu, K.; Eisenberg, A., Soluble Stoichiometric Complexes from Poly(N-ethyl-4-vinylpyridinium) Cations and Poly(ethylene oxide)-block-polymethacrylate Anions. *Macromolecules* **1996**, 29, (21), 6797-6802.
76. Gohy, J.-F.; Varshney, S. K.; Jerome, R., Water-Soluble Complexes Formed by Poly(2-vinylpyridinium)-block-poly(ethylene oxide) and Poly(sodium methacrylate)-block-poly(ethylene oxide) Copolymers. *Macromolecules* **2001**, 34, (10), 3361-3366.
77. Katayose, S.; Kataoka, K., Water-Soluble Polyion Complex Associates of DNA and Poly(ethylene glycol)-Poly(L-lysine) Block Copolymer. *Bioconjugate Chemistry*. **1997**, 8, (5), 702 - 707.
78. Gohy, J.-F., Block Copolymer Micelles. *Advances in Polymer Science. Block Copolymers II*. **2005**, 190, 65-136.
79. Gillies, E. R.; Fréchet, J. M. J., Development of Acid-Sensitive Copolymer Micelles for Drug Delivery. *Pure and Applied Chemistry* **2004**, 76, (7-8), 1295–1307.
80. Bakeev, K. N.; Shu, Y. M.; Zezin, A. B.; Kabanov, V. A.; Lezov, A. V.; Mel'nikov, A. B.; Kolomiets, I. P.; Rjuntsev, E. I.; MacKnight, W. J., Structure and Properties of Polyelectrolyte-Surfactant Nonstoichiometric Complexes in Low-Polarity Solvents. *Macromolecules* **1996**, 29, (4), 1320-1325.
81. Bakeev, K. N.; Shu, Y. M.; MacKnight, W. J.; Zezin, A. B.; Kabanov, V. A., A novel Ttype of Ionomer Based on a NonStoichiometric Polyelectrolyte-Surfactant Complex. *Macromolecules* **1994**, 27, (1), 300-302.
82. Sergeyev, V. G.; Pyshkina, O. A.; Lezov, A. V.; Mel'nikov, A. B.; Ryumtsev, E. I.; Zezin, A. B.; Kabanov, V. A., DNA Complexed with Oppositely Charged Amphiphile in Low-Polar Organic Solvents. *Langmuir* **1999**, 15, (13), 4434-4440.

83. Lokshin, N. A.; Sergeyev, V. G.; Zezin, A. B.; Golubev, V. B.; Levon, K.; Kabanov, V. A., Polyaniline-Containing Interpolymer Complexes Synthesized in Low-Polar Organic Media. *Langmuir* **2003**, 19, (18), 7564-7568.
84. Pergushov, D. V.; Remizova, E. V.; Zezin, A. B.; Kabanov, V. A., Interpolyelectrolyte Complex Formation is Possible in Low-Polarity Organic Media. *Doklady Physical Chemistry* **2006**, 406, (Part 2), 38-42.
85. Sergeyev, V. G.; Pyshkina, O. A.; Gallyamov, M. O.; Yaminsky, I. V.; Zezin, A. B.; Kabanov, V. A., DNA-Surfactant Complexes in Organic Media. *Progress in Colloid & Polymer Science* **1997**, 106, 198-203.
86. Emerich, D. F.; Thanos, C. G., The pinpoint promise of nanoparticle-based drug delivery and molecular diagnosis. *Biomolecular Engineering* **2006**, 23, (4), 171-184.
87. Pison, U.; Welte, T.; Giersig, M.; Groneberg, D. A., Nanomedicine for Respiratory Diseases. *European Journal of Pharmacology* **2006**, 533, (1-3), 341-350.
88. Kaparissides, C.; Alexandridou, S.; Kotti, K.; Chaitidou, S., Recent Advances in Novel Drug Delivery Systems. *Journal Of Nanotechnology Online* **2006**, 2, 1-11.
89. Gao, F.; Zhang, Z.; Bu, H.; Huang, Y.; Gao, Z.; Shen, J.; Zhao, C.; Li, Y., Nanoemulsion Improves the Oral Absorption of Candesartan Cilexetil in Rats: Performance and Mechanism. *Journal of Controlled Release* **2011**, 149, (2), 168-174.
90. Torchilin, V. P., Multifunctional Nanocarriers. *Advanced Drug Delivery Reviews* **2006**, 58, (14), 1532-1555.
91. Schmaljohann, D., Thermo- and pH-Responsive Polymers in Drug Delivery. *Advanced Drug Delivery Reviews* **2006**, 58, (15), 1655-1670.
92. Limayem Blouza, I.; Charcosset, C.; Sfar, S.; Fessi, H., Preparation and Characterization of Spironolactone-Loaded Nanocapsules for Pediatric Use. *International Journal of Pharmaceutics* **2006**, 325, (1-2), 124-131.
93. Mora-Huertas, C. E.; Fessi, H.; Elaissari, A., Pharmaceutical Nanotechnology. Polymer-Based Nanocapsules for Drug Delivery. *International Journal of Pharmaceutics* **2010**, 385, (1-2), 113-142.

94. Fessi, H.; Puisieux, F.; Devissaguet, J. P.; Ammoury, N.; Benita, S., Nanocapsule Formation by Interfacial Polymer Deposition Following Solvent Displacement. *International Journal of Pharmaceutics* **1989**, 55, (1), R1-R4.
95. Desgouilles, S.; Vauthier, C.; Bazile, D.; Vacus, J.; Grossiord, J.-L.; Veillard, M.; Couvreur, P., The Design of Nanoparticles Obtained by Solvent Evaporation: A Comprehensive Study. *Langmuir* **2003**, 19, (22), 9504-9510.
96. Quintanar-Guerrero, D.; Allemann, E.; Doelker, E.; Fessi, H., A Mechanistic Study of the Formation of Polymer Nanoparticles by the Emulsification-Diffusion Technique. *Colloid and Polymer Science* **1997**, 275, (7), 640-647.
97. Couvreur, P.; Vauthier, C., Polyalkylcyanoacrylate Nanoparticles as Drug Carrier: Present State and Perspectives. *Journal of Controlled Release* **1991**, 17, (2), 187-198.
98. Dange, C.; Michel, C.; Aprahamian, M.; Couvreur, P.; Devissaguet, J. P., Nanocapsules as Carriers for Oral Peptide Delivery. *Journal of Controlled Release* **1990**, 13, (2-3), 233-239.
99. Kreuter, J., Nanoparticles - a Historical Perspective. *International Journal for Pharmaceutics* **2007**, 331, (1), 1-10.
100. Al Khouri Fallouh, N.; Roblot-Treupel, L.; Fessi, H.; Devissaguet, J. P.; Puisieux, F., Development of a New Process for the Manufacture of Poly(isobutyl cyanoacrylate) Nanocapsules. *International Journal of Pharmaceutics* **1986**, 28, (2-3), 125-132.
101. Gallardo, M. M.; Roblot-Treupel, L.; Mahuteau, J.; Genin, I.; Couvreur, P.; Plat, M.; Puisieux, F., Nanocapsules and nanospheres of alkyl cyanoacrylate. Interactions of the drug with the polymer. *Proceeding APGI, 5th. International Conference on Pharmaceutical Technology* **1989**, 4, 36-45.
102. de Faria, T. J.; Machado de Campos, A.; Senna, E. L., Preparation and Characterization of Poly(D,L-lactide) (PLA) and Poly(D,L-lactide)-Poly(ethylene glycol) (PLA-PEG) Nanocapsules Containing Antitumoral Agent Methotrexate. *Macromolecular Symposia* **2005**, 229, (Advanced Polymeric Materials), 228-233.

103. Bouchemal, K.; Briancon, S.; Perrier, E.; Fessi, H., Nano-Emulsion Formulation Using Spontaneous Emulsification: Solvent, Oil and Surfactant Optimisation. *International Journal of Pharmaceutics* **2004**, 280, (1-2), 241-251.
104. Moghimi, S. M.; Hunter, A. C.; Murray, J. C., Long-circulating and target-specific nanoparticles: Theory to practice. *Pharmacological Reviews* **2001**, 53, (2), 283-318.
105. Florence, A. T., The Oral Absorption of Micro- and Nanoparticulates: Neither Exceptional Nor Unusual. *Pharmaceutical Research* **1997**, 14, (3), 259-266.
106. Soo, P. L.; Luo, L.; Maysinger, D.; Eisenberg, A., Incorporation and Release of Hydrophobic Probes in Biocompatible Polycaprolactone-block-poly(ethylene oxide) Micelles: Implications for Drug Delivery. *Langmuir* **2002**, 18, (25), 9996-10004.
107. Hillery, A. M.; Florence, A. T., The Effect of Adsorbed Poloxamer 188 and 407 Surfactants on the Intestinal Uptake of 60-nm Polystyrene Particles After Oral Administration in the Rat. *International Journal for Pharmaceutics* **1996**, 132, (1-2), 123-130.
108. Gref, R.; Domb, A.; Quellec, P.; Blunk, T.; Mueller, R. H.; Verbavatz, J. M.; Langer, R., The Controlled Intravenous Delivery of Drugs Using PEG-coated Sterically Stabilized Nanospheres. *Advanced Drug Delivery Reviews* **1995**, 16, (2,3), 215-233.
109. Gref, R.; Minamitake, Y.; Peracchia, M. T.; Trubetskoy, V.; Torchilin, V.; Langer, R., Biodegradable long-circulating polymer nanospheres. *Science* **1994**, 263, (5153), 1600-1603.
110. Blume, G.; Cevc, G., Molecular Mechanism of the Lipid Vesicle Longevity in vivo. *Biochimica et Biophysica Acta* **1993**, 1146, (2), 157-168.
111. Woodle, M. C.; Lasic, D. D., Sterically Stabilized Liposomes. *Biochimica et Biophysica Acta* **1992**, 1113, (2), 171-199.
112. Morkhade, D. M.; Nande, V. S.; Barabde, U. V.; Patil, A. T.; Joshi, S. B., PEGylated Rosin Derivatives: Novel Microencapsulating Materials for Sustained Drug Delivery. *AAPS PharmSciTech* **2007**, 8, (2), E1-E9.

113. De Geest, B. G.; Mehuys, E.; Laekeman, G.; Demeester, J.; De Smedt, S. C., Pulsed Drug Delivery *Expert Opinion on Drug Delivery* **2006**, 3, (4), 459-462.
114. Kikuchi, A.; Okano, T., Pulsatile drug release control using hydrogels. *Advanced Drug Delivery Reviews* **2002**, 54, (1), 53-77.
115. Washington, C., Drug Release from Microdisperse Systems: a Critical Review. *International Journal for Pharmaceutics* **1990**, 58, (1), 1-12.

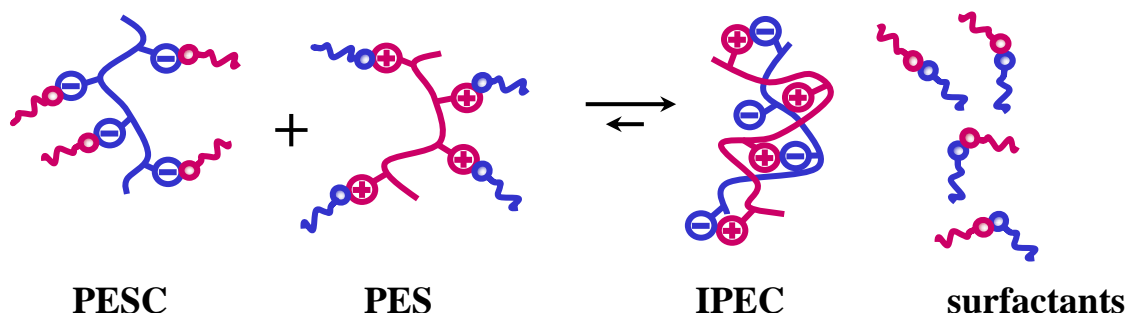
2. OVERVIEW OF THIS THESIS

The research presented in this work was focused on two areas: novel interpolyelectrolyte complexation in low polarity organic solvent and formulation of nanocapsules using diblock copolymers. The thesis consists of five chapters, three of them are articles submitted to or published in scientific journals.

Chapter 3 describes how interpolyelectrolyte complexation between two homopolyelectrolytes oppositely charged was performed in chloroform; this system served as a “model system”. The precursor of the homopolyelectrolytes, poly(*t*-butyl acrylate) (PtBA) and poly(2-(dimethylamino)ethyl methacrylate) (PDMAEMA) were synthesized via ATRP. Poly(acrylic acid) (PAA) was obtained by hydrolysis of PtBA. Interpolyelectrolyte complexation was carried out in a “*two-step*” approach. The first step is the preparation of polyelectrolyte-surfactant complexes (PESCs). This was performed by the addition of aqueous solution of surfactant to an oppositely charged polyelectrolyte at constant ionic strength (0.1M NaCl). Specifically, cetyltrimethylammonium bromide (CTAB), a cationic surfactant, was added slowly to an aqueous solution of PAA at pH = 9 until a precipitated of poly(cetyltrimethylammonium acrylate) ($PA^- CTA^+$) was formed (ratio 1:1). Analogously, sodium dodecyl sulfate (SDS), an anionic surfactant, was added to an aqueous solution of PDMAEMA to form poly[2-(methacryloylolethyl)dimethylammonium dodecyl sulfate] ($PDMAEMAQ^+ DS^-$). Both products were thoroughly washed to remove unreacted surfactant and low molecular weight salts and then dried until constant weight was reached. The second step, interpolyelectrolyte complexation, was performed by direct mixing in chloroform of two complementary PESCs as shown in

Scheme 1. Interpolyelectrolyte complexes (IPEC) are formed with the release of the surfactant counterions previously complexed with the polyelectrolytes.

Scheme 1. Schematic representation for interpolyelectrolyte complexation in low polarity organic media



The complexation was followed by turbidimetric titration and depending on the mixing ratio of PESC (Z or Z*) soluble or insoluble complexes can be formed. The values Z and Z* correspond to the molar mixing ratio, i.e., $Z = [\text{PDMAEMAQ}^+\text{DS}^-]/[\text{PA}^-\text{CTA}^+]$ and $Z^* = [\text{PA}^-\text{CTA}^+]/[\text{PDMAEMAQ}^+\text{DS}^-]$. Figure 1 shows how transmission at 500 nm decreases as Z or Z* increases indicating the formation of insoluble IPECs.

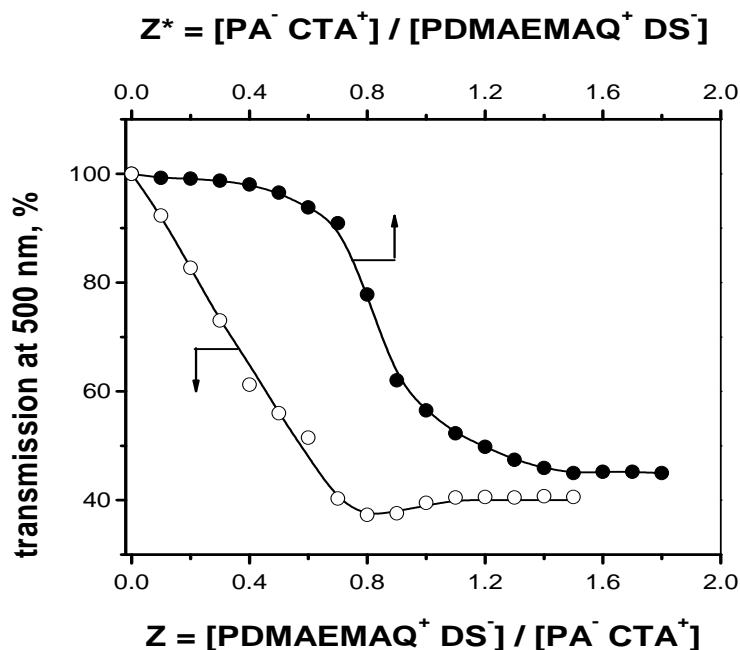


Figure 1. Turbidimetric titration curves of a chloroform solution of $\text{PA}^- \text{CTA}^+$ with a chloroform solution $\text{PDMAEMAQ}^+ \text{DS}^-$ (open circles, bottom x-axis $Z = [\text{PDMAEMAQ}^+ \text{DS}^-] / [\text{PA}^- \text{CTA}^+]$) and a chloroform solution of $\text{PDMAEMAQ}^+ \text{DS}^-$ with a chloroform solution of $\text{PA}^- \text{CTA}^+$ (solid circles, top x-axis $Z^* = [\text{PA}^- \text{CTA}^+] / [\text{PDMAEMAQ}^+ \text{DS}^-]$).

IPECs were characterized by dynamic light scattering to determine the hydrodynamic radii, and by TEM and SFM to visualize the morphology. Possible structures of the formed IPEC particles are given in the in Figure 2. Essentially, the left hand side structure resembles the so-called “surface excess” model to describe the structure of aggregated IPECs formed in aqueous media, which considers them as substantially stoichiometric IPECs whose particles are stabilized in aqueous media by charged fragments of the excess polymeric component. At the same time, vesicles (“polymersomes”) might be formed.

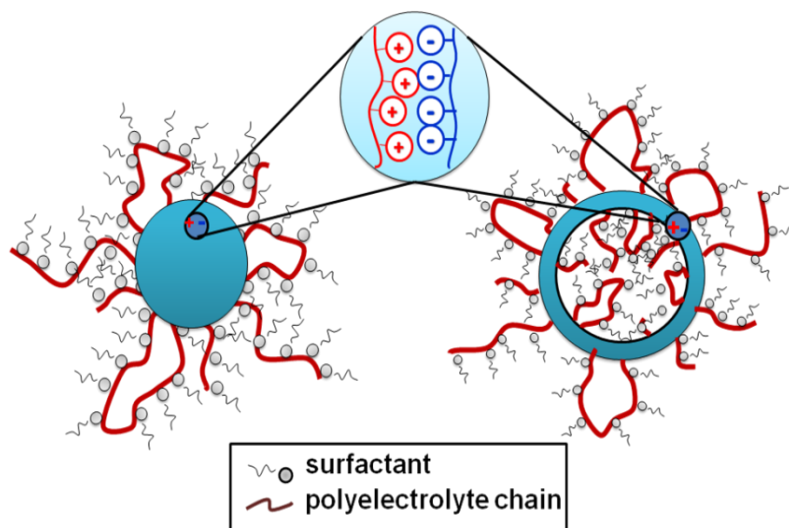


Figure 2. Schematic representation of possible structures of co-assemblies, which might form in the excess of PDMAEMAQ⁺ DS⁻.

Chapter 4 deals with (i) the synthesis of diblock copolymers polystyrene-*block*-poly(acrylic acid) (PS-*b*-PAA) via ATRP, using PS as macroinitiator for *t*-butyl acrylate (*t*BA) protected monomer and (ii) the interpolyelectrolyte complexation in chloroform of these copolymers with PDMAEMAQ⁺DS⁻. To obtain the respective polyelectrolyte, the PtBA segments were hydrolyzed to poly(acrylic acid) (PAA). The copolymers were purified and well characterized. Figure 3 shows the GPC traces of a synthesized copolymer PS-*b*-PtBA. Traces of the macroinitiator, PS, were still present in the copolymer. To remove unreacted PS, the hydrolyzed copolymers were purified using a soxhlet extraction with toluene. The purity of copolymer was verified dissolving the copolymers in THF and adding a concentrated solution of NaOH to the PAA blocks to yield poly(sodium acrylate) (PANa). In THF, reverse micelles are formed and no traces of PS macroinitiator were observed.

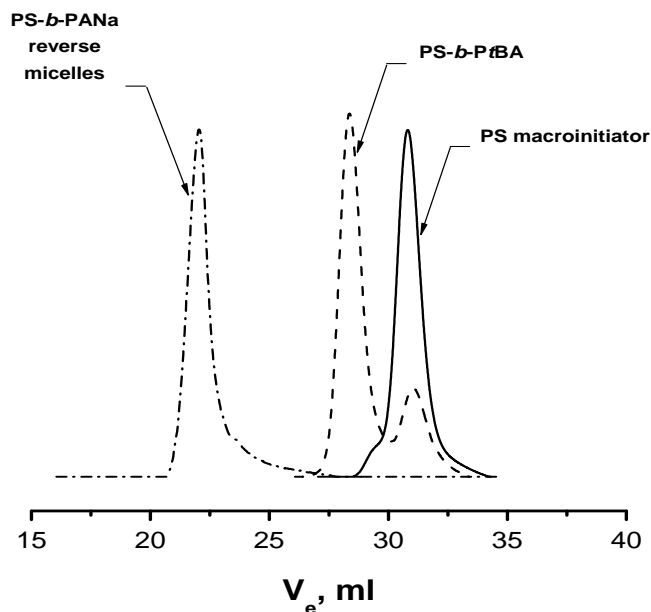


Figure 3. GPC traces of the precursor PS_{84} (—), $PS_{84}\text{-}b\text{-}PtBA_{115}$ (-----) and reverse micelles of $PS_{84}\text{-}b\text{-}PANa_{115}$ (-·-·-·-) after extraction of the residual PS. THF was used as the eluent.

Table 1 resumes the results from SLS and DLS. It is clearly seen that IPECs present much higher molecular weights than the precursors, being within $M_w = 10^8 - 10^9$ g/mol. This provides clear evidence for interpolyelectrolyte complexation and suggests that the co-assemblies formed comprise a large number of macromolecules of the constituting polymeric components, and shows that complexes are stable upon dilution. The positive values of the second virial coefficient indicate that chloroform is a good solvent for the IPEC species formed. The ratio $\rho = \langle R_g^2 \rangle^{0.5} / \langle R_h \rangle_z$, which characterizes the shape of the scattering particles, ranges from 1.18 to 1.24, thus being in good agreement with the values for star-shaped polymers with a high number of arms. The aggregation number, N_{agg} , also gives evidence that thousands of polymeric components assemble to produce IPECs.

Table 1. SLS/DLS results for the IPEC particles formed in the chloroform mixtures of $\text{PS}_{84}\text{-}b\text{-(PA}^-\text{CTA}^+)_x$ with $\text{PDMAEMAQ}^+\text{DS}^-$ at $Z^* = 0.4$ (2.5-fold molar excess of the $(\text{DMAEMAQ}^+\text{DS}^-)$ units)

	$10^{-8} M_w$, g/mol	$10^{-3} N_{\text{agg}}$ ($N_{\text{PS-}b\text{-}A^-} +$ $N_{\text{PDMAEMAQ}^+/\text{PDMAEMA}}$ $Q^+\text{DS}^-$)	$10^7 A_2$, mol ml/g ²	$\langle R_h \rangle_z$, nm	$\langle R_g^2 \rangle^{0.5}$, nm	ρ
$\text{PS}_{84}\text{-}b\text{-(PA}^-\text{CTA}^+)_{115}$	3.05	4.6 (2.6 + 8.9)	5.16	80	94	1.18
$\text{PS}_{84}\text{-}b\text{-(PA}^-\text{CTA}^+)_{410}$	9.60	8.9 (2.5 + 6.4)	8.46	76	90	1.18
$(\text{PA}^-\text{CTA}^+)_{415}$	2.29	2.2 (0.6 + 1.6)	1.24	76	95	1.24

The morphology of soluble IPECs was evaluated using TEM. We proposed a structure consisting of a compact core built up with fragments of the stoichiometric oppositely charged polyelectrolytes blocks, i.e., PA^- and PDMAEMAQ^+ . In the excess of $\text{PS}_{84}\text{-}b\text{-(PA}^-\text{CTA}^+)_x$, the solubilizing corona should be formed by the PS blocks and those fragments of the PA^-CTA^+ blocks, which are not involved in the interpolyelectrolyte complexation (Fig. 4, right structure). In the excess of $\text{PDMAEMAQ}^+\text{DS}^-$, the solubilizing corona comprises both the PS blocks and those fragments of the $\text{PDMAEMAQ}^+\text{DS}^-$ blocks, which are not involved in the interpolyelectrolyte complexation (Fig. 4, left structure).

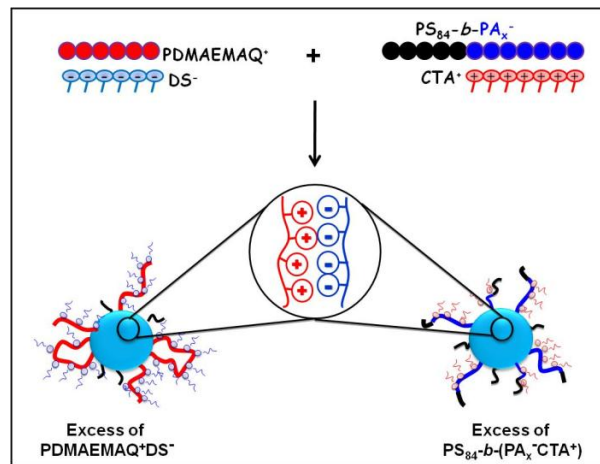


Figure 4. Schematic representation of tentative, idealized structures of macromolecular co-assemblies formed in chloroform mixtures of $\text{PS}_{84}\text{-}b\text{-(PA}^-\text{CTA}^+)_x$ and $\text{PDMAEMAQ}^+\text{DS}^-$.

Chapter 5 presents the results of the research focused in the formulation of novel vesicular nanocarriers from a mixture of poly(ϵ -caprolactone) (PCL) and PMMA-*b*-PDMAEMA. Two diblock copolymers with different PDMAEMA block lengths were synthesized via ATRP using PMMA as macroinitiator. The aim of this research was to formulate nanocapsules (NC) that can be loaded with the drug melatonin. Nanocapsules are vesicular nanoparticles composed with an oily core surrounded by a thin polymer wall. There are several methods to prepare nanocapsules either by polymerization of dispersed monomers or using pre-formed polymers. Here, a technique called interfacial deposition in water was used to obtain NCs. It consists in incorporating a mixture of polymers, oil, drug and surfactant, previously dissolved in an organic solvent like acetone, into water which might or might not contain a surfactant. Surfactants and/or stabilizers are used to avoid drug leakage and/or flocculation and sedimentation of particles. NCs are formed instantaneously by the fast diffusion of a water-miscible solvent with the polymer, drug and oil into an aqueous solution. Nevertheless, our strategy is based on the hypothesis that a new generation of vesicular carrier can be built directly by the mixture of both polymers (PCL and PMMA-*b*-PDMAEMA) in acetone with no need of any surfactant. PCL is a linear polyester widely used as polymer wall in NC formulations while PMMA-*b*-PDMAEMA is an amphiphilic copolymer with potential applications chosen by its solubility in acetone, the ability to anchor at the polymer wall of nanocapsules and to interact with water at the interface.

One important property to evaluate is the size of the nanocarrier. Formulations here prepared were macroscopically homogeneous and stable. Particle size and size distribution were determined by means of DLS. Figure 5A shows the typical linear q^2 dependence of the decay rate, Γ , evidencing the diffusive behavior of the investigated particles. Thus, the Stokes-Einstein equation can be applied to determine reliable hydrodynamic radii from

DLS. Figure 5B indicates unimodal size distributions. Hydrodynamic radii were between 95-180 nm (mean diameter between 180 and 360 nm) what might be suitable for oral administration.

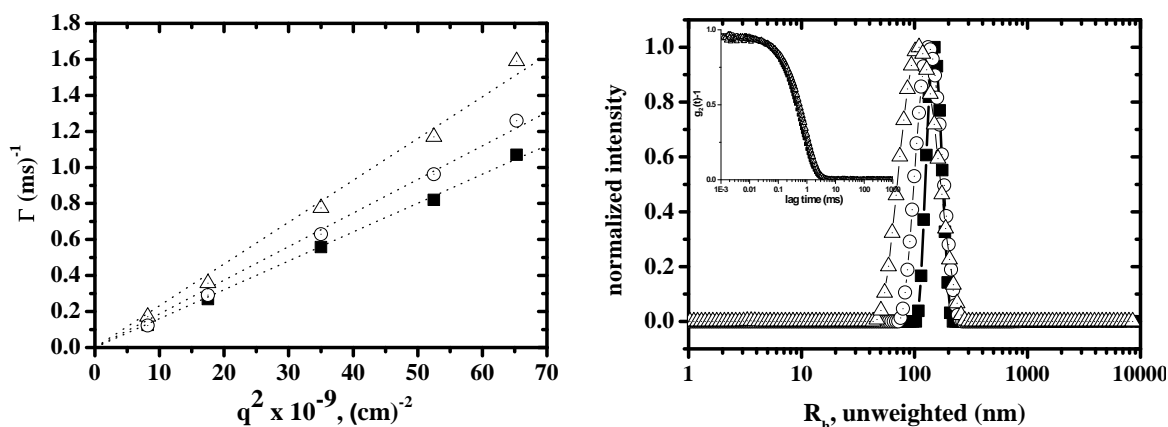


Figure 5. Angular dependence of decay rate obtained from DLS data of diluted nanoparticles loaded with melatonin ($C_{\text{NaCl}} = 1 \text{ mM}$) (Δ = NC1- M₄₀D₁₀₈-Mel-A; \circ = NC1- M₄₀D₄₇₁-Mel-A; \blacksquare = NC2- M₄₀D₄₇₁-Mel-A).

Exhaustive morphological characterization was performed to elucidate the structure of the NCs. Standard TEM, cryo-TEM and SEM showed that all NC presented spherical shape. Also NCs were loaded with Pt nanoparticles using hexachloroplatinum acid (H_2PtCl_6) with a posterior reduction by NaBH_4 . It is expected that the Pt nanoparticles interact with the amino group presents in PDMAEMA, however, no preferential location of the metallic nanoparticles were observed. The fact that NCs were built up with a polymer containing amino groups opens up the possibility to create a wide variety of nanoparticles with promising biomedical applications by complexation with metallic nanoparticles.

The efficiency of encapsulating melatonin was assessed by HPLC. Results showed that melatonin could be encapsulated inside the nanocarrier in ca. 30%. Low encapsulation efficiency might be attributed to the solubility of melatonin in water (0.1 mg/ml) or to the poor diblock ability to keep the drug encapsulated inside the oily core.

Individual Contributions to Joint Publications

In the following, the contributions of each author to the related publications are indicated. The asterisks indicate the corresponding authors.

Chapter 3

This work has been published in *Langmuir*, 2010, 26, 7813-7818 under the title:

Interpolyelectrolyte Complexation in Chloroform

By Evis K. Penott-Chang, Dmitry V. Pergushov, Alexander B. Zezin, and Axel H. E. Müller

I conducted most of the experiments included in this article and wrote the manuscript: Synthesis of polymers used, ^1H NMR, turbidimetric titrations, dynamic light scattering measurements and scanning force microscopy.

Dr. Dmitry V. Pergushov helped with the interpolyelectrolyte complexation reactions and the turbidimetric titrations.

Dr. Pergushov, Prof. Dr. Alexander B. Zezin and Prof. Dr. Axel H. E. Müller were involved with the scientific discussions and corrections of the manuscript.

Chapter 4

This work has been accepted in *Polymer* in July 2011.

DOI: 10.1016/j.polymer.2011.07.017

Interpolyelectrolyte Complexes of Diblock Copolymers via Interaction of Complementary Polyelectrolyte-Surfactant Complexes in Chloroform.

By Evis K. Penott-Chang, Markus Ruppel, Dmitry V. Pergushov, Alexander B. Zezin, Axel H.E. Müller.

I conducted most of the experiments included in this article and wrote the manuscript: the synthesis of all polymers used, ^1H NMR, turbidimetric titrations, static (SLS) and dynamic (DLS) light scattering measurements.

Markus Ruppel helped me with SLS measurements and with SLS/DLS analysis, also with the corrections of the article.

Dr. Pergushov, Prof. Dr. Alexander B. Zezin and Prof. Dr. Axel H. E. Müller were involved with the scientific discussions and corrections of the manuscript.

Chapter 5

This article was submitted to *Journal of Biomedicine Nanotechnology* in March 2010.

Amphiphilic Diblock Copolymer and Polycaprolactone to produce New Vesicular Nanocarriers

By Evis Penott-Chang, Andreas Walther, Pierre Millard, Alessandro Jäger, Eliezer Jäger, Axel H. E. Müller, Silvia S. Guterres, Adriana R. Pohlmann

I synthesized the polymers used in this work. Also prepared all formulations employed and performed DLS and wrote the manuscript.

Andreas Walther performed standard-TEM and cryo-TEM and was involved in the scientific discussions.

Pierre Millard performed HPLC measurements.

Alessandro Jäger Jäger and Eliezer Jäger trained me in the preparation of nanocapsules and were involved with the discussions of the article.

Prof. Dr. Axel H.E. Müller, Prof. Dr. Silvia Guterres and Prof. Dr. Adriana Polhmann were involved in the scientific discussions and the corrections of the manuscript.

3. INTERPOLYELECTROLYTE COMPLEXATION IN CHLOROFORM

Evis K. Penott-Chang^a, Dmitry V. Pergushov^b, Alexander B. Zezin^b, Axel H. E. Müller^{a,}*

^aMakromolekulare Chemie II and Bayreuther Zentrum für Kolloide und Grenzflächen,
Universität Bayreuth, D-95440 Bayreuth, Germany

^bDepartment of Polymer Science, School of Chemistry, Moscow State University,
Vorob'evy Gory, 119991, Moscow, Russia.

*** Corresponding Author and Mailing Address:**

Prof. Dr. Axel Müller:

Lehrstuhl für Makromolekulare Chemie II.

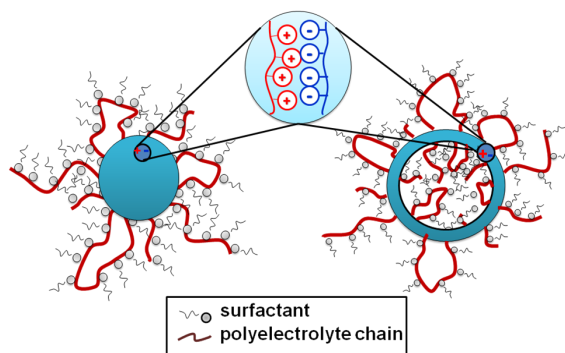
Universität Bayreuth Universitätsstr. 30.

Gebäude NW II D-95447 Bayreuth

Telephone: +49 921 553399

Fax: +49 921 553393

Email: axel.mueller@uni-bayreuth.de



Published in Langmuir (2010), 26, 7813-7818

Evis Penott-Chang: epenott@usb.ve

Abstract

Interpolyelectrolyte complexes (IPECs) were formed in chloroform from complementary polyelectrolyte-surfactant complexes (PESCs), i.e., linear polyelectrolytes whose counterions were substituted by surfactants to dissolve them in the low polarity organic solvent. The interaction between such complementary PESCs was followed by turbidimetry, ^1H NMR, and dynamic light scattering. The experimental results, together with those from transmission electron microscopy and scanning force microscopy provide evidence on the formation IPECs in the system. This process is apparently driven by the entropically favorable release of the pairs of the oppositely charged surfactant ions. If the mixing base-molar ratio between the complementary PESCs, Z , is below a certain threshold value, their chloroform mixtures are colloiddally stable, containing relatively large aggregates. These aggregates are attributed to particles of the formed IPECs stabilized by the fragments of the excess polymeric component. Otherwise, the mixtures of the PESCs undergo phase separation (most pronounced at $Z = 1$) with the formation of an insoluble top phase (attributed to insoluble IPEC) and a clear bottom phase enriched with the surfactant counterions. Electron and scanning force micrographs indicate a rather broad size distribution of the soluble macromolecular co-assemblies with a close to spherical shape.

Keywords: *macromolecular co-assembly, interpolyelectrolyte complexes, polyelectrolyte-surfactant complexes*

3.1 Introduction

Oppositely charged linear polyelectrolytes interacting in a cooperative manner in aqueous media can form stable complexes,^{72, 115-117} often referred to as interpolyelectrolyte complexes (IPECs). They have found a number of important applications, e.g., in drug delivery,¹¹⁸ in non-viral gene transfection¹¹⁹ and in the modification of surfaces using the layer-by-layer technique.¹²⁰ IPEC formation takes place due to strong Coulomb attractive forces, which lead to spontaneous co-assembly of the oppositely charged macromolecules, this process being accompanied by the concomitant, entropically favorable release of small counterions. The structure and the properties of IPECs are governed by several factors such as nature of the interacting polymeric components, their mixing ratio and concentrations, pH, ionic strength, etc. Depending on these parameters, either colloiddally stable complex nanoparticles are obtained or phase separation occurs, resulting in the formation of complex flocculates or complex coacervates. Stoichiometric IPECs (with base-molar ratio of the oppositely charged polymeric components equal to unity) are neutral because charges of the coupled polymeric components are mutually screened. As a rule, such stoichiometric IPECs undergo fast secondary aggregation followed by precipitation from aqueous solutions. When polyelectrolytes with weak ionic groups and with a remarkable difference in molecular weights are complexed at non-stoichiometric mixing base-molar ratios, the reaction can yield water-soluble IPECs consisting of a long host polyion and shorter sequentially attached guest polyions of the opposite charge. Such water-soluble non-stoichiometric IPECs have been thoroughly investigated previously by Kabanov and Zezin with their co-workers.⁸

Only a few authors attempted to realize interpolyelectrolyte complexation in organic media, in particular, of low polarity. Schrage *et al.*⁹ described the formation of vesicles (often referred to as “polymersomes”) by simple mixing solutions of poly(1,2-butadiene)-*block*-poly(cesium methacrylate) and polystyrene-*block*-poly(*N*-methyl-4-vinylpyridinium iodide) micelles in THF. Lokshin *et al.*¹⁰ reported the formation of IPECs containing polyaniline and either DNA or poly(styrenesulfonate) in chloroform. More recently, Pergushov *et al.*¹¹ investigated interpolyelectrolyte complexation in chloroform between complementary polymeric components, viz., surfactant-modified linear polyions, poly(dioctadecyldimethylammonium methacrylate) and poly(*N*-ethyl-4-vinylpyridinium dodecylsulfate).

In these latter two publications,^{10,11} a “two-step” approach was used, whereby the insolubility of ionic polymers in organic solvents of low polarity was successfully overcome by the prior substitution of small counterions of the polyelectrolytes by sufficiently hydrophobic surfactant counterions, viz., dioctadecyldimethylammonium cations and dodecylsulfate or dodecylbenzenesulfonate anions. To perform such a modification, aqueous solutions of oppositely charged polyelectrolyte and surfactant were mixed at equimolar ratio of ionic groups. This resulted in the precipitation or flocculation of the formed polyelectrolyte-surfactant complexes (PESCs). These PESCs are insoluble in water due to the compensation of ionic charges by the hydrophobic surfactant counterions. However, after thorough drying they are soluble in a number of low polarity organic solvents, such as chloroform or benzene.¹²⁻¹⁴

Analogously to the formation of IPECs in aqueous media, interpolyelectrolyte complexation is expected to take place upon the direct mixing organic solutions of two complementary PESCs. This process should be accompanied by an entropically favorable release of the surfactant counterions (in low polarity organic solvents in the form of ion pairs or their aggregates) previously associated with ionic groups of the polymeric components into the bulk solution.

Our interest in the synthesis of IPECs in organic solvents is that it opens up the possibility to vary solvent polarity in a rather broad range, which may lead to some novel nanoarchitectures. Moreover, IPECs prepared in organic media of low polarity are substantially free of water and can be further almost completely dried from a volatile organic solvent to form fine and highly porous powders, which may be afterwards used, for example, for design of novel separation membranes. In low polarity organic solvents, hydrophobic interaction can be cancelled, and thus, essentially only electrostatic interaction plays a role in the complexation process. These electrostatic interactions are naturally expected to be very strong in low permittivity media, thereby leading to non-equilibrium (“frozen”) macromolecular co-assemblies.

In this work, we have synthesized IPECs in chloroform using the interaction between poly(cetyltrimethylammonium acrylate) ($\text{PA}^- \text{CTA}^+$) and poly[(methacryloylethyl)dimethylethylammonium dodecyl sulfate] ($\text{PDMAEMAQ}^+ \text{DS}^-$). The latter PESC is derived from quaternized poly(2-dimethylaminoethyl methacrylate). In contrast to the previous papers where the formation of only insoluble IPECs was

reported,^{10,11} herein we demonstrate for the first time that in the excess of one of the polymeric component they can be colloiddally stable or even soluble in chloroform.

3.2 Experimental Section

3.2.1 Materials

Monomers, *t*-butyl acrylate (*t*-BuA, donated by BASF SE) and 2-dimethylaminoethyl methacrylate (DMAEMA, donated by BASF SE), were stirred over CaH₂, distilled from CaH₂, and degassed in high vacuum. CuBr (95%, Aldrich) and CuCl (97%, Aldrich) were purified by stirring overnight in acetic acid. After filtration, they were washed with ethanol, then with ether, and afterwards dried under vacuum. N,N,N',N'',N''-pentamethyldiethylenetriamine (PMDETA, 99%, Aldrich) and ethyl-2-bromo-2-isobutyrate (EBIB, 98%, Aldrich) were distilled and degassed. 1,1,4,7,10,10-Hexamethyltriethylenetetramine (HMTETA, 97%, Aldrich), *p*-toluenesulfonyl chloride (*p*-TsCl, 99%, Aldrich), trifluoroacetic acid (CF₃COOH, 99%, Aldrich), ethyl bromide (Aldrich, 99%), sodium dodecylsulfate (SDS) and cetyltrimethylammonium bromide, (CTAB) (both 99%, Aldrich) and chloroform (anhydrous, 99%, Aldrich) were commercially obtained and used without further purification.

3.2.2 Polymer Synthesis

Polymers were synthesized through atom transfer radical polymerization (ATRP) of DMAEMA and *t*-BuA. All polymerizations were carried out inside a glovebox under nitrogen atmosphere. The prepared polymers, poly(2-dimethylaminoethyl methacrylate) (PDMAEMA) and poly(*tert*-butylacrylate) (PtBA), were characterized by ¹H NMR and GPC to determine their structures as well as molecular weight distributions. Table 1 summarizes the experimental data for both polyelectrolyte precursors. GPC traces (not shown) indicated a unimodal molecular weight distribution in each case. Hydrolysis of PtBA performed under mild conditions with CF₃COOH was verified by means of ¹H NMR through the disappearance of proton signals corresponding to the *t*-butyl groups. Quaternization of PDMAEMA with ethyl bromide was verified by ¹H NMR and quantified by elemental analysis.

Table 1. Experimental conditions and results of the synthesis of polyelectrolyte precursors.

Polymer	[M] ₀ : [I] ₀ : [Cu]: [L]	T, °C	10 ³ M _{n, GPC} (PDI)	DP _{n, GPC}	Conversion (%)
PDMAEMA	520:1:1:1	90	61.0 (1.43) ^a	390 ^a	32 ^c
PtBA	380:1:1:1	60	53.0 (1.08) ^b	415 ^b	83 ^d

^{a)} Determined by GPC in THF with tetrabutylammonium bromide using PS calibration. ^{b)} Determined by GPC in THF using PtBA calibration. ^{c)} Determined by gas chromatography. ^{d)} Determined by ¹H NMR.

3.2.2.1 Synthesis and quaternization of poly(2-dimethylaminoethyl methacrylate) (PDMAEMA).

The polymerization of DMAEMA was carried out according to the procedure reported by Gan *et al.*¹⁵ DMAEMA monomer (20 g, 0.127 mol) was added to a round bottom flask containing CuCl (0.0252 g, 0.254 mmol), HMTETA (0.0586 g, 0.254 mmol), and anisole (10.0 g, 50 wt%). The solution was stirred until the Cu complex was formed, which was easily observed by the dissolution of the copper and the change of the solution from colorless to light yellow-green. After the Cu-ligand complex formation, *p*-TsCl (0.0485 g, 0.254 mmol) was added to the mixture and the initial sample was taken. The flask was sealed with a plastic cap and reaction solution was immersed for 180 min into an oil bath thermostated at 90°C. The final conversion was determined by gas chromatography. PDMAEMA (2g, 0.012 mol) was exhaustively quaternized with a 10-fold molar excess of ethylbromide in methanol at room temperature. The degree of quaternization, as determined by elemental analysis of bromine, was equal to ca 90%.

3.2.2.2 Synthesis of poly(acrylic acid) (PAA).

CuBr (0.0589 g, 0.411 mmol), PMDETA (0.0714 g, 0.411 mmol), *t*-BuA (20g, 0.156 mol), and ethyl acetate (5g, 25 wt%) were added into a round bottom flask and the mixture was stirred until complete dissolution of the Cu complex. When the Cu catalyst was formed, the initiator, EBIB (0.0802 g, 0.411 mmol), was added. The flask was placed for 22.5 h into an oil bath thermostated at 60°C. The conversion of the double bonds was confirmed by ¹H-NMR. The hydrolysis of *t*-butyl groups was carried out via dissolving PtBA in CH₂Cl₂ and adding a 5-fold molar excess of CF₃COOH. The mixture was stirred at room temperature for 24 h while PAA gradually precipitated in CH₂Cl₂. The solvent and

CF₃COOH were afterwards removed by rotating evaporation followed by freeze-drying. The polymer was finally dried under vacuum at 40°C overnight.

3.2.3 Preparation of Polyelectrolyte-Surfactant Complexes (PESCs).

PESCs soluble in chloroform were successfully synthesized with a yield of more than 90% following a procedure similar to that reported by Pergushov *et. al.*¹¹ Specifically, the aqueous solution of the surfactant was added to an aqueous solution of the oppositely charged polyelectrolyte at constant ionic strength (0.1M NaCl). PDMAEMAQ, (5mM) was dissolved in Millipore water, and SDS (0.01M) was added dropwise under continuous stirring. At the 1 : 1 ratio between concentrations of ionic groups of PDMAEMAQ and SDS, the formed PESC precipitated and a ca. 5% molar excess of surfactant was added. The PESC, referred to as PDMAEMAQ⁺ DS⁻, was filtered under vacuum using a funnel with a glass frit and rinsed with distilled water to remove unreacted surfactant and low molecular weight salt. Afterwards, the PESC was allowed to dry first in an oven at 40°C for 4 h, and then under vacuum at room temperature for 10 days. Complexation between the sodium salt of PAA, PANA (5mM), and CTAB was performed in a similar manner in 0.01M TRIS·HCl buffer (pH 9) to ensure a complete ionization of acrylic acid units. The obtained PESC is referred to as PA⁻ CTA⁺. The degree of substitution of the small counterions by the corresponding surfactant-counterions was determined by elemental analysis of nitrogen for PA⁻ CTA⁺ as 87%. For PDMAEMAQ⁺ DS⁻, elemental analysis of nitrogen and sulfur resulted a degree of substitution of 98 %.

3.2.4 Characterization

¹H NMR spectra were recorded with a Bruker AC-250 spectrometer at room temperature using deuterated chloroform. Molecular weight distributions were measured by gel permeation chromatography (GPC) with THF as the eluent. In the case of PDMAEMA, GPC analysis was performed using THF with tetrabutylammonium bromide as the eluent. The instrument was operated at a flow rate of 1.0 mL/min at room temperature. A column set, 5μ SDV gel, 10²-10⁵ Å, 30 cm each (PSS, Germany), was used together with a differential refractometer and an UV-detector operated at the wavelength of 254 nm. Polystyrene standards (PSS, Germany) were used for the calibration of the column set. Turbidimetric titrations were carried out with a Perkin-Elmer Lambda 15 UV/vis-spectrophotometer at the wavelength of 500 nm. At this wavelength, polymers do not

absorb light; therefore, optical density values are attributed only to the light scattering. Particle size distributions were determined by means of *dynamic light scattering measurements (DLS)* with an ALV DLS/SLS SP 5022F equipment and a He-Ne laser ($\lambda=632.8$ nm) as a light source. Prior to measurements, samples were filtered using PTFE filter (Millipore) with a pore size of 1 μm . The CONTIN program was employed to analyze the autocorrelation functions measured at the scattering angle of 90° . *Transmission electron microscopy (TEM)* images were taken using a Zeiss EM 922 transmission electron microscope operated at 200 kV. Typically, a 5- μL droplet of IPEC solution in chloroform was deposited onto the copper TEM grid coated with a carbon film. *Scanning force microscopy (SFM)* measurements were performed using a Digital Instrument Dimension 3100 microscope operated in Tapping Mode. Samples were prepared by a dip-coating from dilute solutions of IPECs in chloroform onto freshly cleaved mica surface.

3.3 Results and Discussion

3.3.1 Interpolyelectrolyte Complexation in Chloroform

After being thoroughly dried, the polyelectrolyte-surfactant complexes (PESCs) $\text{PA}^- \text{CTA}^+$ and $\text{PDMAEMAQ}^+ \text{DS}^-$, prepared as described in Experimental Section, were dissolved in anhydrous chloroform. Figure 1 shows that the chloroform solutions of these PESCs are transparent even at relatively high concentrations (ca. 1 wt %). When both transparent chloroform solutions containing complementary PESCs are mixed at the base-molar ratio $Z = [\text{PDMAEMAQ}^+ \text{DS}^-]/[\text{PA}^- \text{CTA}^+]$ or $Z^* = [\text{PA}^- \text{CTA}^+]/[\text{PDMAEMAQ}^+ \text{DS}^-]$ (where the molar concentrations of monomer units complexed with surfactant ions are given in the brackets), equal to unity ($Z = Z^* = 1$), a distinct phase separation occurs. As is clearly seen from Figure 1, insoluble particles float on a transparent bottom phase. This finding strongly suggests that the two complementary PESCs interact in chloroform, generating an insoluble IPEC of PDMAEMAQ^+ and PA^- .

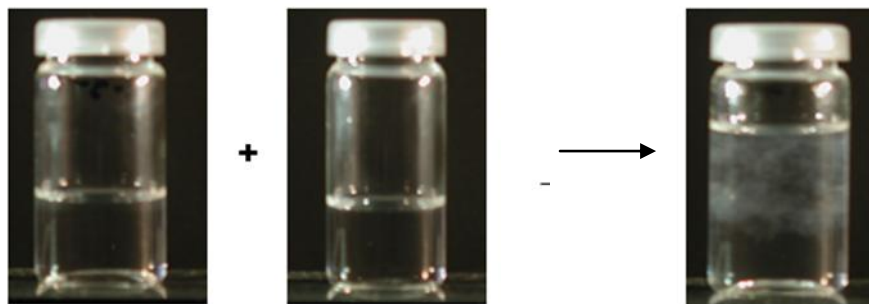


Figure 1. Solutions of PESC s PA $^-$ CTA $^+$ and PDMAEMAQ $^+$ DS $^-$ in chloroform (1 wt %) and their mixture at [PA $^-$ CTA $^+$] = [PDMAEMAQ $^+$ DS $^-$] ca. 5 min after mixing.

The interpolyelectrolyte complexation in chloroform was followed by turbidimetric titration. In Figure 2, the resulting curves are shown for the experiments carried out using the PA $^-$ CTA $^+$ chloroform solution either as the titrand or the titrant. First, a chloroform solution of PA $^-$ CTA $^+$ ([PA $^-$ CTA $^+$] = 4.29 mM) was used as the titrand and a 10 times more concentrated chloroform solution of PDMAEMAQ $^+$ DS $^-$ ([PDMAEMAQ $^+$ DS $^-$] = 42.9 mM) was added as the titrant (open circles). A decrease of the transmittance was already observed on addition of very low amounts of the titrant solution. For the used concentrations of the PESC s , opalescent but colloidally stable mixtures were obtained only at $Z \leq 0.2$. On the other hand, when PDMAEMAQ $^+$ DS $^-$ ([PDMAEMAQ $^+$ DS $^-$] = 4.29 mM) was titrated with a 10 times more concentrated chloroform solution of PA $^-$ CTA $^+$ ([PA $^-$ CTA $^+$] = 42.9 mM), the behavior was different from that observed before (solid circles). Homogeneous mixtures demonstrating virtually no opalescence are formed at $Z^* \leq 0.6$. Further addition of PA $^-$ CTA $^+$ resulted in a gradual pronounced decrease of transmittance due to the formation of insoluble particles and did not lead to the re-dissolution of the aggregates even at $Z^* = 1.8$, that is, at the more than the 1.5-fold excess of PA $^-$ CTA $^+$. This finding can be explained by the formation of substantially “frozen” co-assemblies in this organic media of low permittivity ($\epsilon = 4.8$).

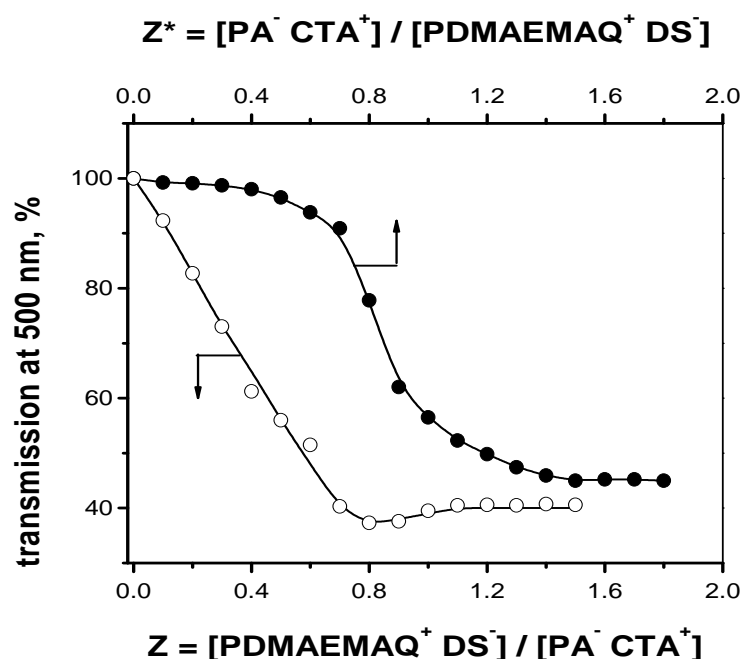
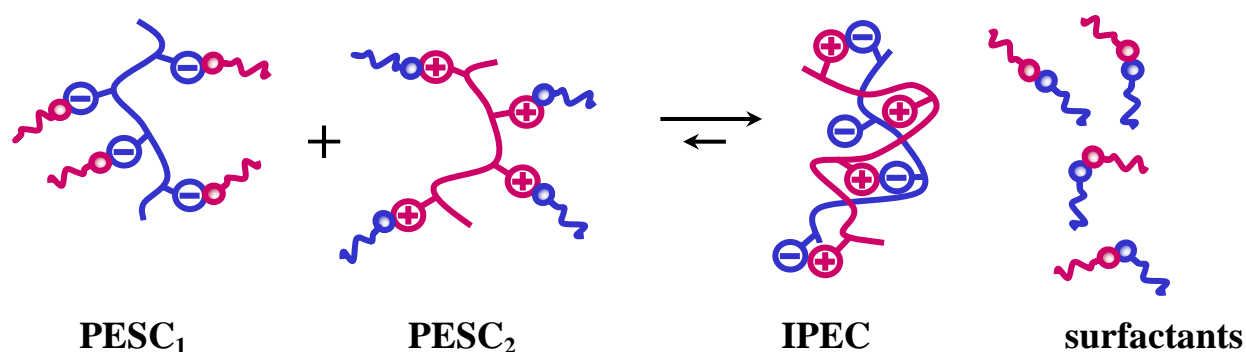


Figure 2. Turbidimetric titration curves of a chloroform solution of $\text{PA}^- \text{CTA}^+$ with a chloroform solution $\text{PDMAEMAQ}^+ \text{DS}^-$ (open circles, bottom x-axis $Z = [\text{PDMAEMAQ}^+ \text{DS}^-] / [\text{PA}^- \text{CTA}^+]$) and a chloroform solution of $\text{PDMAEMAQ}^+ \text{DS}^-$ with a chloroform solution of $\text{PA}^- \text{CTA}^+$ (solid circles, top x-axis $Z^* = [\text{PA}^- \text{CTA}^+] / [\text{PDMAEMAQ}^+ \text{DS}^-]$).

One may attribute the formation of insoluble IPECs already at rather low values of Z (when $\text{PA}^- \text{CTA}^+$ acts as the titrand) to a rather poor solubilizing power of the $\text{PA}^- \text{CTA}^+$ fragments in chloroform. Indeed, not all counterions of PANa are substituted by surfactant counterions (see Experimental Section) and therefore a certain fraction of $\text{A}^- \text{Na}^+$ groups is not balanced by CTA^+ counterions. This would apparently worsen the solubilizing power of $\text{PA}^- \text{CTA}^+$ and may even result in a clustering of such groups in chloroform. Bakeev *et al.*^{13,14} reported that aggregation (intermolecular and even intermolecular) of salt groups of non-stoichiometric PESC with a partial substitution of small counterions by surfactant counterions, may occur in solvents of low polarity.

Scheme 1. Schematic representation for interpolyelectrolyte complexation in low polarity organic media.



It is reasonable to assume that driving force of interpolyelectrolyte complexation in low polarity organic media is the release of surfactant counterions previously associated with the polyelectrolytes. This process is shown in the Scheme 1, the surfactant counterions being released most probably as ion pairs or their aggregates. To verify the release of the surfactant counterions into the bulk solution due to interpolyelectrolyte complexation, the deuterated chloroform solutions of the PESC_s were mixed at $[PA^-CTA^+] = [PDMAEMAQ^+DS^-]$ ($Z = Z^* = 1$) and after macroscopic phase separation the resulting transparent bottom phase was taken out to be analyzed by 1H NMR (Figure 3C). Figures 3A and 3B show the 1H NMR spectra of the used surfactants and the corresponding proton assignments. Due to poor solubility of SDS in chloroform, its 1H NMR spectrum was measured in deuterated water, though chemical shifts are expected to be different from those one would obtain in deuterated chloroform. The 1H NMR spectra for the original PESC_s presented in Figs 3D and 3E were also recorded as reference.

The analysis of the 1H NMR spectra corresponding to the PESC_s (Figs 3D and 3E) indicates that the intensities of the proton signals of the polyelectrolyte components considerably decrease after the complexation with the surfactants (spectra not shown). This may be attributed to the fact that upon incorporation of the surfactant counterions the contribution of the proton signals from the polyelectrolyte components decreases, resulting in their lower intensity. Also, the methylene protons from the surfactants and polyelectrolyte components overlap and clear assignments could not be performed. From the 1H NMR spectrum of the bottom phase after separation of the IPEC (Figure 3C) it can be seen that the assignments of the proton signals correspond rather well to those of the

surfactants. As the signals from protons of the polyelectrolyte components are of very low intensity even for the original PESC, we cannot draw unambiguous inference about their presence or the absence in the bottom phase. At the same time, however, it appears obvious that the bottom phase is rich with surfactant counterions.

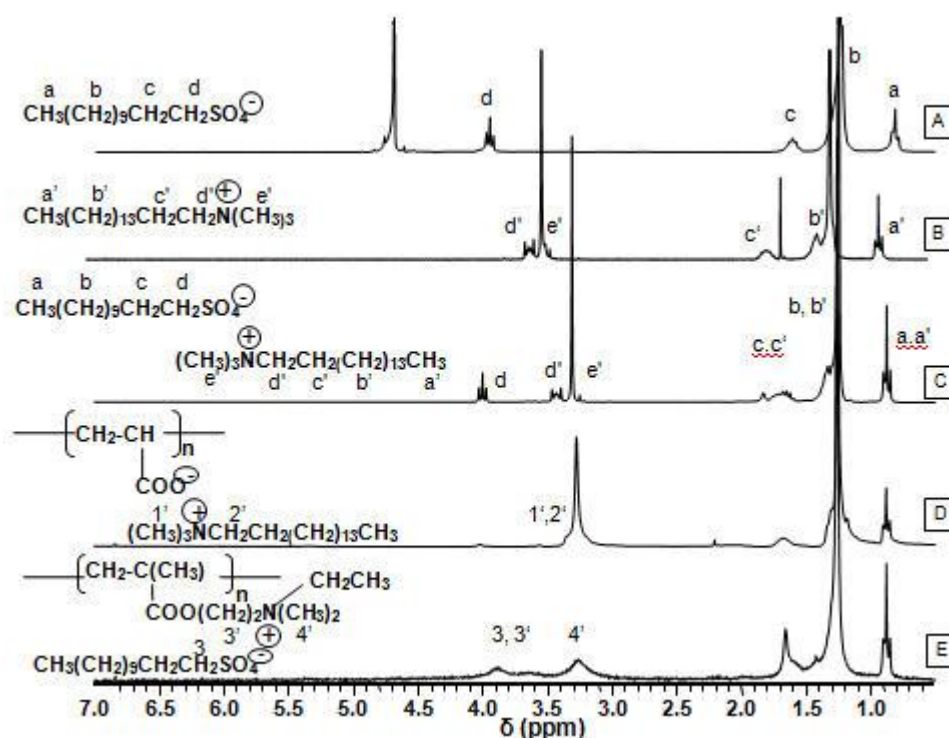


Figure 3. ^1H NMR spectra of (A) the solution of SDS in D_2O , (B) the solution of CTAB in CDCl_3 , (C) the bottom phase formed upon mixing solutions of $\text{PA}^- \text{CTA}^+$ and $\text{PDMAEMAQ}^+ \text{DS}^-$ in CDCl_3 at $[\text{PA}^- \text{CTA}^+] = [\text{PDMAEMAQ}^+ \text{DS}^-]$, (D) the solution of $\text{PA}^- \text{CTA}^+$ in CDCl_3 , (E) the solution of $\text{PDMAEMAQ}^+ \text{DS}^-$ in CDCl_3 .

3.3.2 Characterization of IPECs

Dynamic light scattering (DLS) measurements were performed for chloroform mixtures of $\text{PA}^- \text{CTA}^+$ and $\text{PDMAEMAQ}^+ \text{DS}^-$ at $Z = 0.2$ (5-fold excess of $\text{PA}^- \text{CTA}^+$) or $Z^* = 0.2$ (5-fold excess of $\text{PDMAEMAQ}^+ \text{DS}^-$), respectively. As seen from Figure 4, the resulting CONTIN plots for such mixtures apparently demonstrate the co-existence of two populations of the scattering particles in both cases, with larger species ($\langle R_{h,app} \rangle_z \cong 70$ nm) giving a dominant contribution to the intensity of the scattered light. For comparison, DLS measurements were also performed for the chloroform solutions of the original PESC at

the same concentrations as the concentration of the excess polymeric component in the chloroform mixtures of $\text{PA}^- \text{CTA}^+$ and $\text{PDMAEMAQ}^+ \text{DS}^-$ (results are not shown). In the latter case, the obtained autocorrelation functions were very noisy, the scattering intensities were rather low, and the scattering particles demonstrated a very broad size distribution with the $\langle R_{h,\text{app}} \rangle_z \cong 10 \div 20$ nm. The fact that the pattern of the autocorrelation functions and the scattering behavior of the individual PESCs in chloroform differ substantially from that observed for their chloroform mixtures strongly suggests that the detected large scattering particles can be considered as co-assemblies formed due to interaction between $\text{PA}^- \text{CTA}^+$ and $\text{PDMAEMAQ}^+ \text{DS}^-$. The small scattering particles with $\langle R_{h,\text{app}} \rangle_z \cong 8 \div 10$ nm are most likely either precursors of the large co-assemblies resulting from their secondary aggregation or single PESC unimers not involved in the interpolyelectrolyte complexation.

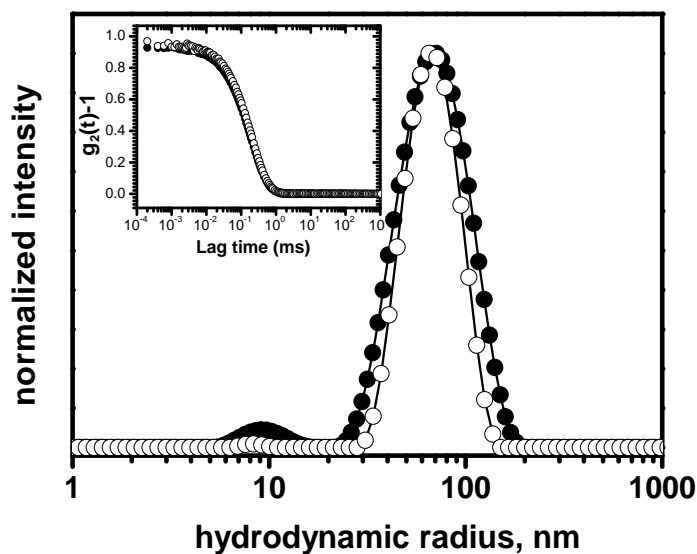


Figure 4. Intensity-weighted distribution of apparent hydrodynamic radii of particles formed in chloroform mixtures of $\text{PA}^- \text{CTA}^+$ and $\text{PDMAEMAQ}^+ \text{DS}^-$ at 5-fold excess of $\text{PA}^- \text{CTA}^+$ ($Z = 0.2$, open circles) and at 5-fold excess of $\text{PDMAEMAQ}^+ \text{DS}^-$ ($Z^* = 0.2$, solid circles). Total base-molar concentration of the excess polymeric component was equal to 2.6 g/L.

We anticipated that the interaction between the PESCs in the excess of one of the polymeric components would result in macromolecular co-assemblies of micellar type with a rather compact core assembled from the oppositely charged fragments of PA^- and PDMAEMAQ^+ , which substantially represents a stoichiometric IPEC, surrounded by a

swollen corona built up from fragments (loops/tails) of the excess polymeric component, providing solubility for the whole complex species in low polarity organic media. Figure 5 shows transmission electron microscopy (TEM) images of IPECs formed in the excess of PDMAEMAQ⁺ DS⁻ at $Z^* = 0.2$. In general, the observed particles demonstrate a spherical shape with a rather broad particle size distribution. The number-average radius, $\langle R \rangle_n$, (and its standard deviation) of the IPEC particles obtained from the TEM images presented in Figure 5 was evaluated as $\langle R \rangle_n = 60 \pm 26$ nm, which compares well to the z-average hydrodynamic radius of the corresponding large complex aggregates measured by DLS, $\langle R_{h,app} \rangle_z \cong 70$ nm (Figure 4), taking into account the collapsed state of the aggregates in TEM and the different averages. At the same time, micrograph 5A apparently indicates a rather complex structure of the generated macromolecular co-assemblies. Indeed, the dark ring and the dark circle with a bright ring of the thickness ca. $40 \div 50$ nm in between clearly observed in the enlargement of some of the objects given in the TEM images (Figure 5), pointing to a vesicular structure. Possible structures of the formed IPEC particles are given in the bottom chart in Figure 5. Essentially, the left hand side structure resembles the so-called “surface excess” model proposed earlier^{16,17} to describe the structure of aggregated IPECs formed in aqueous media, which considers them as substantially stoichiometric IPECs whose particles are stabilized in aqueous media by charged fragments of the excess polymeric component. At the same time, vesicles (“polymersomes”) were observed earlier by Schrage *et al.*⁹ upon the interaction of micelles of poly(1,2-butadiene)-*block*-poly(cesium methacrylate) and polystyrene-*block*-poly(1-methyl-4-vinylpyridinium iodide) in THF.

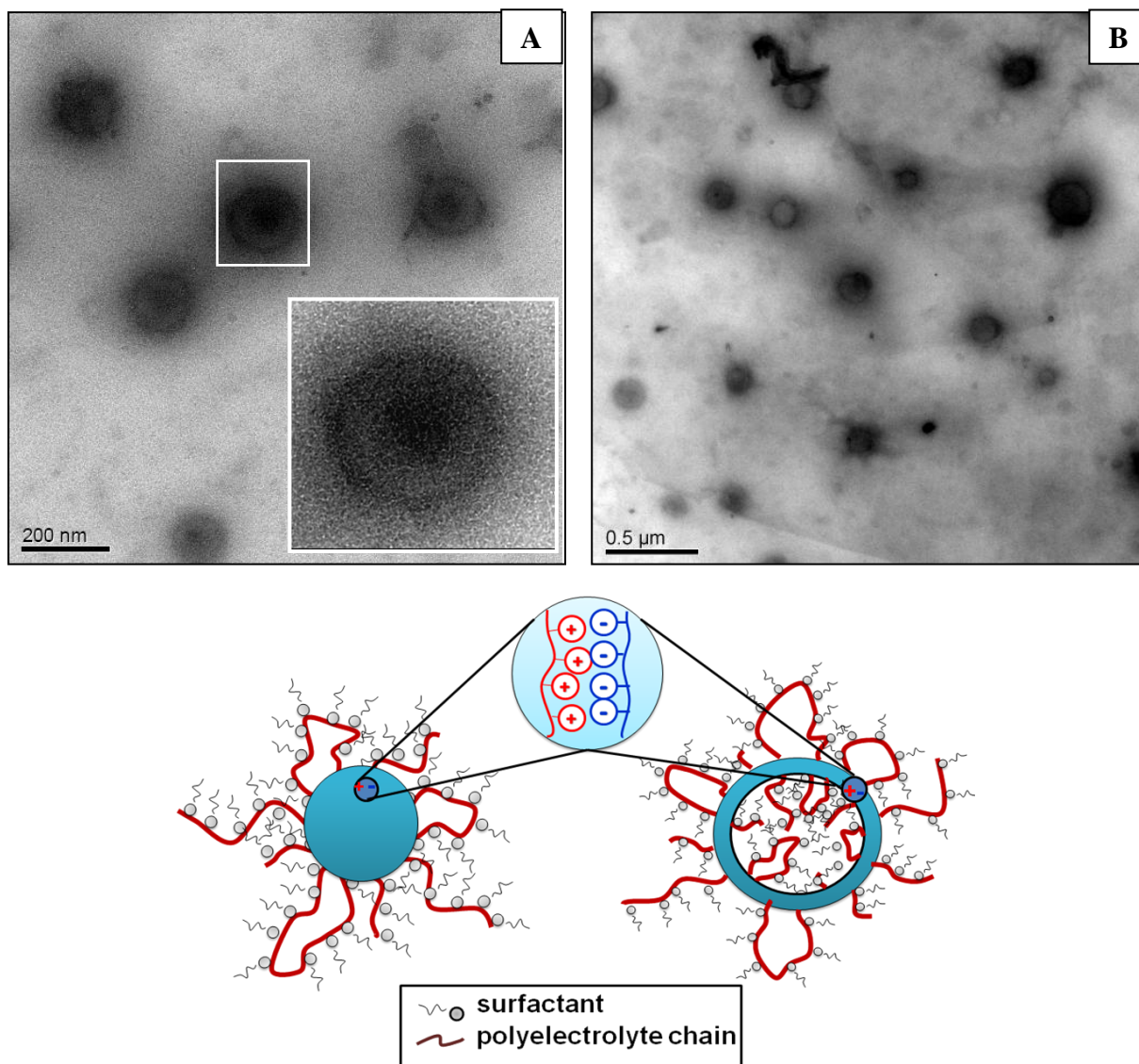


Figure 5. TEM images of the IPEC particles formed in the chloroform mixture of $\text{PA}^- \text{CTA}^+$ and $\text{PDMAEMAQ}^+ \text{DS}^-$ at $Z^* = 0.2$ (top). Schematic representation of possible structures of co-assemblies, which might form in the excess of $\text{PDMAEMAQ}^+ \text{DS}^-$ (bottom).

Tapping mode scanning force microscopy (SFM) was used to image the same IPEC that was measured by TEM. Figure 6 shows the obtained phase and height images. As was observed in the TEM images (Figure 5), the observable objects show a close to spherical shape and rather high polydispersity with a number-average radius from 80 up to 160 nm. Taking into account the convolution of the signal by the finite size of the of the SFM cantilever tip (typically around 20 nm), these values are in good agreement with $\langle R_{h,\text{app}} \rangle$ and $\langle R_{\text{TEM}} \rangle$ (Figs 4 and 5). The observed high polydispersity can most probably be

attributed to the formation of so-called “frozen” structures upon mixing chloroform solutions of both PESC which do not re-arrange once they are formed.

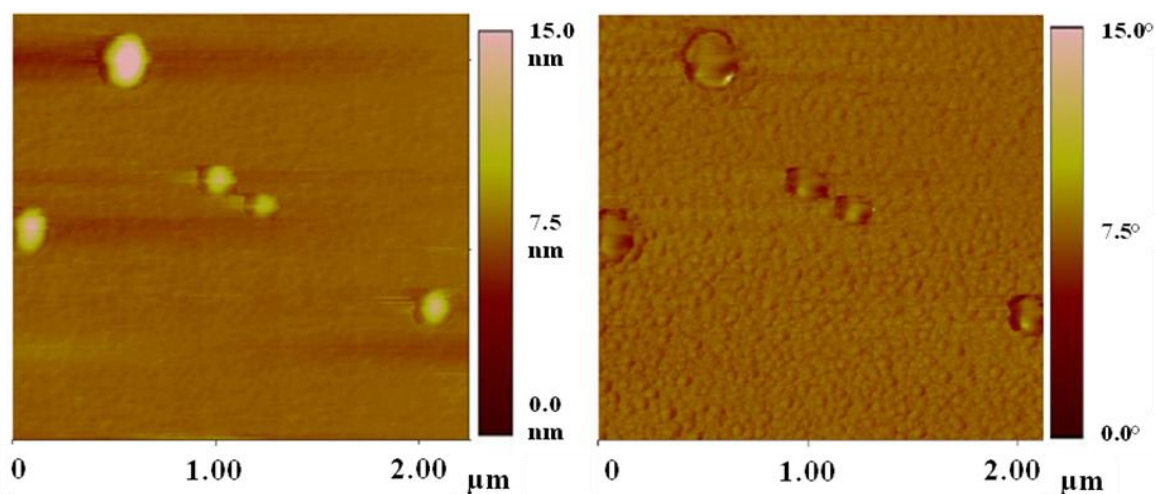


Figure 6. SFM images of IPEC particles formed in the chloroform mixture of $\text{PA}^- \text{CTA}^+$ and $\text{PDMAEMAQ}^+ \text{DS}^-$ in the excess of $\text{PDMAEMAQ}^+ \text{DS}^-$ at $Z^*=0.2$. Dip coating onto mica. Left: height image, right: phase image.

3.4 Conclusions

Our experimental results provide evidence that interpolyelectrolyte complexation in chloroform, a low polarity organic solvent, can be realized if low molecular weight counterions of the complementary polyelectrolytes are substituted by sufficiently hydrophobic surfactant counterions. This process results in the formation of aggregated complex particles. Analogously to aqueous media where the driving force for interpolyelectrolyte complexation is the release of low molecular weight counterions into bulk solution, such a process in organic media of low polarity is most probably driven by a concomitant release of surfactant counterions (apparently, as pairs of oppositely charged surfactant ions). TEM and SFM show close to spherical particles with a rather broad particle size distribution, most likely due to frozen structures.

Acknowledgements

This work was supported by the EU Marie Curie Research and Training Network POLYAMPHI, (project no. EU MCRTN-CT-2003-505027). D.V.P. thanks the Deutsche Forschungsgemeinschaft for the financial support of his research stays at Universität Bayreuth.

References

- (1) Smid, J.; Fish, D., *In Encyclopedia of Polymer Science and Engineering*; Mark, H.F., Bikales, N.M., Overberger, C.G., Menges G., Eds.; Wiley: New York, 1988, Vol. 11, pp. 720-739.
- (2) Philipp, B.; Dautzenberg, H.; Linow, K.-J.; Kötz, J.; Dawydoff, W., *Progr. Polym. Sci.*, **1989**, *14*, 91-172.
- (3) Kabanov, V.A., *In Macromolecular Complexes in Chemistry and Biology*; Dubin, P., Bock, J., Davies, R.M., Schulz, D.N., Thies C. Eds.; Springer: Berlin, 1994, pp. 151-174.
- (4) Thünemann, A.F.; Müller, M.; Dautzenberg, H.; Joanny, J.F.; Löwen, H., *Adv. Polym. Sci.*, **2004**, *166*, 113-171.
- (5) Kabanov, A.V.; Kabanov, V.A., *Adv. Drug Delivery Rev.*, **1998**, *30*, 49-60.
- (6) Wong, S.Y.; Pelet, J.M.; Putnam, D., *Progr. Polym. Sci.*, **2007**, *32*, 799-837
- (7) Decher, G., *Science*, **1997**, *277*, 1232-1237.
- (8) Kabanov, V.A.; Zezin, A.B., *Pure Appl. Chem.*, **1984**, *56*, 343-354.
- (9) Schrage, S.; Sigel, R.; Schlaad, H., *Macromolecules*, **2003**, *36*, 1417-1420.
- (10) Lokshin, N.A.; Sergeyev, V.G.; Zezin, A.B.; Golubev, V.B.; Levon, K.; Kabanov, V.A., *Langmuir*, **2003**, *19*, 7564-7568.
- (11) Pergushov, D.V.; Remizova, E.V.; Zezin, A.B.; Kabanov, V.A., *Doklady Phys. Chem.*, **2006**, *406*, Part 2, 38-42.
- (12) Bakeev, K.N.; Shu, Y.M.; Zezin, A.B.; Kabanov, V.A., *Doklady Akademii Nauk* (in Russian) **1993**, *332*, 450-453.
- (13) Bakeev, K.N.; Shu, Y.M.; MacKnight, W.J.; Zezin, A.B.; Kabanov, V.A., *Macromolecules*, **1994**, *27*, 300-302.
- (14) Bakeev, K.N.; Shu, Y.M.; Zezin, A.B.; Kabanov, V.A.; Lezov, A.V.; Mel'nikov, A.B.; Kolomiets, I.P.; Rjuntsev, E.I.; MacKnight, W.J., *Macromolecules*, **1996**, *29*, 1320-1325.
- (15) Gan, L.-H.; Ravi, P.; Mao, B.W.; Tam, K.-C., *J. Polym. Sci. A: Polym. Chem.*, **2003**, *41*, 2688-2695.
- (16) Pergushov, D.V.; Buchhammer, H.-M.; Lunkwitz, K., *Colloid Polym. Sci.*, **1999**, *277*, 101-107.

- (17) Chen, J.; Heitmann, J.A.; Hubbe, M.A., *Colloids Surf. A: Physicochem. Eng. Aspects*, **2003**, 223, 215-230.

4. INTERPOLYELECTROLYTE COMPLEXES OF DIBLOCK COPOLYMERS VIA INTERACTION OF COMPLEMENTARY POLYELECTROLYTE-SURFACTANT COMPLEXES IN CHLOROFORM

Evis K. Penott-Chang^{a,†}, Markus Ruppel^{a,‡}, Dmitry V. Pergushov^b, Alexander B. Zezin^b,

Axel H. E. Müller^{a,}*

^aMakromolekulare Chemie II and Bayreuther Zentrum für Kolloide und Grenzflächen, Universität Bayreuth, D-95440 Bayreuth, Germany

^bDepartment of Polymer Science, School of Chemistry, Moscow State University, Vorob'evy Gory, 119991, Moscow, Russia.

*** Corresponding Author and Mailing Address:**

Prof. Dr. Axel Müller:

Lehrstuhl für Makromolekulare Chemie II.

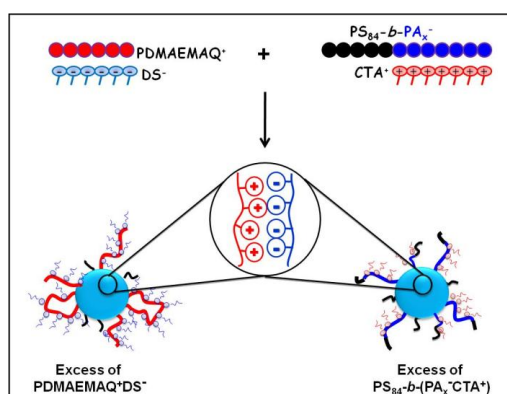
Universität Bayreuth Universitätsstr. 30.

Gebäude NW II D-95447 Bayreuth

Telephone: +49 921 553399

Fax: +49 921 553393

Email: axel.mueller@uni-bayreuth.de



Accepted in Polymer, July 2011

DOI: 10.1016/j.polymer.2011.07.017

Abstract

We have studied the interpolyelectrolyte complexation in chloroform between polystyrene-block-poly(cetyltrimethylammonium acrylate), (PA-CTA⁺), and poly(2-(methacryloyloxy)ethyl dimethylethylammonium dodecyl sulfate) (quaternized poly(2-(dimethylamino)ethyl methacrylate) complexed with sodium dodecyl sulfate), (PDMAEMAQ⁺DS⁻). Turbidimetry, dynamic/static light scattering, and transmission electron microscopy show the formation of large aggregated interpolyelectrolyte complex species, which are colloidally stable in chloroform or even chloroform-soluble if the certain conditions are met. We suggest such co-assemblies to be micellar species with a core assembled from electrostatically coupled fragments of the polymeric components. The corona is built up either from a mixture of polystyrene blocks and excessive fragments of (PDMAEMAQ⁺DS⁻) chains or from a mixture of polystyrene blocks and excessive fragments of (PA-CTA⁺) blocks, depending on which polymeric component was taken in excess for the interpolyelectrolyte complexation. However, their real structures may deviate from such idealized consideration because of the non-equilibrium character of interpolyelectrolyte complexation in organic media of low polarity.

Keywords: *interpolyelectrolyte complexes, macromolecular co-assembly, polymer-surfactant complexes, interpolyelectrolyte complexation in organic solvent.*

4.1 Introduction

Interpolyelectrolyte complexation taking place upon simple mixing aqueous solutions of the oppositely charged polymeric components represents an easy and attractive way to design macromolecular co-assemblies, so-called interpolyelectrolyte complexes (IPECs) [1-5], which have remarkable and often even unique properties. The use of ionic amphiphilic diblock copolymers, which are well known to undergo self-assembly in water [6], thereby generating micelles, offers possibilities to obtain novel IPECs of micellar type with peculiar core-shell-corona (also referred to as “onion-like”) structure [7]. Previously, we thoroughly investigated the interaction of star-like micelles generated in aqueous solutions of ionic amphiphilic diblock copolymers, viz., polyisobutylene-*block*-poly(sodium methacrylate), with a strong cationic polyelectrolyte, viz., exhaustively quaternized poly(4-vinylpyridine), and demonstrated the formation of such micellar IPECs [7-11].

At the same time, interesting complex macromolecular architectures of micellar/vesicular type can result from interpolyelectrolyte complexation performed in organic media, in particular in organic media of low polarity. Schrage *et al.* [12] studied the interaction between polybutadiene-*block*-poly(cesium methacrylate) and polystyrene-*block*-poly(*N*-methyl-4-vinylpyridinium iodide) micelles in THF and demonstrated the formation of complex vesicles (often referred to as “polymersomes”), where the vesicle wall consisted of the IPEC assembled from two oppositely charged polyelectrolyte blocks. Recently [13], we have successfully achieved to match poly(cetyltrimethylammonium acrylate) (PA⁻CTA⁺) and poly(2-(methacryloyloxy)ethyl dimethylethylammonium dodecyl sulfate) (derived from poly(2-(dimethylamino)ethyl methacrylate) via its quaternization with ethyl bromide followed by complexation of the quaternized product with sodium dodecyl sulfate) (PDMAEMAQ⁺DS⁻) and demonstrated for the first time that colloiddally stable in chloroform or even chloroform-soluble macromolecular co-assemblies can result from this process.

To realize interpolyelectrolyte complexation in organic media of low polarity, the insolubility of the ionic polymers in chloroform was advantageously overcome by their prior modification by sufficiently hydrophobic surfactants, leading to efficient substitution of small counterions of those polymers by surfactant counterions. Provided that considerable fraction of the small counterions are substituted by the hydrophobic surfactant counterions, such polyelectrolyte-surfactant complexes (PESCs) can be dissolved in some

low-polar organic solvents [14-17], among which chloroform appears to be the best. Solubility of those PESC is obviously granted by strong affinity of hydrocarbon tails of the surfactant counterions to the organic solvent.

Further direct mixing of organic solutions of two complementary PESC leads to the formation of IPECs, which can be either insoluble [13,18] or soluble [13], depending on the conditions used. We assume [13,18] that interpolyelectrolyte complexation in low-permittivity organic media is predominantly driven by an entropically favorable release of surfactant counterions previously associated with ionic groups on the polymeric components into the bulk solution (in the form of ion pairs or their aggregates). As the electrostatic interaction in organic solvents of low polarity is naturally expected to be very strong, essentially non-equilibrium (“frozen”) IPECs, apparently result from the interaction between such two complementary PESC. Our recent results [8] indicate that the interaction between PA^-CTA^+ and $PDMAEMAQ^+DS^-$ in chloroform leads to the formation of relatively large (aggregated) macromolecular co-assemblies, which appear to be “frozen” vesicles or micelles.

Apart from a fundamental aspect, our interest in the synthesis of IPECs in organic solvents of low polarity is based on the fact that they can be prepared substantially free of water and further almost completely dried from a volatile organic solvent to form fine and highly porous powders, which, for example, are suitable as modifiers and fillers of traditional polymer materials. Additionally, chloroform-soluble IPECs discovered by us recently [13] comprise both IPEC (core) and PESC (corona) compartments, whose fractions can be varied in a broad range, and therefore, from our point of view, might be promising candidates for a design of novel separation membranes, e.g., via casting films from chloroform. Such films, which can be easily prepared, are expected to attractively combine membrane properties of both such complexes within a single material.

In this publication, we report on the interaction of a surfactant-modified ionic amphiphilic diblock copolymer polystyrene-*block*-poly(cetyltrimethylammonium acrylate) ($PS-b-PA^-CTA^+$), with a surfactant-modified homopolyelectrolyte, poly(2-(methacryloyloxyethyl)dimethylethylammonium dodecyl sulfate) ($PDMAEMAQ^+DS^-$), which was derived from poly(2-(dimethylamino)ethyl methacrylate) via its quaternization with ethyl bromide followed by complexation of the quaternized product with sodium dodecyl sulfate, in chloroform. The obtained results strongly suggest that this interaction is a non-equilibrium process and can lead to macromolecular co-assemblies, which are

colloidally stable in chloroform or even chloroform-soluble, if one of the polymeric components is present in the certain excess and apparently have structure of micellar type.

4.2 Experimental Part

4.2.1 Materials

Monomers, *t*-butyl acrylate (*t*-BuA), styrene, and 2-(dimethylamino)ethyl methacrylate (DMAEMA), all donated by BASF SE, were stirred over CaH₂, distilled from CaH₂, and degassed in high vacuum. All other reagents were obtained from Aldrich. CuBr (95%) and CuCl (97%) were purified by stirring in acetic acid overnight. After filtration, they were washed with ethanol, then with ether, and afterwards dried under vacuum. N,N,N',N'',N'''-pentamethyldiethylenetriamine (PMDETA, 99%) and ethyl-2-bromo-2-isobutyrate (EBIB, 98%) were distilled and degassed. 1,1,4,7,10,10-Hexamethyltriethylenetetramine (HMTETA, 97%), *p*-toluenesulfonyl chloride (*p*-TsCl, 99%), trifluoroacetic acid (CF₃COOH, 99%), ethyl bromide (EtBr, 99%), sodium dodecyl sulfate (SDS, 99%), cetyltrimethylammonium bromide, (CTAB) (99%), and chloroform (anhydrous, 99%) were used without further purification.

4.2.2 Synthesis of Polymers

The syntheses of poly(acrylic acid) (PAA, M_n = 30000 g/mol, PDI = 1.08, DP_n = 415) and of poly(2-(dimethylamino)ethyl methacrylate) (PDMAEMA, M_n = 61000 g/mol, PDI = 1.43, DP_n = 390) followed by quaternization of the latter with EtBr to derive poly(2-(methacryloyloxyethyl)dimethylethylammonium bromide) (PDMAEMAQ) are reported elsewhere [13]. Below, we describe in detail the synthesis of diblock copolymers polystyrene-*block*-poly(acrylic acid) (PS-*b*-PAA_x) via atom transfer radical polymerization (ATRP), using polystyrene (PS) as a macroinitiator for polymerization of *t*-BuA, followed by acid-catalyzed hydrolysis of *t*-BuA moieties. All polymerizations were carried out inside a glovebox under nitrogen atmosphere.

4.2.2.1 Synthesis of Polystyrene Macroinitiator.

CuBr (0.2754 g, 1.92 mmol), PMDETA (0.3328 g, 1.92 mmol), styrene (20 g, 0.192 mol) and anisole (10 g, 50 wt%) were added in a round bottom flask and the mixture was stirred until complete dissolution of the copper complex. After the formation of the catalyst, the initiator, EBIB (0.3745 g, 1.92 mmol), was added. The flask was sealed and placed into an oil bath thermostated at 100°C for 2.5 h. The final conversion (48.5%) was determined by means of gas chromatography (GC). The reaction mixture was dissolved in acetone and treated with DOWEX ion exchange resin for 1 h and then passed through a silica column to remove the copper catalyst from the macroinitiator. The solvent was removed by rotating evaporation, the polymer was redissolved in ether and precipitated in methanol; this procedure was repeated twice. The purified PS macroinitiator was dried under vacuum and characterized by means of ^1H NMR and gel permeation chromatography (GPC). The number-average molecular weight of the synthesized PS macroinitiator was $M_{n, \text{PS}} = 8740$ g/mol (PDI = 1.07), i.e., $DP_{n, \text{PS}} = 84$.

4.2.2.2 Synthesis of Polystyrene-block-Poly(acrylic acid) (PS-*b*-PAA_X) Diblock Copolymers.

Syntheses of two precursor polystyrene-*block*-poly(*tert*-butylacrylate) (PS₈₄-*b*-PtBA_X, X denotes the DP_n of the PtBA block) diblock copolymers was carried out under the similar conditions as those described above, except that PS was used as a macroinitiator and placed first together with CuBr. The general procedure is as follows. The PS macroinitiator, CuBr, *t*-BuA, and the solvent (50 wt % anisole) were put into a round-bottom flask. After complete dissolution of the PS macroinitiator, the ligand, PMDETA, was added and an initial sample was taken as a reference to determine the conversion. The flask was finally sealed and placed into an oil bath thermostatted at 60°C. The final conversion was determined by means of GC. The obtained copolymers were purified by the same procedure that was used for the PS macroinitiator, although in this case a water-methanol mixture (50/50 v/v) was used to precipitate the copolymers. Then, the precursor copolymers were analyzed by means of ^1H NMR and GPC; their molecular weight characteristics are given in Table 1. To prepare the PS₈₄-*b*-PAA_X diblock copolymers, the *t*-BuA groups of the precursor copolymers were hydrolyzed for 24 h using a 5-fold excess of CF₃COOH in CH₂Cl₂ at room temperature. The precipitated polymers were separated, washed with CH₂Cl₂, dried under vacuum, and then purified using soxhlet extraction with toluene to remove traces of PS. The quantitative hydrolysis of the *t*-BuA groups of the

prepared copolymers was confirmed by means of ^1H NMR through the disappearance of the signals corresponding to the protons of the *t*-butyl groups ($\delta = 1.5$ ppm). As $\text{PS}_{84}\text{-}b\text{-PAA}_X$ diblock copolymers cannot be directly analyzed by means of GPC in THF, their purity was confirmed using a procedure developed by Zhang *et al.* [19]. Briefly, copolymers are dissolved in THF and the PAA blocks are neutralized with a concentrated solution of NaOH to yield poly(sodium acrylate) (PANa). As is seen, only peak was observed (Fig. 1), which can be reasonably attributed to reversed micelles of the $\text{PS}_{84}\text{-}b\text{-PANa}_X$ diblock copolymers, each comprises a PANa core and a PS corona, which form in THF, hereby indicating successful purification.

Table 1. Experimental Conditions and Results of the Synthesis of $\text{PS}_{84}\text{-}b\text{-PtBA}_X$

$\text{PS}_{84}\text{-}b\text{-PtBA}_X$ copolymer ^a	$[\text{M}]_0:[\text{I}]_0:[\text{Cu}]:[\text{L}]$	$M_{n, \text{PS-}b\text{-PtBA}}$ ^b , g/mol (PDI) ^c	$w_{t\text{-BA}}$, %	w_{AA} , %
$\text{PS}_{84}\text{-}b\text{-PtBA}_{115}$	120:1:1:1	25300 (1.16)	65.5	48.7
$\text{PS}_{84}\text{-}b\text{-PtBA}_{410}$	520:1:1:1	61300 (1.26)	85.7	77.2

^a $M_{n, \text{PS}} = 8740$ g/mol (PDI = 1.07) from GPC analysis in THF using PS calibration. ^bDetermined by ^1H NMR. ^cFrom GPC analysis in THF using PtBA calibration.

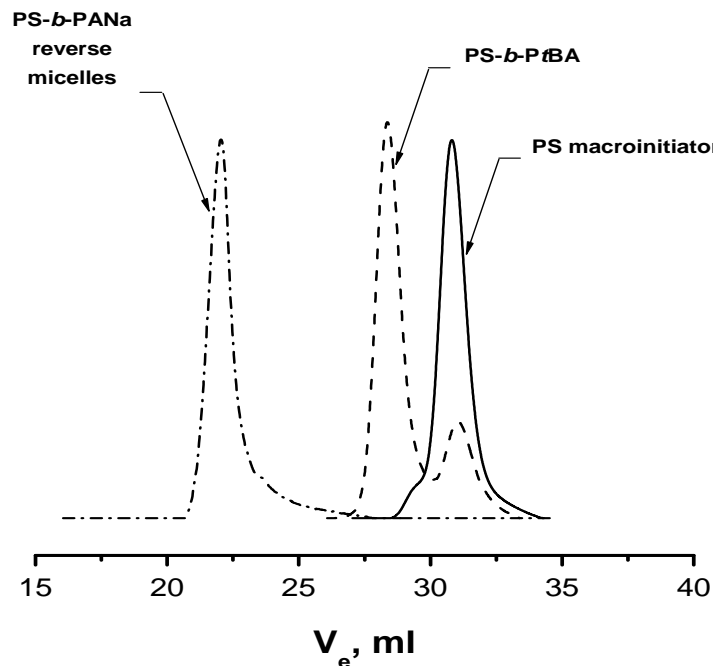


Figure 1. GPC traces of the precursor PS_{84} (—), $PS_{84}\text{-}b\text{-}PtBA_{115}$ (-----) and reverse micelles of $PS_{84}\text{-}b\text{-}PANa_{115}$ (-·-·-·-) after extraction of the residual PS. THF was used as the eluent.

4.2.3 Preparation of Polyelectrolyte-Surfactant Complexes (PESCs)

PDMAEMAQ was dissolved in Millipore water. $PS_{84}\text{-}b\text{-}PAA_x$ diblock copolymers were dissolved upon heating at ca. 100°C under continuous stirring in 0.01 M TRIS·HCl buffer (pH 9) containing the equivalent molar amount (with respect to carboxylic groups of the copolymers) of NaOH. SDS was dissolved in Millipore water while CTAB was dissolved in 0.01 M TRIS·HCl buffer (pH 9). PESCs were successfully synthesized with a yield of more than 90% according to a procedure reported in our previous publication [10]. Specifically, the aqueous solution of the surfactant was added to an aqueous solution of the oppositely charged polyelectrolyte or ionic amphiphilic diblock copolymer at 0.1 M NaCl until 1 : 1 ratio between molar concentrations of ionic groups of the polymeric component and the surfactant was reached. At this concentration ratio, the formed PESCs precipitated. Then, ca 5 % molar excess of the surfactant was added. Afterwards, the PESCs, referred to as $PS_{84}\text{-}b\text{-}(PA^-CTA^+)_x$ and $PDMAEMAQ^+DS^-$, respectively, were filtered under vacuum using a funnel with a glass frit and rinsed with distilled water to remove unreacted surfactant and low molecular weight salt. Next, the PESCs were dried at 40°C for 4 h and then under vacuum at room temperature for 10 days. The degree of substitution of the

small counterions by the corresponding surfactant counterions was determined by means of elemental analysis of nitrogen content for $\text{PS}_{84}\text{-}b\text{-(PA}^-\text{CTA}^+)_x$ while by means of elemental analysis of sulfur and nitrogen contents (S/N ratio) for $\text{PDMAEMAQ}^+\text{DS}^-$ (Table 2). The obtained PESCes easily dissolved in chloroform, yielding absolutely transparent solutions even at rather high polymer concentrations.

Table 2. Results of the Elemental Analysis of PESCes.

PESC	N, % (calc.)	S, % (calc.)	degree of substitution of small counterions, %
$\text{PS}_{84}\text{-}b\text{-(PA}^-\text{CTA}^+)_{115}$	3.27 (3.24)	-	100
$\text{PS}_{84}\text{-}b\text{-(PA}^-\text{CTA}^+)_{410}$	3.69 (3.72)	-	99
$\text{(PA}^-\text{CTA}^+)_{415}$	3.38 (3.90)	-	87 (Ref.[13])
$\text{PDMAEMAQ}^+\text{DS}^-$	2.65 (2.85)	6.08 (6.53)	98 (Ref. [13])

4.2.4. Characterization

Gel Permeation Chromatography (GPC).

Molecular weight distributions were measured by means of GPC with THF or in the case of PDMAEMA with THF containing tetrabutylammonium bromide as the eluents. The instrument was operated at a flow rate of 1.0 mL/min at room temperature. A column set, 5 μ SDV gel, 10²–10⁵ Å, 30 cm each (PSS, Germany), was used together with a differential refractometer and an UV detector operated at the wavelength of 254 nm. PS and poly(*tert*-butyl methacrylate) standards (PSS, Germany) were used for the calibration of the column set.

Turbidimetric Titrations

Measurements were carried out with a Perkin-Elmer Lambda 15 UV/vis spectrophotometer at the wavelength of 500 nm. At this wavelength, the (co)polymers do not absorb light; therefore, optical density values are attributed only to the light scattering. The molar concentrations of a titrand and a titrant in terms of (A^-CTA^+) or $(\text{DMAEMAQ}^+\text{DS}^-)$ were

4.29 mM and 42.9 mM, respectively. The time interval between successive additions of a titrant was equal to 4 min.

Dynamic Light Scattering (DLS).

Size distributions of co-assemblies formed in chloroform mixtures of PS-*b*-(PA⁻CTA⁺)_X and PDMAEMAQ⁺DS⁻ were determined by means of DLS with an ALV DLS/SLS SP 5022F equipment and a He-Ne laser ($\lambda = 632.8$ nm) as a light source. The total polymer concentrations were ranging between 1 and 3 mg/mL. Prior to measurements, sample mixtures were filtered using PTFE filters (Millipore) with a pore size of 1 μ m. The CONTIN program was employed to analyze the autocorrelation functions measured at the scattering angle of 90° and at room temperature.

Static Light Scattering (SLS).

Molecular weight characteristics of co-assemblies formed in chloroform mixtures of PS-*b*-(PA⁻CTA⁺)_X and PDMAEMAQ⁺DS⁻ were determined by means of SLS. A mother mixture of the polymeric components in chloroform at the specified molar mixing ratio $Z^* = 0.4$ between the (A⁻CTA⁺) units and the (DMAEMAQ⁺DS⁻) units, $Z^* = [\text{PA}^- \text{CTA}^+]/[\text{PDMAEMAQ}^+ \text{DS}^-]$, was prepared at the concentration of PDMAEMA⁺DS⁻ in its mixtures with PS-*b*-(PA⁻CTA⁺)_X equal to ca. 2.6 g/L. Then, a set of sample mixtures was prepared by subsequent dilutions of the obtained mother mixture with chloroform to cover a concentration range for PDMAEMA⁺DS⁻ between 0.6 to 2.6 g/L. Afterwards, the sample mixtures were thoroughly filtered using PTFE filters with a pore size of 1 μ m. SLS measurements were carried out at room temperature on a Sofica goniometer equipped with a He-Ne laser ($\lambda = 632.8$ nm). The data were analyzed by Berry extrapolation. Refractive index increments, dn/dc , were measured at room temperature with a differential refractometer (Dn/Dc 2010/620, PSS, $\lambda = 620$ nm). The dn/dc values determined for the interpolyelectrolyte complexes in chloroform PS₈₄-*b*-(PA⁻CTA⁺)_X with PDMAEMAQ⁺DS⁻ at $Z^* = 0.4$ are: 0.029 ± 0.003 for PS₈₄-*b*-(PA⁻CTA⁺)₁₁₅, 0.083 ± 0.001 for PS₈₄-*b*-(PA⁻CTA⁺)₄₁₀, and 0.0266 ± 0.0007 for (PA⁻CTA⁺)₄₁₅.

Transmission Electron Microscopy (TEM).

TEM images were taken using a Zeiss EM 922 transmission electron microscope operated at 200 kV. Typically, a 5 μ L droplet of a sample solution in chloroform was deposited onto a copper TEM grid coated with a carbon film. Zero/loss filtered images ($\Delta E = 0$ eV) were

taken under reduced dose conditions (100–1000 e/nm²). All images were registered digitally by a bottom-mounted CCD camera system (Ultrascan 1000, Gatan, München, Germany) combined and processed with a digital imaging processing system (Digital Micrograph 3.9 for GMS 1.4, Gatan).

4.3 Results and Discussions

4.3.1. Interpolyelectrolyte Complexation in Chloroform

After being thoroughly dried, the PESC_s, PS₈₄-*b*-(PA⁻CTA⁺)_X and PDMAEMAQ⁺DS⁻, prepared as described in the Experimental Section, were each dissolved in anhydrous chloroform, giving absolutely transparent solutions. On addition of a chloroform solution of PDMAEMAQ⁺DS⁻ to a chloroform solution of PS₈₄-*b*-(PA⁻CTA⁺)_X, opalescence appears already at rather low molar mixing ratios, *Z*, between the (DMAEMAQ⁺DS⁻) units and the (A⁻CTA⁺) units, $Z = [\text{PDMAEMAQ}^+ \text{DS}^-] / [\text{PA}^- \text{CTA}^+]$, thus indicating the formation of IPECs assembled from the PA⁻ blocks and PDMAEMAQ⁺ chains, while the surfactant counterions (CTA⁺ and DS⁻) are released into the bulk solution in the form of surfactant ion pairs or their aggregates. Such opalescent mixtures of the complementary PESC_s remain stable on the colloidal level at molar mixing ratios $Z \leq \text{ca } 0.2$ (Fig. 2A). For $Z > 0.6$, the transmittance remains nearly constant with further addition of the titrant. As is also seen, the presence of the PS block in one of the polymeric components does not cause the mixtures of the complementary PESC_s to be less turbid as it might be intuitively expected since chloroform is a good solvent for PS. Moreover, the increasing content of PS in PS₈₄-*b*-(PA⁻CTA⁺)_X for $X = 115$ as compared to $X = 410$ apparently makes such mixtures even more turbid. In the case of addition of a chloroform solution of PS₈₄-*b*-(PA⁻CTA⁺)_X to a chloroform solution of PDMAEMAQ⁺DS⁻, the mixtures of the complementary PESC_s appear to remain transparent or slightly opalescent at molar mixing ratios $Z^* \leq \text{ca } 0.6$ between the (A⁻CTA⁺) units and the (DMAEMAQ⁺DS⁻) units (Fig. 2B), $Z^* = [\text{PA}^- \text{CTA}^+] / [\text{PDMAEMAQ}^+ \text{DS}^-]$. This finding strongly suggests the formation of chloroform-soluble IPECs in the case of at least 1.5-fold or more molar excess of the (DMAEMAQ⁺DS⁻) units in the mixtures of the complementary PESC_s. The excess fragments (tails/loops) of PDMAEMAQ⁺DS⁻ are considered to provide a stabilization effect for the formed IPECs. A similar behavior was observed for a reference system, that

is, for a chloroform solution of PDMAEMAQ⁺DS⁻ titrated with a chloroform solution of (PA⁻CTA⁺)₄₁₅ (cf. Fig. 2B, squares and also Ref. [13]). It is also worthy to emphasize that at $Z^* < 1$ turbidimetric titration curves for chloroform solutions of PDMAEMAQ⁺DS⁻ titrated with chloroform solutions of PS₈₄-*b*-(PA⁻CTA⁺)_X as well as with a chloroform solution of (PA⁻CTA⁺)₄₁₅ demonstrate only small differences.

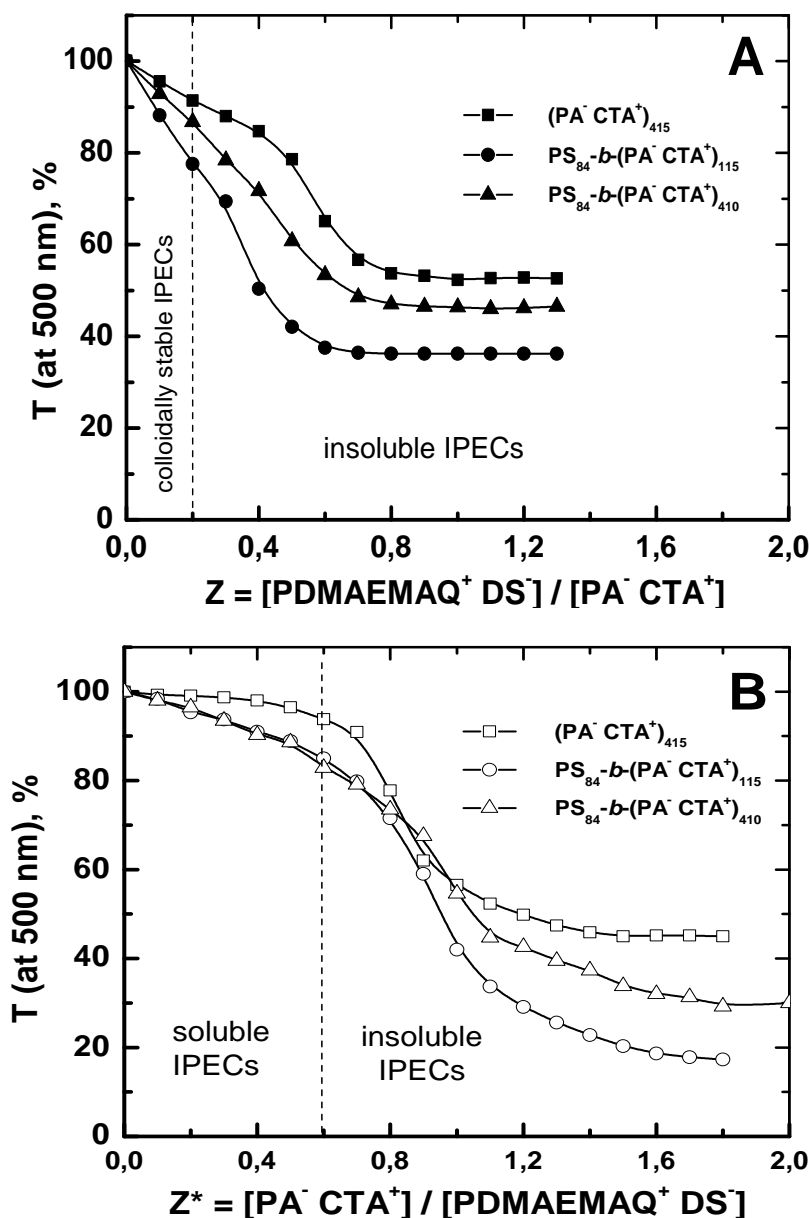


Figure 2. Turbidimetric titration curves of (A) chloroform solutions of PS₈₄-*b*-(PA⁻CTA⁺)_X with a chloroform solution of PDMAEMAQ⁺DS⁻ and (B) a chloroform solution of PDMAEMAQ⁺DS⁻ with chloroform solutions of PS₈₄-*b*-(PA⁻CTA⁺)_X. The turbidimetric titration curves of a chloroform solution of (PA⁻CTA⁺)₄₁₅ with a chloroform solution of PDMAEMAQ⁺DS⁻ or vice versa are also given in both plots for a comparison purpose.

The dashed vertical lines denote boundaries between colloidally stable or soluble IPECs (to the left of) and insoluble IPECs (to the right of).

4.3.2 Characterization of IPECs

Transparent (or slightly opalescent) chloroform mixtures of $\text{PS}_{84-b}\text{-(PA}^-\text{CTA}^+)_x$ and $\text{PDMAEMAQ}^+\text{DS}^-$ were at first examined by means of DLS. Typical size distributions (following from CONTIN analysis of the obtained autocorrelation functions) of the scattering particles formed in mixtures of $\text{PS}_{84-b}\text{-(PA}^-\text{CTA}^+)_x$ and $\text{PDMAEMAQ}^+\text{DS}^-$ at $Z^* = 0.4$ (2.5-fold molar excess of the $(\text{DMAEMAQ}^+\text{DS}^-)$ units) are given in Fig. 3. These distributions are obviously characterized by a dominant contribution to the intensity of the scattered light from particles with $\langle R_h \rangle_z = 75 - 80$ nm. A very similar size distribution was obtained for chloroform mixtures of $(\text{PA}^-\text{CTA}^+)_{415}$ and $\text{PDMAEMAQ}^+\text{DS}^-$ (Fig. 3). In analogy to previous assignments [13] of the scattering particles formed in chloroform mixtures of $(\text{PA}^-\text{CTA}^+)_{415}$ and $\text{PDMAEMAQ}^+\text{DS}^-$, such rather large scattering particles are attributed to aggregated IPECs resulting from the interaction between $\text{PS}_{84-b}\text{-(PA}^-\text{CTA}^+)_x$ and $\text{PDMAEMAQ}^+\text{DS}^-$. Smaller scattering species with $\langle R_h \rangle_z \cong 6$ nm (the mixture of $(\text{PA}^-\text{CTA}^+)_{415}$ with $\text{PDMAEMAQ}^+\text{DS}^-$) or $\langle R_h \rangle_z \cong 20$ nm (the mixture of $\text{PS}_{84-b}\text{-(PA}^-\text{CTA}^+)_{410}$ with $\text{PDMAEMAQ}^+\text{DS}^-$) (indicated by arrows in Fig. 3) could be observed in the corresponding size distributions but give a small or even negligible contribution to the intensity of the scattered light. These much smaller scattering species, as is already mentioned in our previous publication [13], may be considered as either precursors of the large co-assemblies resulting from the secondary aggregation of the initially generated IPECs or single PESC unimers that are not involved in the interpolyelectrolyte complexation.

In the case of IPEC particles formed upon addition of a chloroform solution of $\text{PS}_{84-b}\text{-(PA}^-\text{CTA}^+)_x$ to a chloroform solution of $\text{PDMAEMAQ}^+\text{DS}^-$ (a molar excess of the $(\text{DMAEMAQ}^+\text{DS}^-)$ units), their hydrodynamic radii were found to considerably decrease with lowering Z^* from $Z^* = 0.4$ to $Z^* = 0.2$ (Table 3), thereby presumably indicating the formation of less aggregated IPECs, which therefore comprise lower numbers of macromolecules of the constituting polymeric components. It is also interesting that the values of $\langle R_h \rangle_z$ of the aggregated IPECs in chloroform mixtures of $\text{PS}_{84-b}\text{-(PA}^-\text{CTA}^+)_x$ or $(\text{PA}^-\text{CTA}^+)_{415}$ with $\text{PDMAEMAQ}^+\text{DS}^-$ appear to be only marginally dependent on whether IPEC species are formed at the 5-fold molar excess of the $(\text{DMAEMAQ}^+\text{DS}^-)$

units ($Z^* = 0.2$) or at the 5-fold molar excess of the (A^-CTA^+) units ($Z = 0.2$) in the mixtures of the complementary PESCs.

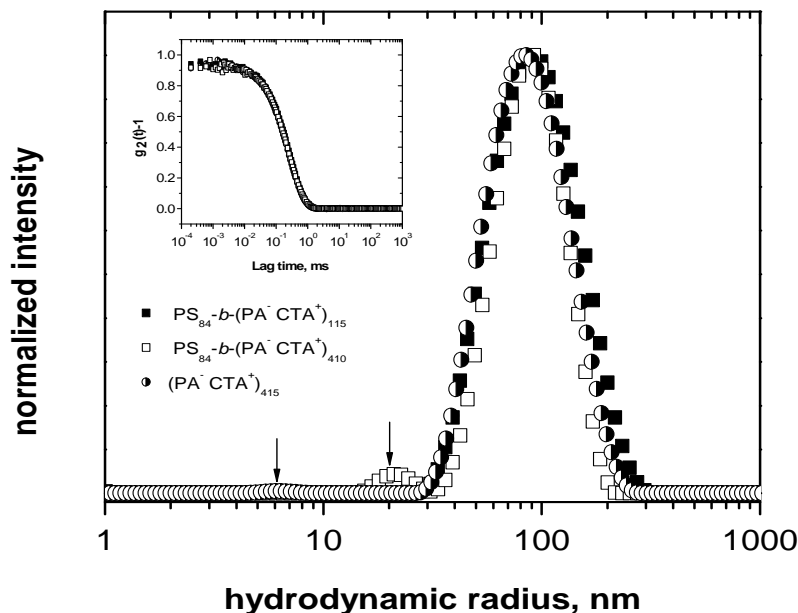


Figure 3. Intensity-weighted distributions of apparent hydrodynamic radii, $\langle R_h \rangle_z$, of the scattering particles formed in chloroform mixtures of $PS_{84}\text{-}b\text{-}(PA^-CTA^+)_X$ and $PDMAEMAQ^+DS^-$ at $Z^* = 0.4$ (2.5-fold molar excess of the ($DMAEMAQ^+DS^-$) units). The corresponding size distribution for the chloroform mixture of $(PA^-CTA^+)_{415}$ is also given for a comparison purpose. Total concentration of $PDMAEMAQ^+DS^-$ (the excess polymeric component) was equal to 2.6 g/L.

Table 3. Apparent hydrodynamic radii, $\langle R_h \rangle_z$, of the aggregated IPECs formed in the chloroform mixtures of $PS_{84}\text{-}b\text{-}(PA^-CTA^+)_X$ with $PDMAEMAQ^+DS^-$

	$\langle R_h \rangle_z$, nm $Z^* = 0.2$	$\langle R_h \rangle_z$, nm $Z^* = 0.4$	$\langle R_h \rangle_z$, nm $Z = 0.2$
$PS_{84}\text{-}b\text{-}(PA^-CTA^+)_{115}$	42	80	44
$PS_{84}\text{-}b\text{-}(PA^-CTA^+)_{410}$	51	76	61
$(PA^-CTA^+)_{415}$	64	76	65

Since small scattering particles give only a minor contribution to the intensity of the scattered light, SLS measurements to evaluate the molecular weight characteristics of the

large co-assemblies formed upon the interaction between $\text{PS}_{84}\text{-}b\text{-(PA}^-\text{CTA}^+)_x$ and $\text{PDMAEMAQ}^+\text{DS}^-$ are feasible. As a representative example, Fig. 4 shows a typical Berry plot for the chloroform mixture of $\text{PS}_{84}\text{-}b\text{-(PA}^-\text{CTA}^+)_{115}$ with $\text{PDMAEMAQ}^+\text{DS}^-$ at $Z^* = 0.4$ (2.5-fold molar excess of the $(\text{DMAEMAQ}^+\text{DS}^-)$ units). Extrapolations of $(Kc/R)^{1/2}_{\Theta \rightarrow 0}$ and $(Kc/R)^{1/2}_{c \rightarrow 0}$ are close to linear within the used concentration range. Besides, DLS measurements do not give any evidence for considerable changes of hydrodynamic size of the IPEC species, at least in the concentration range from 1 to 3 g/L with respect to $\text{PDMAEMA}^+\text{DS}^-$. Thus, both SLS and DLS measurements suggest that the IPECs formed in chloroform are stable macromolecular co-assemblies, which demonstrate no tendency to their disintegration or dissociation upon dilution of the system with chloroform. This is naturally expected, as the Coulomb attraction in organic media of low permittivity is very strong.

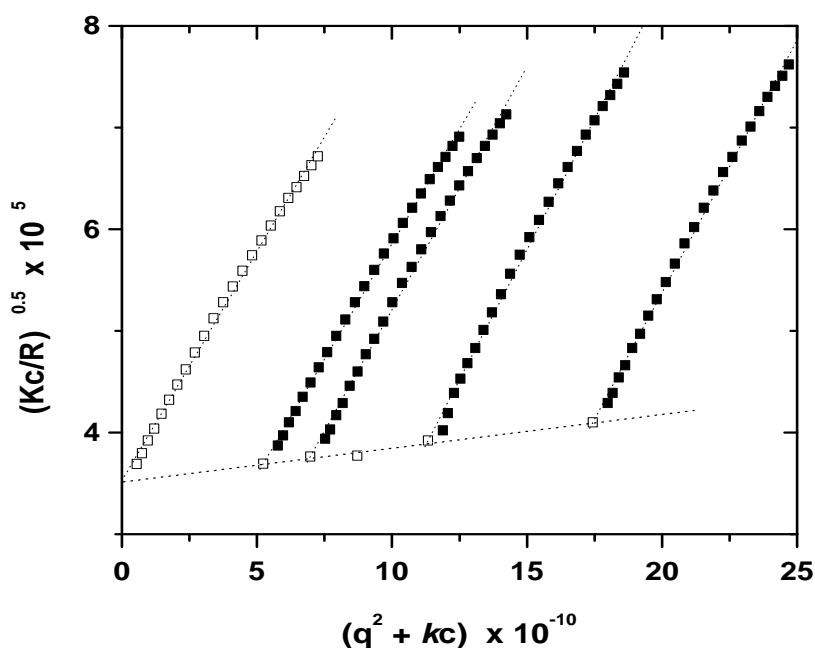


Figure 4. Typical Berry plot obtained for the chloroform mixture of $\text{PS}_{84}\text{-}b\text{-(PA}^-\text{CTA}^+)_{115}$ and $\text{PDMAEMAQ}^+\text{DS}^-$ at $Z^* = 0.4$ (2.5-fold molar excess of the $(\text{DMAEMAQ}^+\text{DS}^-)$ units).

Table 4 shows that the weight-average molecular weights, M_w , of the formed IPEC species are within $M_w = 10^8 - 10^9$ g/mol, at least three orders of magnitude higher than those of the precursor PESC. This finding provides clear evidence for interpolyelectrolyte complexation and suggests that the co-assemblies formed comprise a large number of

macromolecules of the constituting polymeric components. The positive values of the second virial coefficient ($A_2 = 10^{-7} - 10^{-6} \text{ mol ml/g}^2$), indicate that chloroform should be a good solvent for the IPEC species formed. The ratio $\rho = \langle R_g^2 \rangle^{0.5} / R_h$, which characterizes the shape of the scattering particles, ranges from 1.18 to 1.24, thus being in good agreement with the values for star-shaped polymers with a high number of arms [20]. At the same time, the decreasing length of the $\text{PA}^- \text{CTA}^+$ block in the polymeric component to be interacted with $\text{PDMAEMAQ}^+ \text{DS}^-$ significantly decreases molecular weight of the IPEC species, thus indicating smaller number of macromolecules of the constituent polymeric components incorporated into them.

Table 4. SLS/DLS results for the IPEC particles formed in the chloroform mixtures of $\text{PS}_{84}\text{-}b\text{-(PA}^- \text{CTA}^+)_x$ with $\text{PDMAEMAQ}^+ \text{DS}^-$ at $Z^* = 0.4$ (2.5-fold molar excess of the $(\text{DMAEMAQ}^+ \text{DS}^-)$ units)

	10^{-8} M_w , g/mol	$10^{-3} N_{\text{agg}}$ ($N_{\text{PS-}b\text{-PA}^-} +$ $N_{\text{PDMAEMAQ}^+/\text{PDMAEMAQ}^+ \text{DS}^-}$)	$10^7 A_2$, mol ml/g ²	$\langle R_h \rangle_z$, nm	$\langle R_g^2 \rangle^{0.5}$, nm	ρ
$\text{PS}_{84}\text{-}b\text{-(PA}^- \text{CTA}^+)_{115}$	3.05	4.6 (2.6 + 8.9)	5.16	80	94	1.18
$\text{PS}_{84}\text{-}b\text{-(PA}^- \text{CTA}^+)_{410}$	9.60	8.9 (2.5 + 6.4)	8.46	76	90	1.18
$(\text{PA}^- \text{CTA}^+)_{415}$	2.29	2.2 (0.6 + 1.6)	1.24	76	95	1.24

From the values of M_w given in Table 4, we estimate the total number of polymer chains in each particle, N_{agg} . Here we assume that the molar stoichiometry of the formed IPEC coincides with the molar mixing ratio of the complementary polymeric components and all surfactant counterions of those $(\text{DMAEMAQ}^+ \text{DS}^-)$ and $(\text{A}^- \text{CTA}^+)$ units that form interpolymer salt bonds are released. The estimated numbers of $\text{PS-}b\text{-PA}^-$ and $\text{PDMAEMAQ}^+/\text{PDMAEMAQ}^+ \text{DS}^-$ chains in each complex are given in parentheses. Under the assumptions made, the numbers represent upper limits. To determine N_{agg} , we

first calculate the theoretical molecular weight, M_{calc} , for an IPEC comprising only one chain of $\text{PS-}b\text{-PA}^-$, taking into account a 2.5-fold molar excess of the $(\text{DMAEMAQ}^+ \text{DS}^-)$ units over $(\text{A}^- \text{CTA}^+)$ units in the mixture of the complementary PESC at $Z^* = 0.4$:

$$M_{\text{calc}} = M_{\text{PS}} + \text{DP}_{\text{PAA}} M_{(\text{DMAEMA}^+ \text{A}^-)} + \text{DP}_{\text{PAA}} \left(\frac{1}{Z^*} - 1 \right) M_{(\text{DMAEMA}^+ \text{DS}^-)} \quad (1)$$

Then $N_{\text{PS-}b\text{-PA}^-}$ is calculated as

$$N_{\text{PS-}b\text{-PA}^-} = \frac{M_w}{M_{\text{calc}}} \quad (2)$$

and $N_{\text{PDMAEMAQ}^+/\text{PDMAEMA}^+ \text{DS}^-}$ is given by

$$N_{\text{PDMAEMAQ}^+/\text{PDMAEMA}^+ \text{DS}^-} = N_{\text{PS-}b\text{-PA}^-} Z^* \frac{\text{DP}_{\text{PAA}}}{\text{DP}_{\text{PDMAEMAQ}}} \quad (3)$$

The estimated values of N_{agg} are also presented in Table 4, indicating that the formed IPEC species appear to be built up from thousands of chains of the polymeric components. It is surprising that the presence of the PS block in one of the polymeric components does not facilitate the formation of less aggregated IPEC species in chloroform. Indeed, the values of N_{agg} for IPECs formed in the mixtures of $\text{PDMAEMAQ}^+ \text{DS}^-$ and $\text{PS}_{84}\text{-}b\text{-}(\text{PA}^- \text{CTA}^+)_{\text{X}}$ considerably exceed those IPECs formed in the mixture of $\text{PDMAEMAQ}^+ \text{DS}^-$ and $(\text{PA}^- \text{CTA}^+)_{415}$ (Table 4). This finding manifests a strong tendency of $(\text{PDMAEMAQ}^+ \text{PA}^-)$ fragments to aggregation despite of the presence of excess $\text{PDMAEMAQ}^+ \text{DS}^-$ fragments and PS blocks, both $\text{PDMAEMAQ}^+ \text{DS}^-$ fragments and PS blocks being well-soluble in chloroform.

The morphology of IPEC species formed in chloroform mixtures of $\text{PS}_{84}\text{-}b\text{-}(\text{PA}^- \text{CTA}^+)_{410}$ and $\text{PDMAEMAQ}^+ \text{DS}^-$ at $Z^* = 0.4$ (2.5-fold molar excess of the $(\text{DMAEMAQ}^+ \text{DS}^-)$ units) was also investigated by means of TEM. The obtained micrographs (Fig. 5) indicate particles of close to spherical shape (sometimes deformed spherical shape), apparently with inhomogeneous structure. Furthermore, the observed species are characterized by a rather broad size distribution ($\langle R_{\text{TEM}} \rangle_n = 34 \pm 9$ nm as calculated from Fig. 5B for 136 objects). The TEM micrographs obtained for a comparison purpose for the precursor PESC, $\text{PS}_{84}\text{-}b\text{-}(\text{PA}^- \text{CTA}^+)_{\text{X}}$ and $\text{PDMAEMAQ}^+ \text{DS}^-$ (results are not shown), demonstrate no objects similar to those seen in Fig. 5. The high polydispersity

of IPECs generated in such systems may be reasonably attributed to the formation of substantially “frozen” structures in low-polarity organic media. The fact that the value of $\langle R_{\text{TEM}} \rangle_n$ is ca 2-times lower than the value of $\langle R_h \rangle_z$ can be attributed to a collapse of the IPEC species upon drying as well as the different averages. The inhomogeneity of the observed species might be attributed to incidental entrapping of PS blocks into a core assembled from the oppositely charged fragments of PA^- and PDMAEMAQ^+ as a consequence of the pronounced non-equilibrium character of the interpolyelectrolyte complexation in low-polarity organic solvents.

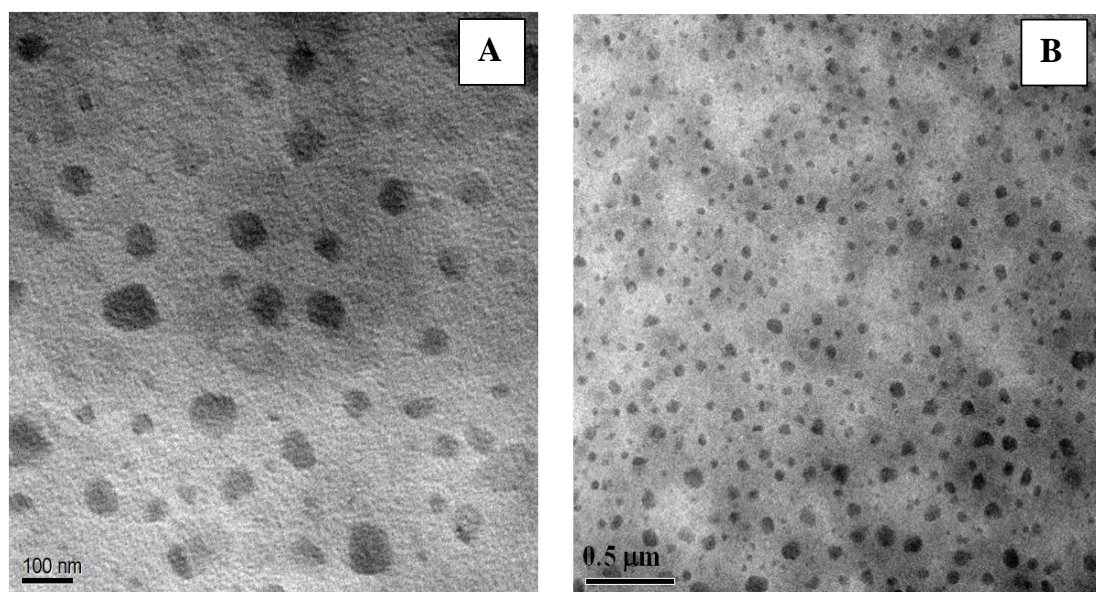


Figure 5. TEM images of IPEC particles formed in the chloroform mixture of $\text{PS}_{84}\text{-}b\text{-(PA}^-\text{CTA}^+)_{410}$ and $\text{PDMAEMAQ}^+\text{DS}^-$ at $Z^* = 0.4$ (2.5-fold excess of the $(\text{DMAEMAQ}^+\text{DS}^-)$ units).

4.3.3. Tentative Structure of IPECs

We anticipated that the interaction between the complementary PESC in the excess of one of the polymeric components would result in macromolecular co-assemblies of a micellar (core-corona) type. A rather compact core assembled from the oppositely charged fragments of PA^- and PDMAEMAQ^+ substantially represents a stoichiometric IPEC comprising the opposite charges of the polymeric components in ca 1 : 1 ratio. In the excess of $\text{PS}_{84}\text{-}b\text{-(PA}^-\text{CTA}^+)_x$, the solubilizing corona should be formed by the PS blocks and those fragments of the PA^-CTA^+ blocks, which are not involved in the

interpolyelectrolyte complexation (Fig. 6, right structure). In the excess of PDMAEMAQ⁺DS⁻, the solubilizing corona comprises both the PS blocks and those fragments of the PDMAEMAQ⁺DS⁻ blocks, which are not involved in the interpolyelectrolyte complexation (Fig. 6, left structure). Thus, the macromolecular co-assemblies formed due to the interaction between PS₈₄-*b*-(PA⁻CTA⁺)_x and PDMAEMAQ⁺DS⁻ in chloroform can be considered as peculiar IPEC/(PESC/PS) nanoparticles of core-corona type, each comprising an IPEC core surrounded by a mixed PESC/PS corona. At the same time, we cannot exclude the possibility that a certain part of the PS blocks is incidentally entrapped into the core assembled from the oppositely charged fragments of PA⁻ and PDMAEMAQ⁺. Indeed, the Coulomb attraction between such oppositely charged fragments is very strong in low-polarity organic media, such as chloroform ($\epsilon = 4.8$), thereby leading to substantially non-equilibrium, “frozen” and therefore non-ideal structures, which cannot rearrange once they are formed. Such entrapment of the PS blocks into (PA⁻PDMAEMAQ⁺) cores of the resultant macromolecular co-assemblies may explain, at least partially, their somewhat inhomogeneous structure, which is apparently observed in the TEM images (Fig. 5).

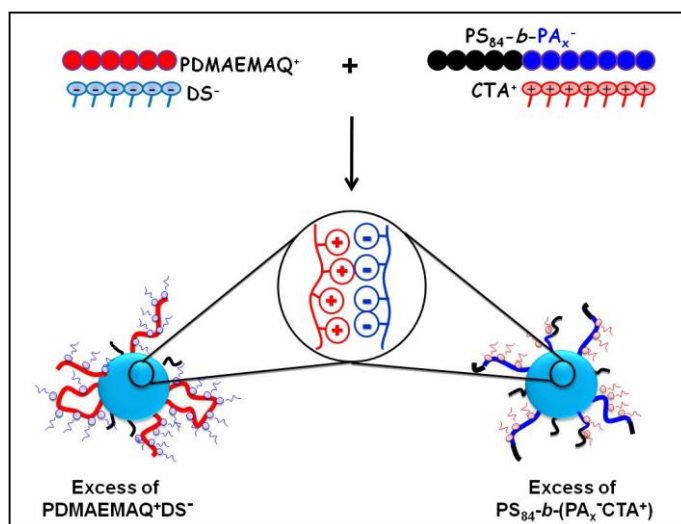


Figure 6. Schematic representation of tentative, idealized structures of macromolecular co-assemblies formed in chloroform mixtures of PS₈₄-*b*-(PA⁻CTA⁺)_x and PDMAEMAQ⁺DS⁻.

4.4 Conclusions

We demonstrate the formation of novel macromolecular co-assemblies with hydrodynamic radii in the range of 40 – 80 nm due to the interaction between two

complementary PESC, viz., $\text{PS}_{84}\text{-}b\text{-(PA}^-\text{CTA}^+)_x$ and $\text{PDMAEMAQ}^+\text{DS}^-$, in chloroform. Such co-assemblies can be either colloiddally stable or even soluble if one of the PESC is present in the system in the certain excess. We suggest the formed colloiddally stable or soluble co-assemblies to be aggregates of micellar type with an IPEC core surrounded by apparently a mixed PESC/PS corona, which grants such co-assemblies solubility in chloroform (good solvent for both PESC and PS). As the electrostatic interaction in low-permittivity organic media is naturally expected to be very strong, the described above co-assemblies are most likely non-equilibrium (“frozen”) macromolecular architectures, whose IPEC cores may contain quite a few PS blocks incidentally entrapped upon the formation of the complex species. Overall, the co-assemblies formed in the chloroform mixtures of $\text{PS}_{84}\text{-}b\text{-(PA}^-\text{CTA}^+)_x$ and $\text{PDMAEMAQ}^+\text{DS}^-$ at Z (or Z^*) $\neq 1$ apparently represent peculiar compartmentalized nanoparticles of core-corona type, which due to the presence of both IPEC (core) and PESC (corona) compartments may possess a number of unique properties and promising applications.

Acknowledgements.

This work was supported by the EU Marie Curie Research and Training Network POLYAMPHI, (project No. EU MCRTN-CT-2003-505027). The authors thank Jeannine Roksel for measuring TEM. D.V.P. thanks the Deutsche Forschungsgemeinschaft for the financial support of his research stays at Universität Bayreuth,

References

1. Smid J, Fish D in: Mark HF, Bikales NM, Overberger CG, Menges G, editors. Encyclopedia of Polymer Science and Engineering, vol. 11. New York: Wiley, 1988. pp. 720-739.
2. Kabanov VA, Zezin AB. Pure Appl. Chem. 1984; 56:343-354.
3. Philipp B, Dautzenberg H, Linow K-J, Kötze J, Dawydoff W. Prog. Polym. Sci. 1989; 14:91-172.
4. Kabanov VA in: Dubin P, Bock J, Davies RM, Schulz DN, Thies C, editors. Macromolecular complexes in chemistry and biology, Berlin: Springer 1994. pp. 151-174.
5. Thünemann AF, Müller M, Dautzenberg H, Joanny JF, Löwen H. Adv. Polym. Sci. 2004; 166:113-171.
6. Förster S, Abetz V, Müller AHE. Adv. Polym. Sci. 2004; 166:173-210.

7. Pergushov DV, Borisov OV, Zezin AB, Müller AHE. *Adv. Polym. Sci.* 2011; 241: 131-61, DOI: 10.1007/12_2010_102.
8. Pergushov DV, Remizova EV, Feldthusen J, Zezin AB, Müller AHE, Kabanov VA. *J. Phys. Chem. B* 2003; 107:8093-8096.
9. Pergushov DV, Remizova EV, Gradzielski M, Lindner P, Feldthusen J, Zezin AB, Müller AHE, Kabanov VA. *Polymer* 2004; 45:367-378.
10. Pergushov DV, Gradzielski M, Burkhardt M, Remizova EV, Zezin AB, Kabanov VA, Müller AHE. *Preprints (American Chemical Society, Division of Polymer Chemistry)* 2004, 45:236-237.
11. Burkhardt M, Ruppel M, Tea S, Drechsler M, Schweins R, Pergushov DV, Gradzielski M, Zezin AB, Müller AHE. *Langmuir* 2008; 24:1769-1777.
12. Schrage S, Sigel R, Schlaad H. *Macromolecules* 2003; 36:1417-1420.
13. Penott-Chang EK, Pergushov DV, Zezin AB, Müller AHE. *Langmuir* 2010; 26:7813-7818.
14. Bakeev KN, Yang MS, Zezin AB, Kabanov AV. *Doklady Akademii Nauk* 1993; 332:450-453.
15. Bakeev KN, Shu YM, MacKnight WJ, Zezin AB, Kabanov VA. *Macromolecules* 1994; 27:300-302.
16. Bakeev KN, Shu YM, Zezin AB, Kabanov VA, Lezov AV, Mel'nikov AB, Kolomiets IP, Rjuntsev EI, MacKnight WJ. *Macromolecules* 1996; 29:1320-1325.
17. Lysenko EA, Bronich TK, Eisenberg A, Kabanov VA, Kabanov AV. *Macromolecules* 1998; 31:4511-4515.
18. Pergushov DV, Remizova EV, Zezin AB, Kabanov VA. *Doklady Physical Chemistry* 2006; 406(Part 2):38-42.
19. Zhang LF, Eisenberg A. *J. Polymer Science Part B: Polymer Physics* 1999; 37:1469-1484.
20. Burchard W. *Adv. Polym. Sci.* 1999; 143:113-194.

5. AMPHIPHILIC DIBLOCK COPOLYMER AND POLYCAPROLACTONE BLENDS TO PRODUCE NEW VESICULAR NANOCARRIERS

*Evis Penott-Chang,^{a,d} Andreas Walther,^a Pierre Millard,^a Alessandro Jäger,^b
Eliezer Jäger,^b Axel H. E. Müller,^{a,*} Silvia S. Guterres,^b Adriana R. Pohlmann^{c,*}*

^a Makromolekulare Chemie II, Universität Bayreuth, D-95440 Bayreuth, Germany

^b Faculdade de Farmácia, Universidade Federal do Rio Grande do Sul, UFRGS, Porto Alegre 91501-970, Brazil

^c Departamento de Química Orgânica, Instituto de Química, Universidade Federal do Rio Grande do Sul, UFRGS, Porto Alegre 91501-970, Brazil

^d Grupo de Polímeros USB, Departamento de Ciencia de los Materiales, Universidad Simón Bolívar, Caracas 1080A, Venezuela

Corresponding Authors and Mailing Address:

Prof. Dr. Axel Müller:

Lehrstuhl für Makromolekulare Chemie II.

Universität Bayreuth Universitätsstr. 30.

Gebäude NW II D-95447 Bayreuth

Telephone: +49 921 553399

Fax: +49 921 553393. **Email:** axel.mueller@uni-bayreuth.de

Prof. Dr. Adriana Pohlmann

Universidade Federal Do Rio Grande Do Sul – UFRGS

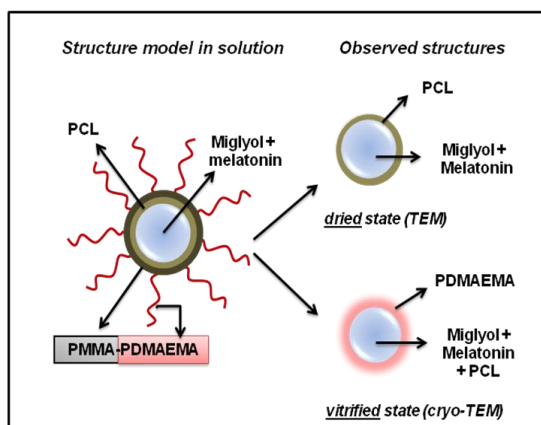
Dpto. Química Orgânica-Instituto de Química

CP 15003 Av. Bento Gonçalves,
9500 Porto Alegre, RS 91501-970

Telephone: +55 51 33087237

Fax: +55 51 33087304

Email: pohlmann@iq.ufrgs.br



Accepted in J. Biomed. Nanotech., March 2011

Abstract

New Melatonin-loaded vesicular nanocarriers were prepared by interfacial deposition using a blend of an amphiphilic diblock copolymer, poly(methyl methacrylate)-*block*-poly(2-(dimethylamino)ethyl methacrylate), PMMA-*b*-PDMAEMA, with poly(ϵ -caprolactone), PCL. Particle size and morphology of the nanocarriers was evaluated. Dynamic light scattering shows that the nanocarriers have hydrodynamic radii between 100 and 180 nm, with unimodal particle size distribution for each formulation. Shape and structure were visualized by transmission electron microscopy (TEM), cryogenic TEM and scanning electron microscopy. Standard TEM for nanocapsules showed an oily core surrounded by a thin layer composed by PCL/PMMA-*b*-PDMAEMA. Cryo-TEM also indicated the presence of spherical nanoobjects with a diffuse polymer corona. Encapsulation efficiencies were determined assaying the nanoparticles by HPLC and higher values of ca. 25% are shown by the nanocapsules. We could successfully incorporate platinum nanoparticles into the nanocarrier as evidenced by TEM, which opens up the possibility for promising applications like monitoring the encapsulated drug in the body.

Keywords: *nanocapsules, amphiphilic block copolymer, caprolactone, PDMAEMA, melatonin, cryo-TEM, DLS,*

5.1. Introduction

Polymeric nanoparticles refer to nanocarriers prepared using polymers, i.e., nanocapsules and nanospheres. A nanocapsule (NC) has a vesicular structure, composed of a central oil core surrounded by a thin polymer wall, whereas a nanosphere (NS) only consists of a polymer matrix. NC and NS are stabilized by surfactants at the particle/water interface, preventing particle agglomeration and/or drug leakage. These colloidal systems (NC and NS) can be prepared either by polymerization of dispersed monomers, so called interfacial polymerization, or using pre-formed polymers by nanoprecipitation, also called interfacial deposition or solvent displacement,^{1,2} solvent evaporation,³ or emulsion-diffusion techniques.⁴ By interfacial polymerization, alkyl cyanoacrylate monomers have been commonly used.^{5,6} Here, the cyanoacrylate monomer is polymerized in the presence of the lipophilic drug. Both monomer and drug are previously dissolved in a mixture of oil and lipophilic solvent. Moreover, the presence of residual monomers or oligomer, as well as the cross-reaction between the components might limit the potential of the nanocapsules. This problem was overcome by Fessi by means of interfacial deposition of preformed polymers.¹ Nanocapsules are formed instantaneously by the fast diffusion of a water-miscible solvent with the polymer, drug and oil into an aqueous solution. In general mixture of surfactants and/or stabilizers is used to avoid drug leakage and/or flocculation and sedimentation of particles.

Some free or unencapsulated oral administered drugs have shown a low bioavailability that can mainly be attributed to the premature degradation and/or poor solubility of drugs in the gastrointestinal tract. In the literature, there are several reports on the encapsulation of some drugs has enhanced the absorption and bioavailability compared to oral-free drugs.⁷⁻¹⁰ The development of drug delivery systems from biodegradable polymers has been gaining great interest because of their multiple advantages for a better control of drug release to achieve a more effective therapy against some diseases. These systems help to minimize drug degradation, reduce its toxicity after the administration, keep the drug level in a desired range and increase the drug availability at the disease site. Drug carriers can include micelles, liposomes, polymeric nanoparticles and nanoemulsions.¹¹⁻¹⁴

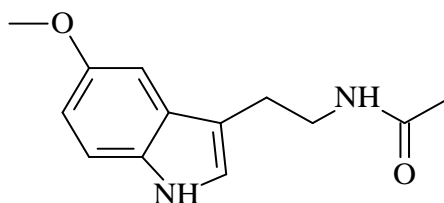
The aim of this work was to obtain a new vesicular nanocarrier using a blend of poly(epsilon-caprolactone), PCL, and poly(methyl methacrylate)-*b*-poly(2-dimethylaminoethyl methacrylate), PMMA-*b*-PDMAEMA. PCL is a linear polyester

widely use as polymer wall in NC, whereas PMMA-*b*-PDMAEMA has been reported to form micelles in aqueous media, for neutral or cationic PDMAEMA block.¹⁵⁻¹⁷ Amphiphilic diblock copolymers have been widely used due to their promising applications.^{13,18-20} Our strategy is based on the hypothesis that a new generation of vesicular carrier can be built directly by the mixture of both polymers in acetone with no need of any surfactant, like polysorbates, phospholipids, sorbitan monostearate or sorbitan monooleate, or stabilizer, as poly(ethyleneglycol) or poloxamers, among others. PMMA-*b*-PDMAEMA was chosen because of its ability to anchor at the polymer wall of nanocapsules and to interact with water at the interface. This diblock presents good solubility in acetone, a solvent which can diffuse through water, allowing the preparation of those new vesicular nanocarriers under similar conditions previously used to obtain conventional NC. The hydrophilic PDMAEMA is a pH and temperature-sensitive polymer with lower critical solution temperature (LCST),²¹ and it is gaining great interest in the industrial and research field because its potential applications as emulsion and dispersion stabilizer, flocculants for water and wastewater treatment, drug delivery, etc.²²⁻²⁴ For instance, the amino function in the PDMAEMA chain can be complexed with metallic nanoparticles as a potential way to monitor particle migration inside the body. In the particular case of polymeric nanocarriers, it can lead to avoid the use of hydrophilic low molecular weight surfactants as stabilizers, traditionally employed for this type of formulations, and it might improve the absorption of orally administered drugs, as shown by Sakuma, who demonstrated that the presence of hydrophilic polymeric chains onto hydrophobic polystyrene surfaces can enhance the absorption in the intestine of orally administered salmon calcitonin.²⁵⁻²⁷ In our first attempt using the PCL/PMMA-*b*-PDMAEMA block copolymer blend, the new vesicular nanocarriers were prepared by interfacial deposition technique. In order to evaluate the ability of those nanocarriers in encapsulating lipophilic drugs, melatonin was used as drug model, due to its relevance in the field of Health Sciences.

The hormone melatonin, N-acetyl-5-methoxytryptamine, (Chart 1), is a major product of the pineal gland in our brain. This hormone is synthesized in our body during the night, and its production decreases with age and has an important role in the regulation of physiological processes like circadian and seasonal changes.²⁸ It is a well-known antioxidant and a free radical scavenger^{29,30} as well as a suppressor of lipid peroxidation.³¹ Furthermore, its properties have been investigated to treat sleep disorders,^{32,33} and

neurodegenerative diseases,³⁴⁻³⁶ such as Alzheimer, Parkinson and Huntington. Additionally, it is adopted as anti-inflammatory and anti-cancer agent.³⁷

Chart 1. Melatonin Structure.



Melatonin has a short half-life of less than 1 hour and a nocturnal secretion pattern over 8 h. When administered orally, it shows a low and variable bioavailability and hence is not a good candidate for conventional immediate-release oral technology. As such, much of the current efforts have been focused on the development of sustained release forms for melatonin.^{38,39} It has been reported that exogenous controlled-release melatonin formulations are clinically more useful for sleep maintenance than fast released melatonin formulations.³² Tusilli⁴⁰ reported that the photostability of melatonin could be enhanced by its encapsulation into lipid microspheres. El-Gibaly *et al.*,³⁹ investigated melatonin-loaded microparticles with a hollow core, which presented encapsulation efficiencies between 36.9-56.2%. They could also evaluate its efficacy against cases of aflatoxicosis, where melatonin microcapsules appeared to be more effective in the reduction of the apoptotic rate than free melatonin.

Melatonin-loaded nanoparticles have been reported by Schaffazick *et al.*^{41,42} The encapsulation was carried out using Eudragit S100[®], and it was demonstrated that c.a. 55% of the drug can be encapsulated inside nanocapsules and nanospheres, and 32% in the nanoemulsions. Additionally, nanoparticulates showed a notable increase in the antioxidant properties of melatonin against lipid peroxidation.

To ensure the quality of the new vesicular nanocarrier suspensions, the colloids were characterized using dynamic light scattering (DLS), probe content (HPLC), standard and cryogenic transmission electron microscopy (TEM and cryo-TEM) and scanning electron microscopy (SEM).

5.2. Experimental Section

5.2.1 Materials

Two amphiphilic diblock copolymers poly(methyl methacrylate)-*b*-poly(2-dimethylaminoethyl methacrylate) ($M_{40}D_{108}$ and $M_{40}D_{471}$), with the same PMMA block length were synthesized by the ATRP technique. All other chemicals were purchased and used without any further purification: Poly(ϵ -caprolactone), PCL ($M_w = 65.000$ g/mol, Aldrich). Miglyol 810[®] (caprylic/capric triglyceride, oil phase, Hulls, France), melatonin (99% purity, Acros Organic).

5.2.2 Synthesis of Poly(methyl methacrylate) macroinitiator

Polymerization was carried out as reported by Matyjaszewski *et al.*⁴³ Methyl methacrylate monomer (20 g, 0.2 mol) was added to a round bottom flask containing CuCl (19.8 mg, 0.2 mmol), 4,4'-di(5-nonyl)-2,2'-bipyridyl (dNbpy) (81.8 mg, 0.2 mmol) and anisole (10.0 g, 50 wt%). *p*-toluene sulfonyl chloride, *p*-TsCl, (0.381 g, 2.0 mmol) was used and initiator and a first sample was removed for conversion determination. The flask was sealed with a plastic cap and reaction solution was immersed into an oil bath thermostated at 90 °C for 5h. Final conversion was determined by GC.

5.2.3 Synthesis of Poly(methyl methacrylate)-*b*-poly(2-dimethylaminoethyl methacrylate)

DMAEMA was copolymerized using PMMA as macroinitiator, CuCl and 1,1,4,7,10,10-hexamethyltriethylenetetramine, HMTETA, as catalyst system in anisole. The flask was sealed with a plastic cap, and immersed into an oil bath at 90 °C. Conversion was determined by GC and the polymer was purified first by passing it through a silica column using THF as eluent to remove the catalyst and then precipitating the copolymer into hexane. The copolymers were characterized by ¹H-NMR and GPC. Table 1 shows the chemical characterization and compositions for both copolymers.

TABLE 1. Molecular Characterization of PMMA-*b*-PDMAEMA

Polymer	M_{n, PMMA}^a (PDI)	M_{n, diblock}^b (PDI)^b	^bComposition (%PMMA)
M ₄₀ D ₁₀₈	4.000 (1.11)	21.000 (1.15)	23%
M ₄₀ D ₄₇₁	4.000 (1.11)	78.000 (1.11)	6%

a) From GPC analysis in THF using PMMA calibration.

b) From ¹H-NMR analysis.

5.2.4 Preparation and Loading of Nanocapsules

Nanocapsules were prepared by interfacial deposition in water. Different copolymer/PCL ratios were employed, an example is as follow: First, the copolymer (100 mg) and PCL (30mg) were dissolved in acetone (27 mL) at 40 °C, after complete polymer dissolution, Miglyol 810[®] (50 μL) and melatonin (5 mg) were added to the mixture. Then, the organic solution was slowly added into MilliQ[®] water (53 mL) under constant magnetic stirring at room temperature for 30 min. Afterwards acetone was removed by rotating evaporation and the aqueous solution was concentrated under reduced pressure. The final volume was adjusted to 10 mL. Nanocarriers without PCL, i.e, NC1, were prepared under similar conditions described above. Control experiments were carried out preparing formulations without melatonin.

5.2.5 Platinum-melatonin loaded nanoparticles

Nanocapsule and nanoemulsion formulations were diluted 50% v/v with water, and a 5-fold excess with respect to amino group in the PDMAEMA block, of H₂PtCl₆ was added under stirring. The sample was dialyzed against pure water for two days. Reduction of PtCl₆ ions was performed using a 5-fold excess NaBH₄, respect to Pt ions, added slowly to the Pt-NC under stirring. Finally, the sample was dialyzed against pure water for two days to remove any excess of reducing agent. Samples were analyzed by TEM.

5.2.6 Notation

Formulations here prepared herein are denoted as follows: NCX-M_nD_m-Mel represents a nanocapsule loaded with melatonin where X corresponds to a number, 1 or 2, depending

on its content of PCL. M_nD_m corresponds to be diblock copolymer used ($M_{40}D_{108}$ and $M_{40}D_{471}$).

5.2.7 Characterization of nanoparticles

pH. Measurements were performed for all samples using a potentiometer (Microanal B-474).

Particle size distribution and polydispersity.

Nanocapsule suspensions, NC1 or NC2, (0.02 mg/mL respect to the PMMA-b-PDMAEMA content) were properly diluted with 1 mM NaCl. Samples were filtered using Nylon filter with a pore size of 0.45 μm (13-HV, Millipore) prior to the measurement, in order to remove dust particles that might cause interference. Their particle size distributions and polydispersity index (PDI) were determined by dynamic light scattering measurements, which were performed with an ALV DLS/SLS SP 5022F equipment with a He-Ne laser ($\lambda=632.8$ nm). The CONTIN algorithm was used to analyze the obtained autocorrelation functions. The measured electric field correlation function $g_1(t)$ was analyzed by means of the a cumulant expansion (eq.1):

$$\ln g_1(t) \approx \Gamma_0 - \Gamma_1 t + \left(\frac{\Gamma_2}{2!}\right)t^2 - \left(\frac{\Gamma_3}{3!}\right)t^3 + \dots \quad (\text{eq.1})$$

The first cumulant, Γ_1 , is related to the apparent diffusion coefficient via equation (eq.2)

$$D = \frac{\Gamma_1}{q^2} \quad (\text{eq.2})$$

Γ_2 , the second cumulant, is related to the relative standard deviation. The average hydrodynamic radius, R_h , can be calculated using the Stokes-Einstein equation (eq.3):

$$D = \frac{k_B T}{6 \pi \eta_0 R_h} \quad (\text{eq.3})$$

where k_B is the Boltzmann constant, T is the absolute temperature, and η_0 is the solvent viscosity. Nanocapsule PDIs were determined using cumulant analysis.

Transmission Electron Microscopy (TEM), Cryogenic TEM (Cryo-TEM) and Scanning Electron Microscopy (SEM).

TEM micrographs were obtained using a Zeiss EM 922 transmission electron microscope operated at 200 kV. NC1 and NC2 suspensions were diluted 10 times in Millipore water (1 mg/mL respect to PMMA-*b*-PDMAEMA content), and a 5- μ L droplet was deposited onto a copper TEM grid (300 mesh) coated with a carbon film, without any further staining process. Cryogenic studies were performed by depositing a drop of the nanocarriers onto the copper TEM grid (600 mesh, Science Services, München, Germany) and removing most of the liquid with a blotting paper, leaving a thin film stretched over the grid holes. The grid was immersed rapidly into liquid ethane and cooled to ca 90 K by liquid nitrogen in a temperature-controlled freezing unit (Zeiss Cryobox, Zeiss NTS GmbH, Oberkochen, Germany, and then transferred via a cryotransfer holder (CT 3500, Gatan, München, Germany) to a Zeiss EM 922 EFTEM. Zero/loss filtered images ($\Delta E = 0$ eV) were taken under reduced dose conditions (100-1000 e/nm²). All images were registered digitally by a bottom-mounted CCD camera system (Ultrascan 1000, Gatan, München, Germany) combined and processed with a digital imaging processing system (Digital Micrograph 3.9 for GMS 1.4). Scanning electron microscopy (SEM) images were recorded using a LEO 1530 Gemini microscope, and the samples of solid powder were loaded on the carbon film substrate.

Encapsulation Efficiency (EE).

Melatonin was assayed by high performance liquid chromatography (HPLC). Measurements were conducted on a thermo separation product chromatographic system composed of a pump P4000, an autosampler AS3000 and an UV-detector UV6000LP with a wavelength $\lambda=229$ nm was used as detector. A reversed phase column C18, 250x4.6 mm ID, 1000 Å pore diameters, with 7 μ m average particle sizes, was employed (Macherey-Nagel). The solvents, acetonitrile (ACN) and water (H₂O), were HPLC grade and used freshly. The solvent composition for the measurements was ACN/H₂O 55/45 (v/v) at 23°C with a flow rate of 0.7 mL/min. These experimental parameters are based on a previous study and where described elsewhere.⁴¹ Predetermined concentration of pure melatonin solutions were used to calibrate the detector and a new calibration curve were done daily. Free melatonin was separated from colloids by ultrafiltration–centrifugation (Ultrafree-MC 10,000 MW, Millipore). Total drug was measured, after dissolution of colloids with acetonitrile. The associated melatonin with the NC1 and the NC2 was calculated from the difference between the total and the free drug concentrations.

5.3. Results and Discussions

The nanocarriers were prepared by interfacial deposition technique using the PMMA-*b*-PDMAEMA block copolymers. Melatonin which is slightly soluble in water but completely soluble at the concentration used in the organic solution of polymer and oil is expected to precipitate after the diffusion of the solvent into the aqueous medium. Here, we refer to so-called nanocarriers NC1 or NC2 for nanocapsules prepared with and without PCL, respectively. PMMA-*b*-PDMAEMA has a long hydrophilic PDMAEMA chain and when PCL was used (NC1), one expects to have a suprastructure like a nanocapsule. The oil core is surrounded by PCL which is anchored with PMMA-*b*-PDMAEMA. When no PCL is used, the expected suprastructure for NC2 is like a nanoemulsion stabilized by the copolymer, acting as an interfacial agent. So, the copolymer is located at the interface surrounding the oil core. The reason to use PCL is related to its ability of stabilizing nanoemulsions by encapsulating it and forming nanocapsules.^{42,44} The LCST behavior of PDMAEMA also opens up another possibility to separate and to collect the nanocarriers from the solution by simple filtration after heating the solution above the cloud point.

The particle size and shape of the nanocarriers play an important role in the efficiency of the drug delivery. For instance, the bioavailability, the timed/controlled release of the drug, the targeting of direct intracellular delivery, the clearance and opsonization processes are strongly related to it. Thus, the determination of this property of the colloidal carriers is one of the key parameters in any study.⁴⁵⁻⁴⁷

5.3.1 Physico-Chemical Characterization

A first important property which needs to be assessed after the preparation of nanoscopic carriers is its size, size distribution and the stability of the formed dispersion. All formulations studied were macroscopically homogeneous and stable. Figure 1 (bottom) shows a representative autocorrelation function and the CONTIN analysis obtained for some of the formulations. Unimodal and narrow distributions were observed in each case. Table 2 summarizes all values obtained for the formulations under study. Hydrodynamic radii ranged between 100-180 nm (i.e. mean diameters between 200-360 nm) optimal for oral drug delivery systems, where a favorable particle size should be lower than < 500 nm.^{8,45,47,48} The sample polydispersity listed in the same table was calculated from the

cumulant analysis at the scattering angle of 90°. For almost all formulations, values were lower than 0.13, indicating a moderate size distribution of the nanoparticles.

Table 2. Physico-Chemical Characterization of nanocarriers loaded with melatonin^a

	Miglyol (μ L)	PCL (mg)	M _n D _m (mg)	R _h (nm)	PDI	pH (\pm 0.02)
NC2- M ₄₀ D ₁₀₈ -Mel-A	250	-	100	143	0.060	8.25
NC2- M ₄₀ D ₄₇₁ -Mel-A	50	-	30	135	0.010	7.88
NC1- M ₄₀ D ₁₀₈ -Mel-A	50	30	100	95	0.060	7.98
NC1- M ₄₀ D ₁₀₈ -Mel-B	250	100	100	128	0.110	8.12
NC1- M ₄₀ D ₁₀₈ -Mel-C	330	100	100	137	0.117	8.30
NC1-M ₄₀ D ₁₀₈ -Mel-D ^b	250	100	100	123	0.120	8.23
NC1- M ₄₀ D ₄₇₁ -Mel-A	50	30	100	115	0.125	7.90
NC1- M ₄₀ D ₄₇₁ -Mel-B	200	30	100	161	0.042	8.14
NC1- M ₄₀ D ₄₇₁ -Mel-C	200	100	100	134	0.009	8.52

a) In all melatonin containing formulations the concentration of melatonin was 0.5 mg/mL

b) melatonin concentration = 1.0 mg/mL

M_nD_m: PMMA-b-PDMAEMA content (mg)

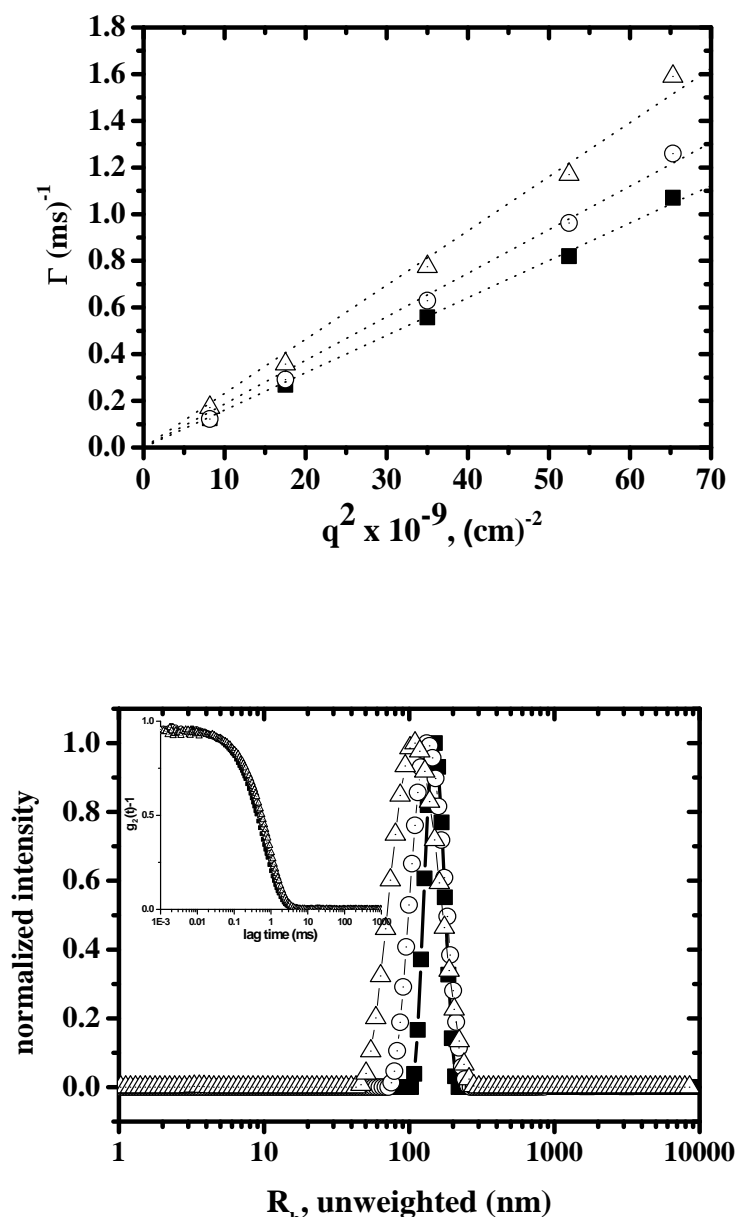


Figure 1. Angular dependence of decay rate obtained from DLS data of diluted nanoparticles loaded with melatonin ($C_{\text{NaCl}} = 1 \text{ mM}$) ($\Delta = \text{NC1- M}_{40}\text{D}_{108}\text{-Mel-A}$; $\circ = \text{NC1- M}_{40}\text{D}_{471}\text{-Mel-A}$; $\blacksquare = \text{NC2- M}_{40}\text{D}_{471}\text{-Mel-A}$).

Figure 1 (top) depicts the typical linear q^2 dependence of the decay rate, Γ , evidencing the diffusive behavior of the investigated particles. Thus, the Stokes-Einstein equation can be applied to determine reliable hydrodynamic radii from DLS.

5.3.2 Morphological Study

The influence of the particle shape in the drug delivery has not been fully elucidated. But certainly, the particle shape along with the size and the chemistry are critical parameters in the designing of drug nanocarriers.⁴⁷ We have investigated the shape and the morphology of the nanocontainers by standard- and cryo-TEM. Figure 2 shows the air-dried TEM micrographs for the NC1 prepared with both diblock copolymers (A and B) and for a NC2-M₄₀D₄₇₁-A. It can be observed from the micrographs that nanocarriers show a well-defined structure with spherical shape. In the case of NC1, it is possible to distinguish a melatonin core surrounded by a thin shell of polymer, possibly PCL. In Figure 2A, this shell has a thickness of approximately 15 nm, and the oily core has a diameter of 154 nm. Particle sizes from TEM presented smaller size compared to the results obtained by DLS. Reductions of the size are attributed to the specificity of the measurements. With DLS a highly soluble and a more expanded structure is measured, the PDMAEMA block is solvated and extended in water, unlike the sizes obtained by standard TEM, where structures collapse in the dried state. In the first case, z-average particle size is determined while by TEM it is a number-average.

Since methacrylates degrade upon electron beam^{49,50} it is not possible to distinguish PCL and PMMA-*b*-PDMAEMA at the interface of the core. Nevertheless, the fact that all colloids were macroscopically homogeneous and no other surfactants were used (the copolymer is acting as surfactant), together with the basic pH values measured, seems to support the structure proposed in the Scheme 1, where the copolymer should be in the outer part of the shell with the hydrophilic PDMAEMA block interacting with the aqueous phase and stabilizing the nanocarriers and in the inner one the PCL and PMMA at the interface of the oily core, with, probably, some chain fragments solubilized inside it. In the TEM picture of the NC2- M₄₀D₄₇₁-Mel-A (micrograph C) the presence of the copolymer is not visible either and due the absence of PCL, no shell was observed.

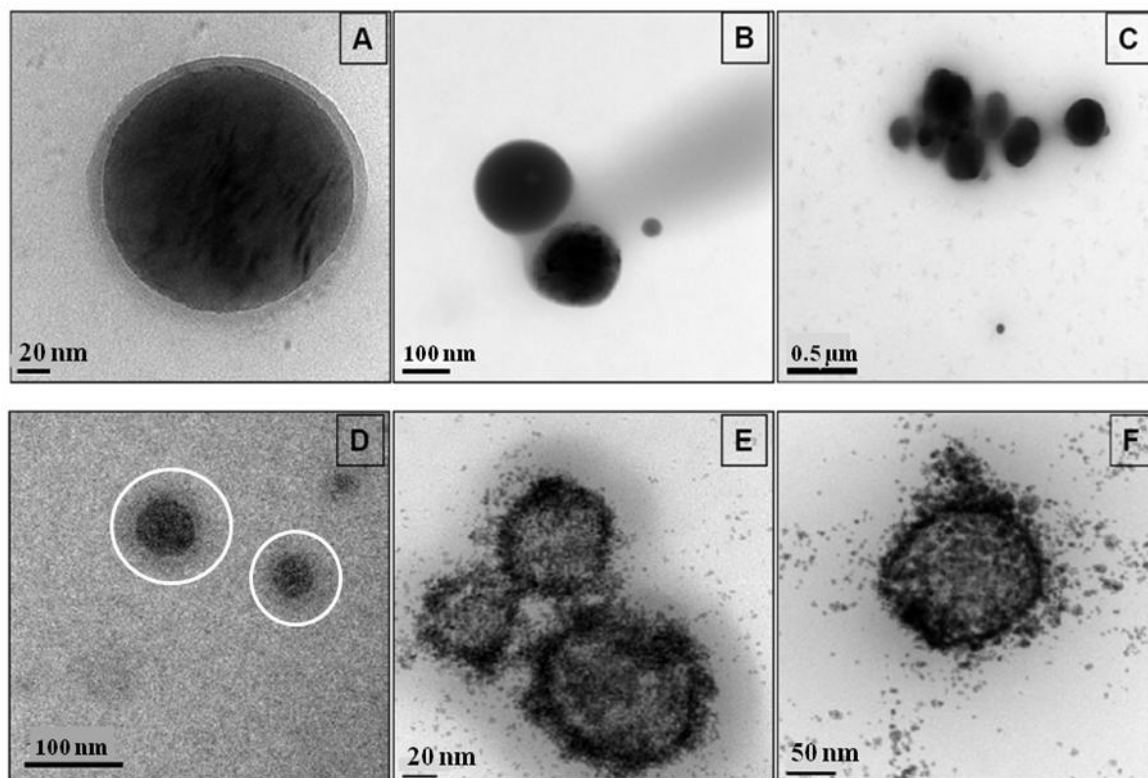


Figure 2. Non-stained TEM images for (A) NC1- $M_{40}D_{471}$ -Mel-A, (B) NC1- $M_{40}D_{108}$ -Mel-A, (C) NC2- $M_{40}D_{471}$ -Mel-A. Cryo-TEM image of NC1-MD₂-Mel-A (D); the circles denote the swollen PDMAEMA shell. TEM images of Pt loaded (E) NC1- $M_{40}D_{471}$ -Mel-A and (F) NC2- $M_{40}D_{471}$

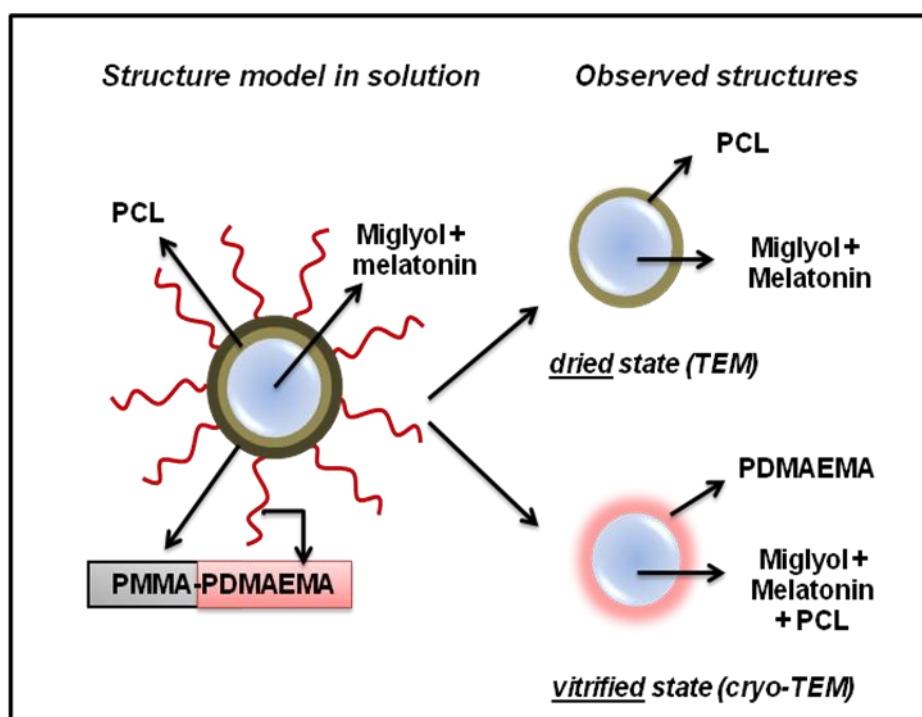
In order to prove the presence of copolymer in the outer part of the NC1, *cryo*-TEM was performed. Cryogenic TEM allows the visualization of particle shape and size *in situ* in solution rather than in a dry state since the sample is vitrified in a thin layer of water before the measurement. Although the shell does not present a high contrast in water, a diffuse shadow surrounding the oily core can be seen, which corresponds to the highly solvated PDMAEMA chains in the mixture PCL/ $M_{40}D_{471}$. Probably PCL is collapsed and would not show a shadow.

To further confirm the location of PMMA-*b*-PDMAEMA, NC1- $M_{40}D_{471}$ -Mel-A and NC2- $M_{40}D_{471}$ were loaded with platinum nanoparticles. Hexachloroplatinum acid specifically binds to amino functions. After the coordination of H_2PtCl_6 , reduction by $NaBH_4$ leads to the generation of Pt nanoparticles inside the corona. As depicted in micrographs E and F, a preferential location of the Pt nanoparticles is not observed, nevertheless, there is a darker and denser ring of metallic nanoparticles localized at the oil-

polymer interface where the diblock should be. Thus, these results together with the cryo-TEM provide convincing evidence for the proposed structural model (Scheme 1).

One of the advantages of employing polymers containing an amino function, like PDMAEMA, is that it opens up the possibility of creating a variety of nanoparticles with promising biomedical applications by complexation with, for instance, fluorescent quantum dots (CdSe, CdS), metallic nanoparticles, plasma probes (Au), resulting in an interesting way of functionalizing drug carriers with probes to monitor particle migration in the body by X-ray, computer tomography or fluorescence microscopy. The possibility of “decorating” the melatonin-loaded nanocarriers with metallic nanoparticles may results in a promising alternative to further investigate its migration and accumulation in cellular and in *in vivo* experiments.

Scheme 1. Hypothetical structural model for melatonin-loaded nanocapsules



The information about the stability of the nanocarriers in the dry state might be useful for the storage of the nanocarriers in the final formulation. To investigate this, NC1-MD₁-Mel-B was frozen with liquid nitrogen and lyophilized without any additional treatment.

The solid sample was analyzed by SEM. The particles that remained intact have a round shape with a rough surface (Figure 3).

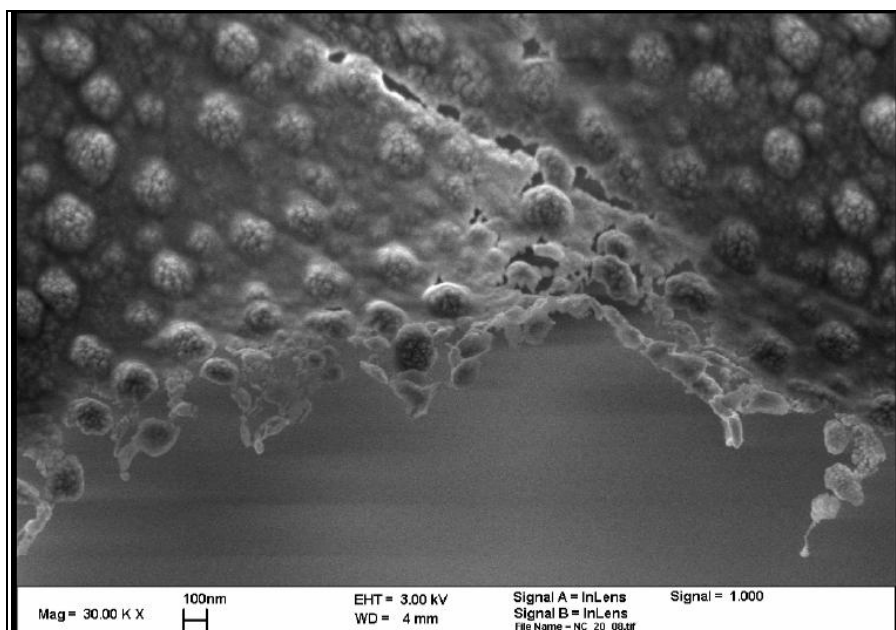


Figure 3. SEM micrograph of a freeze-dried NC1- M₄₀D₁₀₈-MEL-B sample.

5.3.3 Encapsulation Efficiency (EE)

After assessing the size distribution, we evaluated a second important parameter, the encapsulation efficiency (EE), by assaying in HPLC the free melatonin separated previously using ultrafiltration-ultracentrifugation. The efficiencies of melatonin encapsulation ranged mainly between 22.7% and 29.9% (Table 3). The lowest efficiency (2.7%) was observed by the nanocarrier without PCL and with longer PDMAEMA block, NC2- M₄₀D₄₇₁-Mel-A. In general, low encapsulation efficiencies might be attributed to the solubility of melatonin in water (0.1 mg/ml) or to the poor diblock ability to keep the drug encapsulated inside the oily core. To enhance the encapsulation, a nanocapsule with higher melatonin content (1 mg/ml) was prepared and evaluated. The particle size remained slightly unchanged by increasing melatonin concentration (NC1-M₄₀D₁₀₈-Mel-D, in Table 2). As it can be observed in Table 3 by increasing the melatonin by a factor of 2, the efficiency increased to 35.5%, what represent an increase of drug loaded of 18.4%. This result seems to indicate that there is a limit of the capacity of the NC1, prepared under the experimental conditions, to load more melatonin inside the container. Since, it has been reported that the addition of inorganic salts to the nanocarrier formulations may induce changes in the drug entrapment due to the osmotic gradient between the internal and the

external phase,^{51,52} we therefore tried to further optimize the melatonin loading by the addition of a low molecular weight salt (0.01M NaCl). We observed a slight enhancement of the EE, with values ca. 5% higher than those without NaCl added, what means that the melatonin encapsulated increased by ca. 14.7% and 10.7% for NC containing 0.5 and 1.0 mg/ml, respectively.

TABLE 3. Melatonin Encapsulation Efficiencies

Sample	%EE
NC1- M ₄₀ D ₁₀₈ -Mel-A	22.7
NC1- M ₄₀ D ₁₀₈ -Mel-B	29.9
NC1- M ₄₀ D ₁₀₈ -Mel-C	26.4
NC1- M ₄₀ D ₄₇₁ -Mel-A	25.1
NC1- M ₄₀ D ₄₇₁ -Mel-B	23.2
NC1- M ₄₀ D ₄₇₁ -Mel-C	25.7
NC2- M ₄₀ D ₁₀₈ -Mel-A	24.3
NC2- M ₄₀ D ₄₇₁ -Mel-A	2.7
Na-NC1- M ₄₀ D ₁₀₈ -Mel-B	34.3*
Na-NC1- M ₄₀ D ₁₀₈ -Mel-D	39.2*

* samples with 10 mM NaCl added

5.4. Conclusions

Encapsulation of melatonin was carried out by interfacial deposition using an amphiphilic diblock copolymer, PMMA-*b*-PDMAEMA, and a mixture of the linear diblock copolymer with PCL. This first attempt to encapsulate melatonin with a thermoresponsive and multifunctional diblock copolymer allowed the preparation of nanocarriers whose particle size and shape were extensively characterized by DLS, TEM and SEM. By the method employed here, nanocarriers were prepared without using low molecular weight surfactants as stabilizers, as commonly used in these formulations, proving that the amphiphilic behavior of the diblock was sufficient to stabilize the nanoparticles. Drug content measurements indicate that melatonin was loaded with an encapsulation efficiency of mainly ca. 22.7 to 29.9%, depending on the formulation, which

can be slightly enhanced by the addition of NaCl. We could prove that nanocarriers are composed by a core containing oil and melatonin, surrounded by PCL and PMMA-*b*-PDMAEMA. The successful adsorption of platinum nanoparticles to the nanocarriers may provide a promising way to track the migration of the nanocontainers once they are introduced into the body. In summary, the use of a multifunctional diblock copolymer combines easy encapsulation, separation/purification and the ability of incorporating functional nanoparticles and thus presents significant advantages and an alternative to classical low molecular weight surfactants.

Acknowledgments

This work was supported by the European Union within the Marie Curie RTN POLYAMPHI. E. P.-Ch., S.S.G and A.R.P acknowledge travel grants from the DAAD-CAPES academic exchange program E.P-Ch wants to thanks to Dr. G.T Lim for valuable discussions.

References

1. Fessi, H.; Puisieux, F.; Devissaguet, J. P.; Ammoury, N.; Benita, S., Nanocapsule Formation by Interfacial Polymer Deposition Following Solvent Displacement. *International Journal of Pharmaceutics* **1989**, *55*, (1), R1-R4.
2. Mora-Huertas, C. E.; Fessi, H.; Elaissari, A., Pharmaceutical Nanotechnology. Polymer-Based Nanocapsules for Drug Delivery. *International Journal of Pharmaceutics* **2010**, *385*, (1-2), 113-142.
3. Desgouilles, S.; Vauthier, C.; Bazile, D.; Vacus, J.; Grossiord, J.-L.; Veillard, M.; Couvreur, P., The Design of Nanoparticles Obtained by Solvent Evaporation: A Comprehensive Study. *Langmuir* **2003**, *19*, (22), 9504-9510.
4. Quintanar-Guerrero, D.; Allemann, E.; Doelker, E.; Fessi, H., A Mechanistic Study of the Formation of Polymer Nanoparticles by the Emulsification-Diffusion Technique. *Colloid and Polymer Science* **1997**, *275*, (7), 640-647.
5. Couvreur, P.; Vauthier, C., Polyalkylcyanoacrylate Nanoparticles as Drug Carrier: Present State and Perspectives. *Journal of Controlled Release* **1991**, *17*, (2), 187-198.

6. Damge, C.; Michel, C.; Aprahamian, M.; Couvreur, P.; Devissaguet, J. P., Nanocapsules as Carriers for Oral Peptide Delivery. *Journal of Controlled Release* **1990**, 13, (2-3), 233-239.
7. Gao, F.; Zhang, Z.; Bu, H.; Huang, Y.; Gao, Z.; Shen, J.; Zhao, C.; Li, Y., Nanoemulsion Improves the Oral Absorption of Candesartan Cilexetil in Rats: Performance and Mechanism. *Journal of Controlled Release* **2011**, 149, (2), 168-174.
8. Pandey, R.; Ahmad, Z.; Sharma, S.; Khuller, G. K., Nano-Encapsulation of Azole Antifungals: Potential Applications to Improve Oral Drug Delivery. *International Journal of Pharmaceutics* **2005**, 301, (1-2), 268-276.
9. Pandey, R.; Zahoor, A.; Sharma, S.; Khuller, G. K., Nanoparticle Encapsulated Antitubercular Drugs as a Potential Oral Drug Delivery System Against Murine Tuberculosis. *Tuberculosis (Edinburgh, Scotland)* **2003**, 83, (6), 373-378.
10. Ahlin, P.; Kristl, J.; Kristl, A.; Vrecer, F., Investigation of Polymeric Nanoparticles as Carriers of Enalaprilat for Oral Administration. *International Journal of Pharmaceutics* **2002**, 239, (1-2), 113-120.
11. Gref, R.; Minamitake, Y.; Peracchia, M. T.; Trubetskoy, V.; Torchilin, V.; Langer, R., Biodegradable Long-Circulating Polymer Nanospheres. *Science* **1994**, 263, (5153), 1600-1603.
12. Torchilin, V. P.; Trubetskoy, V. S., Which Polymers Can Make Nanoparticulate Drug Carriers Long-Circulating? *Advanced Drug Delivery Reviews* **1995**, 16, (2,3), 141-155.
13. Kwon, G. S.; Kataoka, K., Block Copolymer Micelles as Long-Circulating Drug Vehicles. *Advanced Drug Delivery Reviews* **1995**, 16, (2,3), 295-309.
14. Couvreur, P.; Puisieux, F., Nano- and Microparticles for the Delivery of Polypeptides and Proteins. *Advanced Drug Delivery Reviews* **1993**, 10, (2-3), 141-162.
15. Baines, F. L.; Armes, S. P.; Billingham, N. C.; Tuzar, Z., Micellization of Poly(2-(dimethylamino)ethyl methacrylate-block-methyl methacrylate) Copolymers in Aqueous Solution. *Macromolecules* **1996**, 29, 8151-8159.
16. Baines, F. L.; Billingham, N. C.; Armes, S. P., Synthesis and Solution Properties of Water-Soluble Hydrophilic-Hydrophobic Block Copolymers. *Macromolecules* **1996**, 29, 3416-3420.
17. Gohy, J.-F.; Antoun, S.; Jerome, R., pH-Dependent Micellization of Poly(2-vinylpyridine)-block-poly((dimethylamino)ethyl methacrylate) Diblock Copolymers. *Macromolecules* **2001**, 34, (21), 7435-7440.

18. Harada, A.; Kataoka, K., Supramolecular Assemblies of Block Copolymers in Aqueous Media as Nanocontainers Relevant to Biological Applications. *Progress in Polymer Science* **2006**, 31, (11), 949-982.
19. Kataoka, K.; Harada, A.; Nagasaki, Y., Block Copolymer Micelles for Drug Delivery: Design, Characterization and Biological Significance. *Advanced Drug Delivery Reviews* **2001**, 47, (1), 113-131.
20. Letchford, K.; Burt H. A Review of the Formation and Classification of Amphiphilic Block Copolymer Nanoparticulate Structures: Micelles, Nanospheres, Nanocapsules and Polymersomes. *European Journal of Pharmaceutics and Biopharmaceutics* **2007**, 65, (3), 259-269.
21. Plamper, F. A.; Ruppel, M.; Schmalz, A.; Borisov, O.; Ballauff, M.; Muller, A. H. E., Tuning the Thermoresponsive Properties of Weak Polyelectrolytes: Aqueous Solutions of Star-Shaped and Linear Poly(N,N-dimethylaminoethyl Methacrylate). *Macromolecules* **2007**, 40, 8361-8366.
22. Zhang, M.; Liu, L.; Wu, C.; Fu, G.; Zhao, H.; He, B., Synthesis, Characterization and Application of Well-Defined Environmentally Responsive Polymer Brushes on the Surface of Colloid Particles. *Polymer* **2007**, 48, (/), 1989-1997.
23. Zhao, Q.; Ni, P., Synthesis of Well-Defined and Near Narrow-Distribution Diblock Copolymers Comprising PMMA and PDMAEMA Via Oxyanion-Initiated Polymerization. *Polymer* **2005**, 46, (9), 3141-3148.
24. Chatterjee, U.; Jewrajka, S. K.; Mandal, B. M., The Amphiphilic Block Copolymers of 2-(Dimethylamino)Ethyl Methacrylate and Methyl Methacrylate: Synthesis by Atom Transfer Radical Polymerization and Solution Properties. *Polymer* **2005**, 46, (24), 10699-10708.
25. Sakuma, S.; Sudo, R.; Suzuki, N.; Kikuchi, H.; Akashi, M.; Ishida, Y.; Hayashi, M., Behavior of Mucoadhesive Nanoparticles Having Hydrophilic Polymeric Chains in the Intestine. *Journal of Controlled Release* **2002**, 81, (3), 281-290.
26. Sakuma, S.; Suzuki, N.; Kikuchi, H.; Hiwatari, K.-i.; Arikawa, K.; Kishida, A.; Akashi, M., Absorption Enhancement of Orally Administered Salmon Calcitonin by Polystyrene Nanoparticles Having Poly(N-isopropylacrylamide) Branches on Their Surfaces. *International Journal of Pharmaceutics* **1997**, 158, (1), 69-78.
27. Sakuma, S.; Ishida, Y.; Sudo, R.; Suzuki, N.; Kikuchi, H.; Hiwatari, K.-i.; Kishida, A.; Akashi, M.; Hayashi, M., Stabilization of Salmon Calcitonin by Polystyrene Nanoparticles Having Surface Hydrophilic Polymeric Chains, Against Enzymatic Degradation. *International Journal of Pharmaceutics* **1997**, 159, (2), 181-189.

28. Beyer, C. E.; Steketee, J. D.; Saphier, D., Antioxidant Properties of Melatonin-an Emerging Mystery EPR and Spin Trapping Investigations. *Biochemical Pharmacology* **1998**, 56, (10), 1265-1272.
29. Qi, W.; Reiter, R. J.; Tan, D. X.; Manchester, L. C.; Calvo, J. R., Melatonin Prevents Delta-Aminolevulinic Acid-Induced Oxidative DNA Damage in the Presence of Fe²⁺. *Molecular and Cellular Biochemistry* **2001**, 218, (1-2), 87-92.
30. Matuszak, Z.; Reszka, K. J.; Chignell, C. F., Reaction of Melatonin and Related Indoles with Hydroxyl Radicals: EPR and Spin Tapping Investigations. *Free Radical Biology and Medicine* **1997**, 23, (3), 367-372.
31. Pieri, C.; Marra, M.; Moroni, F.; Recchioni, R.; Marcheselli, F., Melatonin: A Peroxyl Radical Scavenger More Effective Than Vitamin E. *Life sciences* **1994**, 55, (15), PL271-6.
32. Garfinkel, D.; Laudon, M.; Zisapel, N., Improvement of Sleep Quality by Controlled-Release Melatonin in Benzodiazepine-Treated Elderly Insomniacs. *Archives of Gerontology and Geriatrics* **1997**, 24, (2), 223-231.
33. Jan, J. E.; Hamilton, D.; Seward, N.; Fast, D. K.; Freeman, R. D.; Laudon, M., Clinical Trials of Controlled-Release Melatonin in Children with Sleep-Wake Cycle Disorders. *Journal of Pineal Research* **2000**, 29, (1), 34-39.
34. Srinivasan, V.; Pandi-Perumal, S. R.; Maestroni, G. J. M.; Esquifino, A. I.; Hardeland, R.; Cardinali, D. P., Role of Melatonin in Neurodegenerative Diseases. *Neurotoxicity Research* **2005**, 7, (4), 293-318.
35. Harrod, C. G.; Bendok, B. R.; Hunt Batjer, H., Interactions Between Melatonin and Estrogen May Regulate Cerebrovascular Function in Women: Clinical Implications for the Effective Use of HRT During Menopause and Aging. *Medical Hypotheses* **2005**, 64, (4), 725-735.
36. Coyle, J. T.; Puttfarcken, P., Oxidative Stress, Glutamate, and Neurodegenerative Disorders. *Science* **1993**, 262, (5134), 689-95.
37. Anisimov, V. N.; Popovich, I. G.; Zabezhinski, M. A.; Anisimov, S. V.; Vesnushkin, G. M.; Vinogradova, I. A., Melatonin as Antioxidant, Geroprotector and Anticarcinogen. *Biochimica et Biophysica Acta, Bioenergetics* **2006**, 1757, (5-6), 573-589.
38. Lee, B. J.; Choe, J. S.; Kim, C. K., Preparation and Characterization of Melatonin-Loaded Stearyl Alcohol Microspheres. *Journal of Microencapsulation* **1998**, 15, (6), 775-787.

39. El-Gibaly, I.; Anwar, M. M., Development, characterization and in vivo evaluation of polyelectrolyte complex membrane gel microcapsules containing melatonin-resin complex for oral use. *Bulletin of Pharmaceutical Sciences* **1998**, 21, (2), 117-139.
40. Tursilli, R.; Casolari, A.; Iannuccelli, V.; Scalia, S., Enhancement of Melatonin Photostability by Encapsulation in Lipospheres. *Journal of Pharmaceutical and Biomedical Analysis* **2006**, 40, (4), 910-914.
41. Schaffazick, S. R.; Pohlmann, A. R.; de Cordova, C. A. S.; Creczynski-Pasa, T. B.; Guterres, S. S., Protective Properties of Melatonin-Loaded Nanoparticles Against Lipid Peroxidation. *International Journal of Pharmaceutics* **2005**, 289, (1-2), 209-213.
42. Schaffazick, S. R.; Pohlmann, A. R.; Guterres, S. S., Nanocapsules, Nanoemulsion and Nanodispersion Containing Melatonin: Preparation, Characterization and Stability Evaluation. *Die Pharmazie (Berlin)* **2007**, 62, 354-360.
43. Zhang, X.; Matyjaszewski, K., Synthesis of Well-Defined Amphiphilic Block Copolymers with 2-(Dimethylamino)ethyl Methacrylate by Controlled Radical Polymerization. *Macromolecules* **1999**, 32, (6), 1763-1766.
44. Calvo, P.; Vila-Jato, J. L.; J., A. M., Comparative in vitro Evaluation of Several Colloidal Systems, Nanoparticles, Nanocapsules and Nanoemulsions, as Ocular Drug Carrier. *Journal of Pharmaceutical Sciences* **1996**, 85, (%), 530-536.
45. Emerich, D. F.; Thanos, C. G., The pinpoint promise of nanoparticle-based drug delivery and molecular diagnosis. *Biomolecular Engineering* **2006**, 23, (4), 171-184.
46. Moghimi, S. M.; Hunter, A. C.; Murray, J. C., Long-Circulating and Target-Specific Nanoparticles: Theory to Practice. *Pharmacological Reviews* **2001**, 53, (2), 283-318.
47. Champion, J. A.; Katare, Y. K.; Mitragotri, S., Particle Shape: A New Design Parameter for Micro- and Nanoscale Drug Delivery Carriers. *Journal of Controlled Release* **2007**, 121, (1), 3-9.
48. Kaparissides, C.; Alexandridou, S.; Kotti, K.; Chaitidou, S., Recent Advances in Novel Drug Delivery Systems. *Journal Of Nanotechnology Online* **2006**, 2, 1-11.
49. Walther, A.; André, X.; Drechsler, M.; Abetz, V.; Müller, A. H. E., Janus Discs. *Journal of the American Chemical Society* **2007**, 129, (19), 6187-6198.
50. Breiner, U.; Krappe, U.; Thomas, E. L.; Stadler, R., Structural Characterization of the "Knitting Pattern" in Polystyrene-block-Poly(ethylene-co-butylene)-block-Poly(methyl methacrylate) Triblock Copolymers. *Macromolecules* **1998**, 31, (1), 135-141.

51. Peltonen, L.; Aitta, J.; Hyvönen, S.; Karjalainen, M.; Hirvonen, J., Improved Entrapment Efficiency of Hydrophilic Drug Substance During Nanoprecipitation of Poly(l)lactide Nanoparticles. *AAPS PharmSciTech* **2004**, 5, (1), Article 16.
52. Freytag, T.; Dashevskya, A.; Tillmanb, L.; Hardeeb, G. E.; R., B., Improvement of the Encapsulation Efficiency of Oligonucleotide-Containing Biodegradable Microspheres. *Journal of Controlled Release* **2000**, 69 (1), 197–207.

ACKNOWLEDGMENTS

First of all, I would like to thank Prof. Dr. Axel Müller for giving the excellent opportunity to do my PhD in his group, providing me all what I needed to perform my research. It was a wonderful time in MC. The project itself gave me the chance of interacting with some of the most prestigious researchers in the polymer field and presenting the advances of my topic in national and international meetings. But, even more important, I would like to thank you for encouraging me to finish my thesis when I had a moment of weakness.

I am very grateful to Dr. Dmitry Pergushov who initiated me in the “world of polyelectrolytes” and transmitted his passion to this topic and patiently taught and explained to me every necessary thing to carry out, with success, this research. Also, thanks for his valuable contributions and discussions during the elaboration of manuscripts, seminars, posters or a simple report. Dima, muchas gracias!

I want to thank Prof. Dr. Adriana Polhmann and Prof. Dr. Sílvia S. Guterres, who proposed the fascinating topic of drug delivery and nanocontainers. Thank you for all scientific discussions and suggestions. Also to the “Brazilian” team at UFRGS, Porto Alegre, Brazil, specially to Alessandro Jäger, Eliezer Jäger and Scheila Schaffazick, for all the help in the lab and kindness during my stay in Porto Alegre.

None of this would have been possible had it not relied on the excellent team that I found in MC2, where cultural, ethnic and language differences also contributed to my personal enrichment. This diversity allowed me to get to know not only excellent colleagues but also wonderful friends. I apologize for omitting the titles and I hope I do not miss anyone; especially big thanks for the selfless help, support and scientific discussions to: Sandrine Tea, Petar Petrov, Markus Burkhardt, Manuela Schumacher, Andreas Walther, Nemesio Martinez-Castro, Sharmila Muthukrishnan, Felix Schacher, Markus Ruppel, Holger Schmalz, Youyong Xu, Marli Tebbaldi de Sordi, Sabine Wunder, Felix Plamper, Jiayin Yuan, Adriana Boschetti-Fierro, Pierre Millard, Anja Goldmann, Markus Drechsler, Mingfu Zhang, Girish Behera, Andrew Ah Toy, Oliver Colombani, Yanfei Liu, Chih-Cheng Peng (rip), Harald Becker, Denise Danz, Gabi Cantea, Sergey Nosov, Jeannine Rockser, André Gröschel, Stefan Reinicke, Hideharu Mori.

I would like to thank Gaby Rösner-Oliver for all her help, kindness and support not only in those bureaucratic things but also in those little things important in everyday life.

Special thanks to Annette Krökel because without her help I would have gotten lost in the lab.

Thanks to Dr. Goy Teck Lim for his support, corrections and scientific discussions.

I want to express my infinite gratitude to the “latinoamerican connection” in Bayreuth, my beloved friends who made my daily life enjoyable: Deliani Lovera, Nelson Lombana, Beatriz Álvarez, Luis Matamoros, Sandra Romero, Daniel Varon, Luisa Vera, Raúl Pérez, Oscar Valdes and Lucas do Santos, Alfredo Martínez. ¡Muchas gracias amigos!

Last but not the least; I want to thank my colleagues at the Universidad Simon Bolivar for all their support during this time.

For financial support I thank the European Science Foundation for funding the Marie Curie Research and Training Network “Polyamphi” (MC-RTN Polyamphi).

LIST OF PUBLICATIONS

Evis K. Penott-Chang, Dmitry V. Pergushov, Alexander B. Zezin, and Axel H. E. Müller. Interpolyelectrolyte Complexation in Chloroform. *Langmuir*, 2010, 26, 7813-7818.

Evis K. Penott-Chang, Markus Ruppel, Dmitry V. Pergushov, Alexander B. Zezin, Axel H.E. Müller. Interpolyelectrolyte Complexes of Diblock Copolymers via Interaction of Complementary Polyelectrolyte-Surfactant Complexes in Chloroform. Submitted to *Polymer* in April 2011

Evis Penott-Chang, Andreas Walther, Pierre Millard, Alessandro Jäger, Eliezer Jäger, Axel H. E. Müller, Sílvia S. Guterres, Adriana R. Pohlmann. Amphiphilic Diblock Copolymer and Polycaprolactone to produce New Vesicular Nanocarriers. Submitted to *Journal of Biomedicine Nanotechnology* in March 2010.

Felix A. Plamper, Alexander Schmalz, **Evis Penott-Chang**, Markus Arben Jusufi, Matthias Ballauff, and Axel H. E. Müller, Synthesis and Characterization of Star-Shaped Poly(N,N-dimethylaminoethyl methacrylate) and Its Ammonium Salts. *Macromolecules* 2007, 40, 5689-5697.

ERKLÄRUNG

Die vorliegende Arbeit wurde von mir selbstständig verfasst und ich habe keine anderen als die angegebenen Hilfsmittel benutzt.

Ferner habe ich nicht versucht, anderweitig mit oder ohne Erfolg eine Dissertation einzureichen oder mich der Doktorprüfung zu unterziehen.

Bayreuth, 04.05.2011

(Evis Penott-Chang)